DEVELOPING HETEROGENEOUS TRAFFIC STATE MEASUREMENT TECHNIQUES BASED ON IMAGE PROCESSING AND MODELING

SHAH MD MUNIRUZZAMAN
(MSc Engineering, BUET)

A THESIS SUBMITTED

FOR THE DEGREE OF DOCTOR OF PHILOSOPHY

DEPARTMENT OF CIVIL ENGINEERING

MILITARY INSTITUTE OF SCIENCE AND TECHNOLOGY

DECEMBER 2016

The thesis titled **"*DEVELOPING HETEROGENEOUS TRAFFIC STATE MEASUREMENT TECHNIQUES BASED ON IMAGE PROCESSING AND MODELING*"** submitted by *Shah Md Muniruzzaman*, Roll No: *1013110032* Session: *2013-14* has been accepted as satisfactory in partial fulfillment of the requirement for the degree of *Doctor of Philosophy (PhD)* on *15th December, 2016*.

BOARD OF EXAMINERS

1.	Dr. Md. Hadiuzzaman Associate Professor Department of Civil Engineering, BUET, Dhaka.	Chairman (Supervisor)
2.	Brig Gen K M Salzar Hossain, ndc, psc Dean Faculty of Civil Engineering, MIST, Dhaka.	Ex-Officio
3.	Dr. G. M. Jahid Hasan Professor Department of Civil Engineering, MIST, Dhaka.	Member
4.	Maj Mohammed Russedul Islam, PhD, Engrs. Assistant Professor Department of Civil Engineering, MIST, Dhaka.	Member
5.	Dr. Md. Mizanur Rahman Professor Department of Civil Engineering, BUET, Dhaka.	Member (External)
6.	Dr. Farzana Rahman Associate Professor Department of Civil Engineering, UAP, Dhaka.	Member (External)

DECLARATION

I hereby declare that this thesis is my original work and it has been written by me in it entirety. I have duly acknowledged all the sources of information which have been used in the thesis.

This thesis has also not been submitted for any degree in any University previously.

Shah Md Muniruzzaman

15th December, 2016

ACKNOWLEDGEMENT

All praise goes to almighty Allah, the most merciful and the most benevolent. At the outset I would like to express my deepest gratitude to my supervisor Dr. Md. Hadiuzzaman, Associate Professor, Department of Civil Engineering, BUET, Dhaka for his invaluable guidance, inspiration, passionate directions and continuous support throughout the entire journey of my research work.

I also express my sincere appreciation to the members of the Doctoral committee: Brigadear General K M Salzar Hossain, ndc, psc, Dean, Faculty of CE, MIST; Prof Dr G. M. Jahid Hasan, CE Dept., MIST; Prof Dr Hossain Md Shahin, CEE Dept., IUT; Prof Dr Md Tauhid-Ur-Rahman, CE Dept., MIST; Major Khandaker Sakil Ahmed, PhD, Engrs, CE Dept., MIST; and Major Mohammed Russedul Islam, PhD, Engrs, CE Dept., MIST for their constant supervision, constructive criticism fruitful propositions, invaluable observations, and appropriate corrections in taking the research work at the expected level.

I am grateful to Major General Md Siddiqur Rahman Sardar, SGP, hdmc, psc, the ex-commandant, MIST for his visionary decision of introducing PhD program in MIST and inspiring me to enroll in the program. I am also indebted to present Commandant Major General Md. Abul Khair, ndc for his invaluable guidance and moral support. Sincere obligation to Ex and present Dean of Civil Engineering faculty Brigadier General (Rtd.) Habibur Rahman Kamal, ndc, psc and Brigadier General K M Salzar Hossain, ndc, psc for their unceasing support and encouragement. I am also grateful to Director R&D, Brigadier General Md Gazi Ferooz Rahman for his constant backing. Sincere thanks to Lieutenant Colonel G.M. Azizur Rahman (Rtd.) for his continuous insistence for pursuing PhD program.

Sincere appreciations to all the members of the board of examiners for their invaluable suggestions during defense which has definitely added additional impact to the research work.

I am also grateful to MIST; Maj Md Jahidul Islam, PhD, Assistant Professor Kamrul Islam, Major Tarique, Lecturer Tahmida Hossain Shimu, Captain H. M. Imran Kays, Engrs, Captain Sampa Akter, Engrs, Captain A T M Masum, Engrs and Captain

Muntahith Mehadi Orvin, Engrs, CE Dept., MIST; Lecturer Sanjana Hossain, CE Dept., BUET, Research Assistant Sarder Rafee Musabbir, Nazmul Haque, Mohammad Rayeedul Kalam Siam, Department of Civil Engineering, BUET for their extensive support and assistance.

I am indebted to my mother and parents-in-laws for their support and inspiration. Special thanks to my beloved wife Fara Jabin Parvez, son Adnaf Shah and daughter Apsara Munir for their sacrifice and continuous encouragement which helped me to stay focused.

Finally I am grateful to all faculties and staffs of Civil Engineering department for their help, assistance, and inspiration in conducting the research work.

SUMMARY

In Dhaka city traffic operating condition is predominantly non-lane-based and heterogeneous in nature. Accurate measurement of traffic state is the first and principal task for describing and improving such traffic condition. For this, video-based image processing algorithms are preferred over other alternatives. This research initiates with the development of a novel traffic detection algorithm for detecting non-lane-based heterogeneous traffic. The algorithm uses mainly two different parameters: (1) static background; and (2) threshold parameter. The algorithm achieves high accuracy of detection through small computational effort. The qualitative analysis shows that compared to others the proposed algorithm can detect vehicles accurately. The quantitative analysis of the algorithm shows stable Precision-Recall Relationship. The RMSE values computed from ground truth and estimated traffic parameters show that the proposed algorithm outperforms other state of the art algorithms.

Given the difficulty of obtaining variable traffic demands in the real world and the cost and time associated with the field data collection, a controlled environment is needed where the demand can be changed artificially and the overall network performance can be observed. Microscopic simulators (e.g. VISSIM) are capable of providing such controlled environment. In this research a generic calibration tool, VISCAL has been developed, for microscopic simulation parameters in VISSIM environment. The optimization system of the tool is based on three heuristic algorithms: (a) GA; (b) SPSA; (c) SA. VISCAL can be used to calibrate any type (rural, urban etc.) and extent (large, medium etc.) of network.

Again macroscopic traffic flow models play an irreplaceable role in real-time traffic state estimation & prediction and represent the traffic states with the help of aggregated variables. The two most frequently used macroscopic models are the first-order cell transmission model (CTM) and the second-order METANET model.

In this research a 1st order CTM model was developed for non-lane-based heterogeneous urban traffic condition. At first the nature of the fundamental traffic relationships was systematically investigated based on the traffic data. From regression analysis it was concluded that 3rd degree polynomial structure shows the best fit with

the measured traffic data. As classical CTM tends to simulate inappropriate flow and speed behavior due to simple and linear consideration of FD, a new model was proposed in this research. Detail investigation shows that, the non-linear FD plays the most important role in developing CTM model, for estimating traffic state accurately in heterogeneous traffic operating condition.

Again this research proposes a new second-order macroscopic traffic flow model having the following special features: (1) both the flow and speed dynamics have a normally distributed stochastic term; (2) the FD in the speed dynamics follows Zhang's one-parameter polynomial structure and (3) the parameters of the FD are variable over the links. In the model calibration stage, simultaneous optimization of FD parameters and driver-related parameters were conducted. The optimized parameters capture the existing traffic conditions of the respective links quite well. The link-specific FD parameters and the stochastic traffic state influencing terms improve the model performance the most, followed by the Car Following parameter. Proposed model performs most poorly in the absence of FD in the speed dynamics. Thus it can be concluded that FD affects the traffic states very seriously for heterogeneous composition and cannot be dropped off from the speed dynamics for simplicity in control design.

The predicted speed, flow and density from the developed macroscopic model were compared with those from a microscopic simulation model, VISSIM. Four levels of traffic demands viz. light, moderate, heavy and excessive demand levels were applied to evaluate the compatibility of the two models. Based on the performance of the models and comparative analysis, the following main conclusions are found:

i) The prediction of traffic states from the proposed stochastic METANET-based model is generally consistent with that from VISSIM simulation over the whole range of traffic demand levels used in this research.

ii) The MAEs in traffic state estimation of various links do not show any distinct trend with the change of traffic demand levels, thus indicating that the developed macroscopic model performs quite satisfactorily for different traffic demand levels.

DEDICATION

The Thesis is dedicated to the memory of my father Shah Md Shahidullah (1938-1996) who had been the source of inspiration for all my achievements

And

My eldest son Ahnaf Shah Anindo (1998-2014)who left this World on 06th July 2014, only at the age of sixteen and waiting for us in the garden of heaven under the leadership of Hazrat Ibrahim (Peace be upon him).

TABLE OF CONTENTS

LIST OF TABLES

LIST OF FIGURES

LIST OF ABBREVIATIONS

Acronym	Definition
ATM	Active traffic management
ATDM	Active Traffic and Demand Management
AADT	Average annual daily traffic
ANOVA	Analysis of variance
BGS	Background subtraction
BMC	Background model challenge
CTM	Cell transmission model
COV	Coefficient of Variance
CMYK	Cyan-magenta-yellow-black
F	F-measure
FD	Fundamental diagram
FOV	Field of view
FP	False positive
FPR	False positive ratio
FPS	Frames per second
FN	False negative
GA	Genetic algorithm
GMM	Gaussian mixture model
H-CTM	Heterogeneous cell transmission model
HSV	Hue saturation value
ITS	Intelligent transportation systems
J	Jaccard coefficient
KDE	Karnel density estimation
kph	Kilometer per hour
MAE	Mean absolute error
MAPE	Minimum absolute percentage error
MFD	Macroscopic fundamental diagram
MOE	Measure of Effectiveness
MPC	Model predictive control

Acronym	Definition
O-D	Origin-destination
PBAS	Pixel based adaptive segmenter
PCC	Percentage of correct classification
PR	Precission recall
RGB	Red-green-blue
RM	Ramp metering
RMRSE	Root mean relative square error
ROC	Receiver operating characteristics
SA	Simulated annealing
SL	Speed limit
SPSA	Simultaneous stochastic approximation
SQP	Sequential quadratic programming
STD	Standard deviations
TMC	Traffic management center
TN	True negative
TP	True positive
TPR	True positive ratio
TTT	Total travel time
TTS	Total time spent
TTD	Total travel distance
VISCAL	VISSIM calibration tool
VSL	Variable speed limit
vphpl	Vehicle per hour per lane
vpkpl	Vehicle per kilometer per lane
Y	Yule- coefficient

LIST OF NOTATIONS

Symbol	Definition	Unit
A	Area of car	Sq. Pixel
α	Transparency factor	N/A
Δt	Time step	hours
Δx_i	Cell length	miles
B^*	Static background	Pixel
$B(t)$	Actual Background at time t	Pixel
β_i	Off-ramp Split ratio	dimensionless
CC0	Defines the desired distance between stopped cars	m
CC1	The time (in seconds) that a driver wants to keep. The higher the value, the more cautious the driver is	s
CC2	Restricts the longitudinal oscillation or how much more distance than the desired safety distance a driver allows before he intentionally moves closer to the car in front	m
CC3	Threshold for entering Following, controls the start of the deceleration process	-
CC4	Negative Following Threshold	-
CC5	Positive Following Threshold	-
CC6	The Influence of distance on speed oscillation while in following process	-
CC7	Actual acceleration during the oscillation process	m/s^2
CC8	Desired acceleration when starting from standstill	m/s^2
CC9	Desired acceleration at 80 km/h	m/s^2
C_i	flow combination factor for ramp	dimensionless
C_w	Width of a car	Pixel
$d(t)$	Differential Image at time t	Pixel
$d_i(t)$	On-ramp demand in cell i in period t	vph
d_s^j	Average delay obtained from the simulation model for intersection j,	sec
d_o^i	Observed field delay for intersection j, and	sec

Symbol	Definition	Unit
e	Error term	Square Pixel
ξ_i^q	Stochastic flow influencing term	vpm
ξ_i^v	Stochastic speed influencing term	mph
$F(t)$	Intensity of vehicle at time t	Pixel
$I(t)$	Frame at time t	Pixel
$k_1(t)$	Intensity variation due to illumination change at time t	Pixel
$k_2(t)$	Intensity variation due to camera movement at time t	Pixel
L	Length of the strip	Pixel
m	Number of frames	-
$N(t)$	Count at time t	Vehicle
N	Total number of links in the model,	dimensionless
N	Number of cells	dimensionless
N_j	Number of vehicles present at frame j	Vehicle
$n(t)$	Number of entered vehicles at time t	Vehicle
n	Number of intersections under consideration.	dimensionless
$P(t)$	Vehicle Present at time t	Vehicle
Q_i	Cell capacity	vph
$q(t)$	Flow at time t	vph
$q_i(t)$	Flow from cell i to i + 1 in period t	vph
$qu_i(t)$	On-ramp queue size in cell i in period t	no of vehicles
R_i	On-ramp capacity	vph
ρ_j	Jam density	vpm
ρ_c	Critical density	vpm
$\rho_i(t)$	Density in cell i in period t	vpm

Symbol	Definition	Unit
S_i	Off-ramp capacity	vph
$S_{i,t}$	Actual speeds for link i and time t,	mph
$S(\theta)_{i,t}$	Simulated speeds for link i and time t,	mph
s_i	Change in co-ordinate of vehicle	Pixel
$s_i(t)$, $r_i(t)$	Off-ramp, On-ramp flow in cell i in period t	vph
σ_i	flow distribution factor for ramp	dimensionless
T	Total number of time periods t,	dimensionless
$T(t)$	Travel time in period t	hours
$\tau(t)$	Threshold requirement at time t	Pixel
t'	Time interval between consecutive frame	Second
t	Period number	dimensionless
θ	Car-following parameter	dimensionless
$V_{i,t}$	Actual link flow for link i and time t,	vph
$\tilde{V}(\theta)_{i,t}$	Simulated link flow for link i and time t,	vph
v_i	Free flow speed	mph
v_f	Free flow speed	mph
w	Width of counting strip	Pixel
w_1	Weight used to assign more or less value to flows,	dimensionless
w_2	Weight used to assign more or less value to speeds,	dimensionless
w_i	Back wave speed	mph

CHAPTER 1: INTRODUCTION

1.1. Background of the Study

In recent years, rapid increase in travel demand and the number of vehicles on roadways has resulted in serious traffic congestion problem for Dhaka city. According to a study jointly conducted by the Metropolitan Chamber of Commerce and Industry (MCCI) and Chartered Institute of Logistics and Transport Bangladesh in 2010, it was revealed that the annual cost of traffic congestion in capital Dhaka was around tk 1 billion a day. The study found that about 3.2 million business hours were lost every day due to the traffic jams. A more recent assessment concluded that the estimated loss is now 50% more than what it was in 2010, adding up to a staggering amount of about tk 550 billion annually. The traffic jams not only cause tremendous time and monetary losses but also compromise road safety and increase air pollution.

The most widely used strategy to mitigate the congestion problem is to increase roadway capacity by constructing new lanes. However, the growing demand issue cannot be mitigated by only expanding road infrastructure due to constraints like available right-of-way, capital investment, implementation time and environmental concern. Rather, more efficient use of the existing traffic network through Active Traffic Management (ATM) can be a better measure against the congestion problem at the short term. ATM involves the use of appropriate traffic flow models to accurately simulate and predict traffic state variables in real-time and then apply proper control strategy. In the developed countries, ATM has been successfully practiced for decades as a highly effective tool for mitigating traffic congestion and improving safety. Given the extent of the traffic jam problem in Dhaka, it is high time

that the authority starts adopting ATM as a congestion mitigating tool. Again, in Dhaka city, both motorized and non-motorized vehicles of different sizes, shapes and speeds ply over the roads making the traffic operating condition highly heterogeneous. Here the traffic stream comprises of cars, buses, mini-buses, trucks, covered vans, auto-rickshaws and utilities having varying operating characteristics. All these characteristics make the congestion problem more complex and challenging.

In this situation/context accurate measurement of traffic states is the first and principal task for describing and improving traffic condition. For this, video-based sensors are generally preferred over other alternatives as they provide high quality traffic information over spatial and temporal dimensions. The video sensors are centered on image processing algorithms for traffic detection. Over the years, different detection algorithms have been developed which help in the measurement of traffic states in a variety of situations (e.g. stationary (Pletzer et al., 2012), slowly moving (Mandellos et al., 2011), and free-flow conditions (Vargas et al., 2010), at complex maneuvers (lane change, right or left turn) and for incident detection (Zou et al., 2009). However, even with the recent advances in traffic detection technology, there remain some challenging issues in traffic parameters measurement in urban heterogeneous traffic environments, where complex conditions such as dense traffic flow, traffic congestions, or vehicle queues are likely to appear.

For comprehensive traffic study/management both microscopic and macroscopic models need to be analyzed or developed. Macroscopic traffic flow models play an irreplaceable role in real-time traffic state estimation and short-term prediction. The models consider the traffic flow as a compressible fluid and represent the traffic states with the help of aggregated variables: flow, speed and density. As such, they include a lower number of parameters compared to the microscopic models. This results in low

computational effort and relative ease of calibration for real-time application. On the contrary, the microscopic models include a large number of physical or non-physical parameters that should be appropriately specified to reproduce the traffic flow characteristics with the highest possible accuracy. The parameter estimation has intensive computational requirements and is difficult to validate because human behavior in real traffic is difficult to observe and model. Thus, macroscopic traffic flow models are generally preferred over microscopic models for real-time traffic estimation and control.

The two most frequently used macroscopic models are the first-order cell transmission model (CTM) (Daganzo, 1994) and the second-order METANET model (Messmer and Papageorgiou, 1990). Numerous studies like Lin and Ahanotu (1995), Muñoz et al. (2006), Papageorgiou et al. (1990) etc. have found that traffic state estimates of these models show very close agreement with the field data. Over the years, different extensions and modifications of these models have been proposed to adapt for a variety of traffic engineering tasks, such as dynamic traffic assignment, estimation and prediction, control strategy design and synthesis etc. For example, the CTM has been extended in Li (2010), Gomes and Horowitz (2006) and Hadiuzzaman and Qiu (2013) for arterial traffic signal control, freeways with ramp metering control and Variable Speed Limit (VSL) control respectively. Likewise, many extensions of the METANET model can be found in the literature to take into account e.g., weaving effect (Yin, 2014) and lane drops (Papageorgiou et al., 1990); and have been adapted to different models of ATM: variable speed limits (Islam et at., 2013), ramp meter control (Papamichail et al., 2010) and combination of these two (Lu et al., 2011). However these models were mostly developed and validated for homogeneous traffic. But Dhaka city's traffic is comprised of both motorized and non-motorized vehicles

of different sizes, shapes and speeds making the traffic operating condition highly heterogeneous. The behavior of traffic in such heterogeneous operating condition is significantly different from that in homogeneous condition. This necessitates the development of a new macroscopic model which will be able to successfully estimate and predict the heterogeneous traffic conditions of Dhaka city.

Again comprehensive comparison between appropriate 1st and 2nd order models for heterogeneous traffic warrants testing of the model performances under varied traffic demands. Given the difficulty of obtaining variable traffic demands in the real world and the cost and time associated with the field data collection, a controlled environment is needed where the demand can be changed artificially and the overall network performance can be observed. Microscopic simulators (e.g. VISSIM) are capable of providing such controlled environment. However, to be representative of the real world traffic conditions, the microscopic models need to be accurately calibrated and validated. Since the performance and operational characteristics of non-lane based heterogeneous traffic change rather abruptly over space and time, a single set of calibration parameters may not be appropriate for the entire network during the full simulation period. Also, the proper optimization method and the nature of the objective function for such model calibration are subjects of further extensive research.

1.2. Statement of the Problem and Opportunities

1.2.1. Absence of suitable and robust high-resolution data collection technique

Within the vast literature on macroscopic traffic flow modeling, surprisingly few studies have addressed the heterogeneous traffic condition prevalent in many developing countries like Bangladesh, India etc. Such limited research is primarily attributed to the difficulty of high-resolution data collection in the stated traffic

condition. Here loop detectors are unsuitable due to measurement errors caused by non-lane-based movement of vehicles activating either both or neither of two adjacent detectors. Moreover, traffic cameras for vehicle detection are often absent along the corridors. But given that accurate high-resolution traffic data is the pre-requisite for developing a successful traffic flow model, this research attempts to establish a data collection technique based on image processing which will be able to measure traffic states in the non-lane-based heterogeneous operating condition with reasonable accuracy. Also, the developed technique is expected to be robust and easy-to-use.

1.2.2. Adjustment of macroscopic model for heterogeneous traffic

The core of ATM is the macroscopic traffic models for traffic state prediction. The accuracy of traffic state estimation and prediction affects the control decisions that will be assigned for mitigating the congestion problem. Unfortunately, no such model has been developed till date for simulating the non-lane-based heterogeneous traffic conditions of Dhaka city. Hence, as a stepping stone for ATM implementation, an appropriate macroscopic model should be developed for the stated traffic condition by proposing necessary modifications to state-of-art traffic flow models. The modified model should be able to successfully reproduce the wide variation in operating and performance characteristics of vehicles in heterogeneous traffic systems. More specifically, it should be able to capture the rapid change of traffic states along the roadway in the heterogeneous condition. Previous studies (Lu et al., 2011) showed that the speed dynamics of macroscopic simulation models like the METANET cannot catch quick and significant changes in congested traffic conditions. As a result, considerable prediction errors exist between the measured data and the model-predicted traffic states in such operating condition. Moreover, there remains some inherent differences between lane-based and non-lane based operations which affect the overall mobility of the traffic stream. Therefore, these problems should be

investigated thoroughly to improve the sensitivity of the model performance under various traffic conditions.

1.2.3. Compatibility between microscopic and macroscopic simulation models

Now-a-days both microscopic and macroscopic simulations are widely used in transportation studies (Venkatesan et al., 2008; Nair et al., 2011). Microscopic simulations are often used to explicitly capture interactions among individual drivers and represent the driver's response to traffic control devices at the individual vehicle level. However, this type of application is usually off-line and lacks predictive control functions. On the other hand, the application of macroscopic simulation models is aimed at large-scale roadway networks or online (real time) traffic control to reduce congestion and improve mobility.

Due to traffic operation safety and cost constraints, it is not practical, sometimes even impossible, to carry out experiments of various control measures on freeways. Traffic simulation is often used for experimental investigation purposes. The effects of a control strategy are often evaluated prior to the field implementation of online traffic control using microscopic simulations to determine whether the control strategy will have the expected performance. In this way, the optimal control policy for various traffic conditions can be determined based on several experimental settings and then used in actual field traffic control. Thus it is required to check whether both macroscopic and microscopic models provide similar traffic state results under all traffic conditions, including light traffic, moderate traffic, heavy traffic and excessively congested traffic. This issue is investigated in the present study.

1.3. Research Objectives and Scope of Work

This research work mainly aims at developing model-based techniques for traffic state measurement and estimation in non-lane based heterogeneous operating condition. With this end in view, the objectives of the study are listed below:

- To develop a ready-for-practice method using image processing technique that can provide accurate high resolution traffic data (e.g. speed, flow, density) for non-lane-based heterogeneous traffic in stationary, slowly-moving and free-flow conditions.
- To form a CTM-based 1st order model and a METANET-based 2nd order model which are capable of estimating and predicting traffic states (e.g. speed, flow, density) accurately for the stated traffic system.
- To develop an automatic system that is capable of calibrating the car-following and lane-changing parameters of the microscopic simulation model based on different probabilistic optimization methods with different forms of objective functions so that the overall model performance is improved.
- To explore the compatibility of the developed macroscopic models with the calibrated and validated microscopic model under various traffic conditions to determine the traffic demand influences macroscopic simulation performance.

The possible outcomes of this research include a robust traffic state measurement method based on image processing technique and a suitable macroscopic traffic flow model that will accurately estimate and predict heterogeneous traffic states under different demand scenarios.

The scope of this research is restricted to uninterrupted arterials (including on-ramps and off-ramps) having heterogeneous motorized traffic. The test site is the Tongi Diversion Road, a section of the Dhaka-Mymensingh Highway (N3) in Bangladesh (shown in Figure 1.1). It is an 8-lane major artery road in Dhaka, which connects the capital city with the Shahjalal International Airport. The developed model is expected to accurately estimate and predict the complex nature of the prevailing heterogeneous traffic condition of the test site through appropriate modifications and extensions of conventional traffic models.

Although arterial roads with signal controls are not included in the study, the methodologies and principles used here can be extended and applied to other types of roadways. The research is carried out using both simulations and field data obtained from the studied roadway section. The main test site is illustrated in Figure 1.1 and the research flow chart is shown in Figure 1.2.

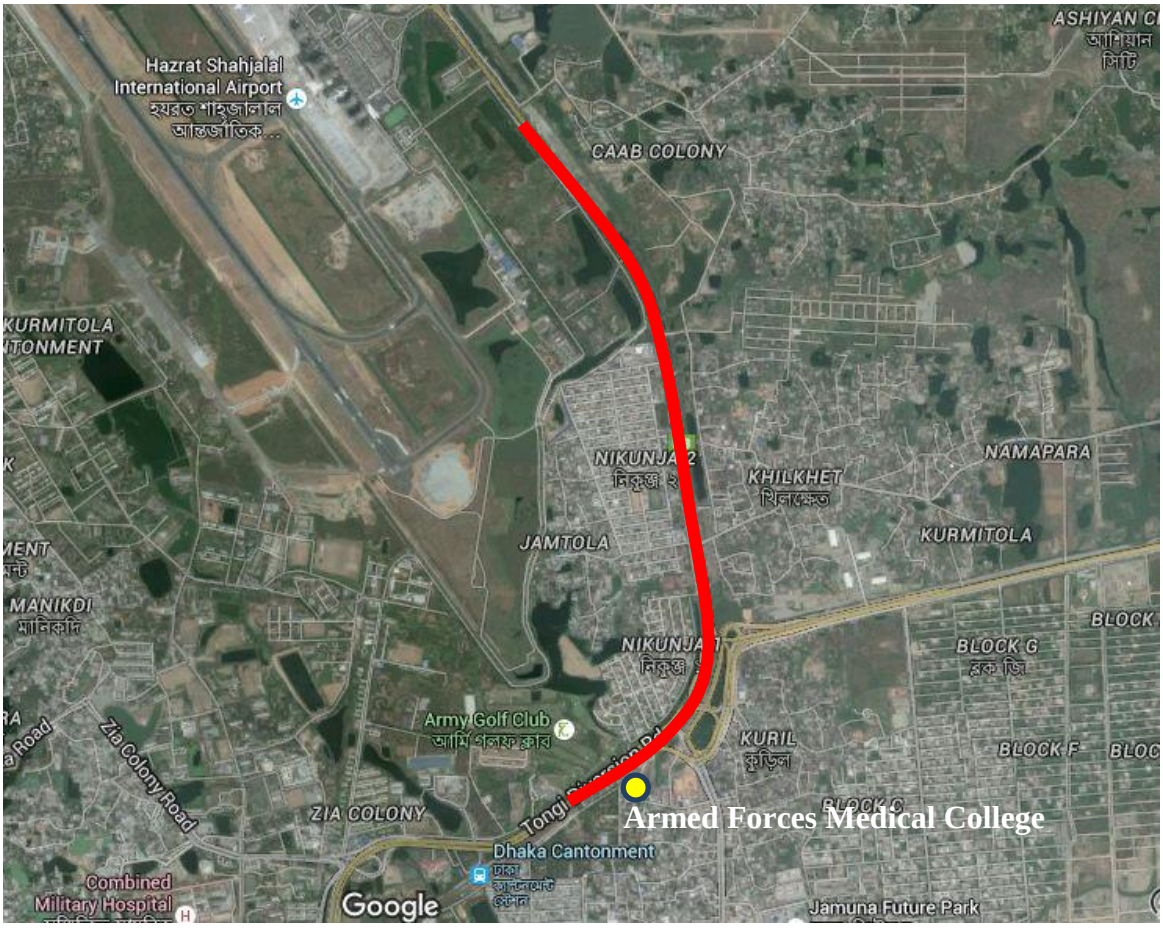

Figure 1.1: The 3.26 km long study site between Armed Forces Medical College (short of army golf club) and CAAB Head Quarters (courtesy: Google maps).

Study Sequence

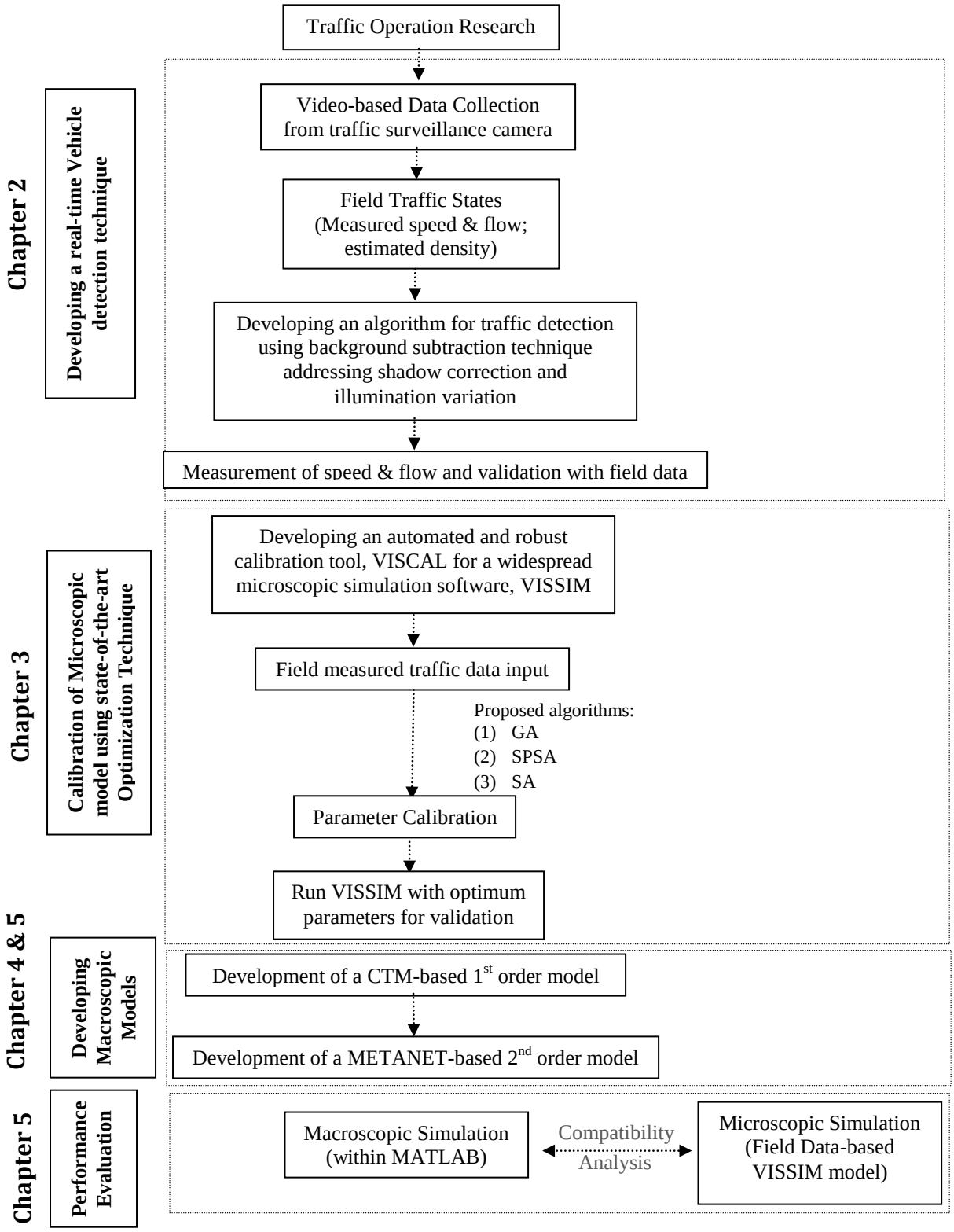

Figure 1.2 Flow chart of the research

1.4. Organization of the Thesis

This thesis consisting of six chapters is structured as follows:

Chapter 1 gives an introduction of the relevant research background, statement of problems as well as the objectives and scope of this research.

Chapter 2 presents a novel algorithm for accurate traffic detection through video sensors. The algorithm involves deterministic parameters, which aid in defining detection challenges and developing solutions. The algorithm detects traffic in three conditions: (1) stationary, (2) slowly moving, and (3) free-flow. The innovation involves the use of transparency effect for frame correction to deal with three challenges: (1) illumination variation, (2) shadow, and (3) camera displacement. To test the applicability of the proposed algorithm, both qualitative and quantitative analysis are performed with respect to four BMC (Background Model Challenges) algorithms such as Kernel Density Estimation (KDE), Gaussian Mixture Model (GMM), Pixel-Based Adaptive Segmenter (PBAS) and Sigma-Delta. The evaluation tasks are performed using synthetic and real-time video dataset. The developed algorithm achieves overall classification accuracy (>95%) with small computational effort (500 frame per second). A set of equations are developed to estimate speed, flow and density which can be readily adopted with other detection algorithms. Finally, correlations between traffic parameters and algorithm evaluation parameters are established to determine the applicability of any image-processing algorithm for traffic state estimation. The increment or decrement of evaluation parameters marks the characteristics of an algorithm, which dictates whether the algorithm is suitable for traffic state estimation.

Chapter 3 presents features of VISCAL (VISSIM CALIBRATION) which is an automated calibration tool for microscopic simulation parameters in VISSIM environment, based on three heuristic optimization algorithms: (a) Genetic Algorithm

(GA); (b) Simultaneous Perturbation Stochastic Approximation (SPSA); (c) Simulated Annealing (SA). It is developed with a goal to automate and ease the tedious process of calibration, offering greater flexibility to the user by providing control on every aspect of the calibration process. It includes multiple features for a generic application tool with the ability to test the significance of the appropriate decision parameter set for a particular network, to determine the most suitable objective function to reflect network characteristics, and to check the suitability of any of the three heuristic optimization algorithms for a particular network. VISCAL also offers four objective function choices into the system: (1) speed, (2) flow, (3) delay, and (4) multi-objective criteria. It is able to calibrate all the driving behavior parameters for any type (urban, rural) and extent of network (small or large network). For this study, the operation of the tool is tested by a dataset obtained from a 3.26 km freeway of Dhaka, Bangladesh.

Chapter 4 describes a first order deterministic macroscopic model–H-CTM (Heterogeneous Cell Transmission Model) based on the basic CTM. The methodological calibration of the model considers the aggregate behavior of heterogeneous traffic under weak lane discipline. Although traffic system of this nature prevails in many urban cities of South Asian countries a suitable first order model has not been proposed till date. To this end, H-CTM incorporates fundamental diagram (FD) modeled for non-lane-based heterogeneous traffic instead of traditional piecewise linear FD. As vehicles from different speed class are mixed together, the shape of FD is found non-linear in nature. For validating the model performance, high resolution traffic data of 20 sec covering both peak and off-peak periods were collected from a 3.26 km major arterial roadway (N3-Highway) of Dhaka city. Then the calibrated FD parameters are used in the newly developed H-CTM to simulate the

traffic. The evolutions of traffic flows show that the H-CTM can be used to describe the traffic dynamics in the stated traffic system.

Chapter 5 illustrates a stochastic macroscopic model developed for traffic state estimation and short-term prediction in such systems. The proposed model takes into account the wide variation in the operating and performance characteristics of vehicles in heterogeneous condition through the use of variable fundamental diagrams (FDs) for different links. The model also allows for the under estimation of flow and speed due to the effect of vehicular influence area in the stated traffic condition. For this, normally distributed stochastic state influencing terms are used with the basic state estimation equations. In addition, an empirical parameter is introduced in the speed dynamics of the model to capture the sensitivity of traffic speed to the speeds of multiple leaders in a heterogeneous mix. To confirm the structure of the FD, initially the speed-density plots of the field data for different links are fitted with four general structures: namely, the linear, logarithmic, exponential and polynomial forms. It is revealed that the 3rd degree polynomial structure is best suited for prevailing traffic condition. The optimized link-specific parameters of the model comply with those obtained from the regression analysis. Field validation with high-resolution traffic data proved that the proposed model can capture traffic dynamics quite accurately. To determine the individual contributions of the proposed model features, different structural variations of the final model are also investigated.

Chapter 6 summarizes the main conclusions of this research and discusses recommendations for future research works related to macroscopic traffic flow models and simulation for heterogeneous traffic.

1.5. Reference

1. Pletzer, F., Tusch, R., Böszörmenyi, L., Rinner, B. Robust traffic state estimation on smart cameras. 9th IEEE International Conference on Advanced Video and Signal-Based Surveillance (AVSS),2012, pp. 434-439.
2. Mandellos, N. A., Keramitsoglou, I., Kiranoudis, C. T. A background subtraction algorithm for detecting and tracking vehicles. Journal of Expert Systems with Applications, 38(3), 2011, pp. 1619-1631.
3. Vargas, M., Milla, J. M., Toral, S. L., Barrero, F. An enhanced background estimation algorithm for vehicle detection in urban traffic scenes. Transactions on Vehicular Technology, 59(8),2011, pp. 3694-3709.
4. Zou, Y., Shi, G., Shi, H., Wang, Y. Image sequences based traffic incident detection for signaled intersections using HMM. Ninth International Conference on Hybrid Intelligent Systems, Vol. 1, 2009, pp. 257-261.
5. Daganzo, C. F. The cell transmission model: A dynamic representation of highway traffic consistent with the hydrodynamic theory. Transportation Research Part B: Methodological 28(4), 1994, pp. 269-287.
6. Messmer, A., and M. Papageorgiou. METANET: A macroscopic simulation program for motorway networks. Traffic Engineering and Control 31, no. 8-9, 1990 pp. 466-470.
7. Lin, W.-H. and D. Ahanotu, Validating the basic cell transmission model on a single freeway link. PATH technical note; 1995, pp 95-103.
8. Muñoz, L., X. Sun, R. Horowitz, and L. Alvarez. Piecewise-linearized cell transmission model and parameter calibration methodology. In *Transportation Research Record: Journal of the Transportation Research Board* 1965, 2006, pp. 183-191.
9. Papageorgiou, M., J.-M. Blosseville, and H. Hadj-Salem, Modelling and real-time control of traffic flow on the southern part of Boulevard Peripherique in Paris: Part I: Modelling. Transportation Research Part A: General, 1990. 24(5): p. 345-359.
10. Li, Z. Modeling arterial signal optimization with enhanced cell transmission formulations. *Journal of Transportation Engineering* 137, no. 7, 2010, pp. 445-454.

11. Gomes, G., and R. Horowitz. Optimal freeway ramp metering using the asymmetric cell transmission model. *Transportation Research Part C: Emerging Technologies* 14, no. 4, 2006, pp. 244-262.
12. Hadiuzzaman, M. and T.Z. Qiu, Cell transmission model based variable speed limit control for freeways. Canadian Journal of Civil Engineering, 2013. 40(1): p. 46-56.
13. Yin, Y., Traffic Flow Modelling to Improve Traffic State Prediction. PhD dissertation, University of Alberta, 2014.
14. Islam, M., M. Hadiuzzaman, J. Fang, T. Z. Qiu, and K. El-Basyouny. Assessing mobility and safety impacts of a variable speed limit control strategy. In *Transportation Research Record: Journal of the Transportation Research Board* 2364, 2013, pp. 1-11.
15. Papamichail, I., A. Kotsialos, I. Margonis, and M. Papageorgiou. Coordinated ramp metering for freeway networks–A model-predictive hierarchical control approach. *Transportation Research Part C: Emerging Technologies* 18, no. 3, 2010, pp. 311-331.
16. Lu, X. Y., T. Z. Qiu, R. Horowitz, A. Chow, and S. Shladover. METANET model improvement for traffic control. In *14th International IEEE Conference on Intelligent Transportation Systems, Washington, DC, USA*, 2011, pp. 2148-2153.

CHAPTER 2: DETERMINISTIC ALGORITHM FOR TRAFFIC DETECTIONING USING VIDEO SENSOR*

2.1. Introduction

Accurate detection of traffic employing various spatial and temporal sensors contributes significantly in describing and improving traffic condition. For this, video-based sensors are most appropriate over other alternatives as they provide high quality traffic information over spatial and temporal dimensions. Video sensors are based on image processing algorithms. These algorithms are involved in image extraction, processing and recording specific information. The ideal requirement of these detection algorithms is dictated by the technique and the parameters involved in analysis. In real-time context, a detection algorithm should be able to detect traffic in a variety of situations. This actually recommends that the algorithms must be robust to various challenges such as shadow, illumination variation, camouflage and noise associated with the video dataset. These challenges affect the accuracy of traffic detection resulting in over estimation or underestimation. For instance, illumination variation causes increase or decrease in the intensity of pixels, resulting in false positive or over estimation. Likewise, lower intensity of illumination causes camouflage, generating false negative or underestimation. Moreover, presence of shadow also disrupts vehicle detection and causes over estimation. Similarly, presence of camera movement induces pixel displacement from its designated position that results in over estimation. All these challenges are generated by natural phenomenon. For example, illumination variation is a natural phenomenon, which occurs gradually

* This chapter is a modified version of a published article in the Journal of Built Environment, Technology and Engineering, Vol. 1 (Sept.), 2016. Muniruzzaman, S. M., Haque, N., Rahman, F., Siam, M. R. K., Musabbir, R., Hadiuzzaman, M., Hossain, S. "Deterministic Algorithm for Traffic Detection in Free-Flow and Congestion using Video Sensor",pp.111-130.

and sometimes suddenly due to weather variation. On the contrary, camouflage depends on the color of the pavement and the vehicle. In any case, when the vehicle color is equivalent or deeper than the pavement, the video sensor faces difficulties in distinguishing traffic. Another practical requirement of the algorithm is that it should be sensitive enough to detect minor changes of traffic flow and stop-and-go situation. In fact, the algorithm should be capable of detecting fast moving, slowly moving, and stationary traffic over the roadway.

Scope of accurate and reliable detection information is that it can be adjusted to enhance incident detection framework, while distinguishing stationary vehicles, complex maneuvers (lane change, right or left turn) and acceleration or deceleration patterns that are indicative of incidents beyond the sensor's field of view (FOV) (Mandellos et al., 2011). Besides, these information can be used to conduct traffic studies, such as examining vehicle maneuvers in weaving sections or bottlenecks, detecting pedestrians (Guo et al., 2012), detecting vehicles in complex traffic scenarios (Mandellos et al., 2011) and extracting individual vehicle data (e.g. spacing, headway, velocity, acceleration), which in due course lead to better traffic flow modeling and an improved understanding of driver behavior.

Coifmanet et al. (1998) investigated vehicle detection and tracking methods and estimated traffic flow parameters from surveillance video. They developed a feature-based tracking algorithm for detecting vehicles under challenging conditions. The algorithms are robust to partial occlusion by tracking certain features of a vehicle instead of the entire vehicle. More recent vehicle detecting approaches are model-based methods that use prior knowledge to detect the desired targets (Lai et al., 2010; Shen, 2008), or deformable templates which are used when targets are matched against known vehicle models in the video frames (Takeuchi et al., 2010), or involving camera calibration and vehicle tracking (Wan et al., 2014; Pletzer et al.,

2012) proposed a robust traffic state estimation technique**,** where the algorithm is integrated on an embedded smart camera and tested in various road sections as well as illumination conditions. The experimental result shows that it performs exceedingly well for stationary traffic. Some researchers also investigated individual flow parameters and exposure such as speed (Mao et al., 2009), flow (Pan et al., 2010) and incident detection (Zou et al., 2009) employing video sensors.

Normally, for vehicle detection, most methods (Gupte et al., 2002; Hsu et al., 2004) are based on the assumption that the camera is static. Given such assumption, fore ground vehicles can be detected by image differencing between current frame and estimated background. For example, (Gupte et al. 2002) presented an algorithm where vehicles in monocular image sequences of traffic scenes are recorded by a stationary camera based on a three level processing approach such as raw images, region level, and vehicle level. For vehicle detection in urban traffic scenes, (Vargas et al. 2010) focused on background subtraction algorithm based on the sigma-delta filter. In the developed model, a reference image is considered to draw a comparison with each video frame. Consequently, this operation helps to eliminate all the stationary objects and extract foreground image of the frame. However, this method cannot cope up with shadow problems and the detection is limited to moving vehicles. Mandellos et al. (2011) proposed an algorithm to reconstruct the actual background color map without the need of any human intervention even in harsh traffic conditions, such as stop-and-go traffic flow, stationary vehicles (i.e. accident) and rain or snow. In a survey approach, (Buch et al. 2011) conducted a comprehensive review on the computer vision techniques employed in urban condition to mark the potential of different algorithms for traffic analysis.

It should be noted that to achieve the primary goal of detection, several type of image processing techniques are available in literature. However, background subtraction

(BGS) technique is the simplest and most computationally efficient among the multitude of techniques (Bouwmans, 2014). General application of BGS based video sensors for detecting vehicles commence by separating the static portion of the scene (background) from the non-static portion (foreground) while only identifying moving objects of interest (i.e. moving vehicles). However, in order to detect and measure accurate traffic flow parameters more emphasis is required to detect the presence of all the significant elements over the carriageway whether static or moving. This specific consideration of static object has not been made valid for many of the detection approaches, which consider object as a moving entity and absorbs long duration static object while in congestion into the background model.

Even with the recent advances in traffic detection technique and technology, still there are challenging issues in vehicle detection, especially when there are: (1) moving objects that merge into the background due to a temporary stop and then become foreground again, after resuming its motion; (2) rapid changes in background lighting; (3) irregular camera displacement; and (4) shadow interference. The goal of this study is to estimate traffic parameters in urban traffic environments, where complex conditions such as dense traffic flow, traffic congestions, or vehicle queues are likely to appear. For this purpose, a novel algorithm for accurate traffic detection is devised. Moreover, a set of equations are developed to estimate traffic parameters that can be readily adopted with other detection algorithms. Interestingly, most of the available methods build on addressing challenges from the image-processing point of view, making it difficult to select a particular method to be useful in traffic application. Thus, correlations between traffic parameters and algorithm evaluation parameters are established to determine the applicability of any image-processing algorithm for traffic state estimation.

2.2. Defining Traffic Detection Challenges

Before approaching towards a solution, it is important to define the problem and the underlying principles that are active in the backdrop. For instance, traffic detection operation faces real-time challenges that affect the analysis and output of an algorithm in particular. In this regard, several mechanisms are required to address specific challenges in the algorithm. Another important consideration is the computational complexity. It is plausible to solve most or all challenges at the expense of computational or automation effort. So there lies a tradeoff between an accurate detection algorithms and the computational complexity, best described by the involved parameters. Actually, the number and type of parameters used in a particular technique affect the rigor or intensity of the analysis procedure. The smaller the number of parameters involved in a methodology the simpler it becomes for analysis. For instance, the interactions of different parameters require rigorous calibration efforts since an optimized set of parameter values are required for a particular set of solution. From this elaboration, it is apparent that a more balanced algorithm is warranted where a small number of parameters are considered and all challenges are addressed accordingly. In short, an algorithm should be capable to generate highly accurate output with least computational requirement.

Table 2.1 represents a list of parameters with a goal to describe and generate solution for the relevant challenges. It is important to focus on the main parameters for the detection algorithm, which are static background and threshold value. The other parameters have been utilized to define the problem and derive a solution. Parameters used for the application of the detection algorithms in determining the traffic state parameters are explained in detail in the application section.

Table 2.1: Parameters involved in analysis and evaluation

Symbols	***Parameter Name***	***Unit***
B^*	Static background	Pixel
$B(t)$	Actual Background at time t	Pixel
$I(t)$	Frame at time t	Pixel
$d(t)$	Differential Image at time t	Pixel
$k_1(t)$	Intensity variation due to illumination change at time t	Pixel
$k_2(t)$	Intensity variation due to camera movement at time t	Pixel
$F(t)$	Intensity of vehicle at time t	Pixel
$\tau(t)$	Threshold requirement at time t	Pixel
e	Error term	Square Pixel
α	Transparency factor	N/A
$P(t)$	Vehicle Present at time t	Vehicle
$n(t)$	Number of entered vehicles at time t	Vehicle
$N(t)$	Count at time t	Vehicle
$q(t)$	Flow at time t	Veh./hour
w	Width of counting strip	Pixel
C_w	Width of a car	Pixel
A	Area of car	Sq. Pixel
L	Length of the strip	Pixel
s_i	Change in co-ordinate of vehicle	Pixel
N_j	Number of vehicles present at frame j	Vehicle
t'	Time interval between consecutive frame	Second
m	Number of frames	-

As mentioned previously, in defining the detection problem, several operations and challenges in the detection algorithms have to be outlined and defined systematically. Since complete understanding of the characteristics aids to generate a solution for individual challenges, such terms are depicted below.

i) Static background B^*: Static background relates to a specific frame, static in nature and temporal dimension. It is selected from a sequence of frames or from the mean of several frames. However, consideration of a static background is faces three challenges, such as: (1) Illumination variation $k_1(t)$; (2) Camera Displacement $k_2(t)$; and (3) Movement of permanent object. For simplicity in analysis procedure, these challenges can globally be termed as noise.

ii) Illumination variation $k_1(t)$: Illumination variation challenge is dynamic in nature and varies temporally. It is directly linked to daily sunlight variation and climatic condition (video censors cannot be used in rainy period and also at night). It attempts to increase or decrease the intensity of a pixel at a certain position with sunlight variation, causing gradual or sudden change in illumination intensity.

iii) Camera displacement $k_2(t)$: The complexity imparted by camera displacement is also dynamic in nature and the occurrence is more uncertain than illumination variation. It is caused due to wind action over the video sensor and other unwanted vibrations. This particular phenomenon displaces image details from its actual position, inducing intensity variation on both pixels origination and destination.

iv) Frame $I(t)$: Frame is a major element of the video and contains all of the information within a field of vision. Frames reside in a video as a static image with particular time signature. They are given certain frame numbers according to the time, when those were captured i.e. 20^{th} frame indicates that the frame has been captured after 19^{th}. This allocation of a frame number depends on the FPS (Frames per second) of a video. However, the FPS of the video depends on the capturing capacity of the camera. Frame consists of pixels; whereas pixels follow a certain structure. Moreover, this structure depends on color channels. Color channels can be of different types i.e. Grayscale, RGB (Red-Green-Blue), CMYK (cyan-magenta-yellow-black), HSV (Hue Saturation value). RGB and grayscale color channels are the most widely used color channel modes. In a particular pixel position, there is respectively 3 and 1 representative numerical value for RGB and grayscale frame. Hence, the number of numerical values depends on the type of color channel. Furthermore, the numerical values corresponding to the pixels are known as pixel intensity. This intensity varies from 0 to 255. 0 stands for the

minimum intensity and 255 for the maximum intensity. Pixels occupy a particular position in a frame and are uniformly distributed along the width and height of the frame maintaining a constant spacing. This spacing is controlled by the visual capacity of the camera. The resolution of frame depends on the number of pixels exist with a frame. If the number of total pixels within a frame is divided by 10^6, the estimate of megapixel unit can be obtained easily.

v) Actual background $B(t)$: Dynamic background contains all information of the current frame except traffic.

Since detection approach focuses on traffic, permanent object movement within the study area can be neglected. Otherwise, the permanent object will act as traffic and the distinction between traffic and permanent object will become invalid.

Considering illumination variation and camera displacement, actual background $B(t)$ can be expressed as $B(t) = B^* + k_1(t) + k_2(t)$. Any frame at time t, $I(t)$ consists of the actual background model at time t, $B(t)$ and intensity of traffic at time t, $F(t)$. The parameter $I(t) = B^* + k_1(t) + k_2(t) + F(t)$, represents a pixel in a frame or the entire pixels of the frame. For the latter one, the parameters act as a 2D matrix for single color channel and 3D matrix for RGB or CMYK color channel.

The differential image $d(t) = I(t) - B(t)$ is obtained from the simple subtraction operation. However, large uncertainty associated with obtaining actual background may limit the availability of $B(t)$. For this, B^* can be adopted instead of $B(t)$ resulting in the expression $d(t) = I(t) - B^*$. Then the traffic extracted can be expressed as, $F(t) = d(t) - k_1(t) - k_2(t)$.The magnitude of $F(t)$ can be both positive and negative, whereas the other parameters are non-negative integers varying from 0 to 255. When the background will have a higher intensity than the respective frame, the traffic

intensity will become negative. Such phenomenon is common when a black colored car travels over the pavement.

In case when the noises due to $k_1(t)$ and $k_2(t)$ become zero, the differential image would result in traffic image. However, this condition will never prevail because of the static background. The resulting traffic image promotes the need of a threshold value $\tau(t)$, the baseline intensity above which the differential image will be considered as traffic. This threshold $\tau(t)$ filters the noises from $d(t)$ and extracts the traffic from the differential image. The threshold requirement depends upon the magnitude of noise; where, the higher intensity of noise requires the increased threshold value. Therefore, $\tau(t)$ can be expressed as a function of noises, such as $\tau(t) = k_1(t) + k_2(t) = f(k_1, k_2)$. Likewise, object in the field of view will be detected as, $F(t) = d(t) - \tau(t)$ when $d(t) \geq \tau(t)$; and $F(t) = 0$ for other considerations. The intensity of the traffic $F(t)$ largely depends upon the selection of the threshold value $\tau(t)$. In fact, a higher threshold value can eliminate the object. On the contrary, the underestimation of threshold value may allow ingression of noise within the detected traffic. For example, when the threshold value $\tau(t)$ increases, severe noises from the image are eliminated. Consequently, the possibility of eliminating the object escalates, especially for $\tau(t) > d(t)$. Therefore the threshold level should be adjusted as minimum as possible towards zero. Understandably, to minimize the effect of noise $d(t)$ must be equal to $F(t)$ and this condition will be fulfilled when $\tau(t)$ becomes zero.

2.3. Appropriate Technique to Address Detection Challenges

A multitude of detection technique involving background subtraction can be found where detection is achieved through methods, such as parametric probabilistic background model (e.g. Gaussian Mixtures Models (GMM)) for each background pixel (Stauffer and Grimson, 1999, Vargas et al., 2010, Zivkovic and Heijden, 2006)

by background reconstruction (Mandellos et al., 2011) by determining the optimal threshold for foreground–background segmentation and object detection (Karasulu and Korukoglu, 2012). Among the stated methods, GMM methodology models each pixel history as a cluster of Gaussian type distributions and uses an on-line approximation to update its parameters. Accordingly, the background is found as the expected value of the distribution corresponding to the most populated cluster (Stauffer and Grimson, 1999). This method is able to tackle low illumination variations whereas rapid variations of illumination and shadows still remain difficult. Furthermore, the learning stage can be inefficient if it is realigned with noisy video frames (Sobral and Vacavant, 2014). Addressing such difficulties, previous GMM methodology is greatly improved on grounds of performance by considering recursive equations to adaptively update the parameters of the Gaussian model (Zivkovic and Heijden, 2006).

In effect, parametric models are tightly coupled with underlying assumptions. They occasionally deviate from conforming to the real data. Moreover, the choice of parameters can be cumbersome, increasing research effort and reducing automation. On the contrary, nonparametric models are more flexible while intensely data oriented. In this regard, Pixel Based Adaptive Segmenter (PBAS) provides a better solution being a nonparametric model. In this technique, multitude of tunable parameters is adaptively adjusted for each pixel separately during runtime for optimal algorithms performance. In this approach, two per-pixel thresholds such as decision threshold and learning parameter are dynamically changed based on an estimate of the background dynamics. However, the method requires extensive tuning while detecting moving objects stopped suddenly, sudden light changes, cast shadows, and moving trees or dynamic background. Another established nonparametric algorithm is Kernel Density Estimation (KDE). It attempts to solve the problem relating to the

presence of a dynamic scene with fast variations or non-stationary properties, where the background cannot be modeled accurately with a set of Gaussians. It tackles the problem by estimating background probabilities at each pixel from many recent samples using KDE (Elgammal et al., 2000).

Another simple yet powerful non-linear background subtraction technique is sigma-delta background estimation (Manzanera and Richefeu, 2007). It consists of incrementing or decrementing the current background estimate by a constant value if it is smaller or greater than the current analyzing frame. The limitations remain in its uni-modal nature which are: (1) one single mode in the density model is inefficient to discriminate moving objects over a complicated background, and (2) one single dispersion estimate, related to one time constant, is not sufficient for certain kind of motion such as remote objects with radial velocity with respect to the optical center.

An algorithm is best described as: (a) variables with known fixed values and connected by a known equation that is deterministic; or (b) variables with random values and connected by a known or unknown equation that is probabilistic. In fact, Deterministic approaches develop systems that are perfectly predictable. Such approaches follow established laws, equations or fixed procedures so that the state of each component and of the entire algorithms can be determined at any time for any time in the past and future. For statistical approach, rules can be derived from a large number of similar events based on experience where directly applicable observations can be transferred to the algorithms or to the event level. On the contrary, probabilistic algorithms involve a degree of uncertainty in predicting behavior and require “random variables” to describe a particular system’s components and their interactions. Moreover, there is no general consensus on the actual meaning of “randomness” of a particular algorithm. For example, randomness could mean generated by chance mechanism, being unpredictable, showing a lack of an apparent

order, etc. Any engineered intervention or an innovative solution should adhere to deterministic approach prior to the path of probabilistic solution since deterministic solution grows over the potential formulations and measures the actual condition to determine the performance of an algorithm. While probabilistic method is apart from deterministic solution, it offers flexibility to address different challenges during analysis such as occlusion, shadow, noise, and camouflage. Generally, probabilistic models (parametric or nonparametric) are robust against rain, snow, sleet, hail, and overcast and handles sensitive motion from swaying branches, rippling water, noise. They also perform under day and night condition. However, they face difficulty in detecting long shadow, object overlapping (object closely spaced from one another) and lighting changes. Moreover, they suffer from errors such as ghost phenomenon that arises when the object remains static for a long duration over time-space dimension, resulting in overestimation. This particular phenomenon governs while the signal timing is more than usual or in congested scenario. Generally probabilistic background models based on greatest occurrence of background pixels in the image sequence, fail to detect such stationary vehicle. Because the stationary vehicle is stored as a part of the image sequence rather than a distinct object, the pixels belonging to an object become the part of the background that consequently eliminates the detected object in the binary image regardless of the opted threshold value.

This study presents a new background subtraction algorithm for detecting vehicles in both moving and stop-and-go situation. In this algorithm, deterministic analytical approach has been adopted instead of conventional probabilistic approach. From the benchmark provided by BMC (Background Models Challenge), a set of four methods are extracted that clearly overtake the existing ones (Sobral and Vacavant, 2014) to test the performance. Quantitative and qualitative analysis of the proposed algorithm

are performed with respect to Kernel Density Estimation (KDE), Gaussian Mixture Model (GMM), Pixel-Based Adaptive Segmenter (PBAS) and Sigma-Delta.

2.4. Solving the Detection Problem: Analytical Approach

In order to derive an analytical solution to the defined challenges of traffic detection, $\tau(t)$ can be taken as τ. Because $\tau = f(k_1, k_2)$ can be written as $\tau = k(t)$ considering the influence of noises (k_1, k_2) upon threshold as they cannot be separated easily. Accordingly, to ensure $\tau = 0$, $k(t)$ corresponds to 0. At this instant, $k(t)$ can only be determined if the actual background $B(t)$ at time t is known,

$$k(t) = B(t) - B^* \tag{1}$$

where, $k(t)$ represents the difference between a static frame and a dynamic frame. The subtracted value can be both positive and negative. For example, when a comparison is drawn between day background and night background, the value of $k(t)$ will be negative. Similarly, when camera displacement causes a pixel to be replaced by a lower intensity value after background selection, $k(t)$ will be negative. On the contrary, when camera displacement causes a pixel to be replaced by a higher intensity value after background selection, $k(t)$ will be positive.

Since acquisition of $B(t)$ involves controlled environment, which may not be feasible in many urban scenarios $I(t)$ can be preferred instead of $B(t)$, where $B(t) \in I(t)$; $B(t) \subset I(t)$). The relationship between $I(t)$ and (B^*), considering $k(t) = 0$ and $k(t) = B(t) - B^*$ is outlined as follows.

$$I(t)^2 + (B^*)^2 = 2I(t)B^* \tag{2}$$

When the equation is true, noise will be eliminated or vice-versa. Because, $B^* = I(t) - k(t) - F(t)$, the Equation *(2)* can be rewritten as follows.

$$I(t)^2 + I(t)^2 + k(t)^2 + F(t)^2 - 2k(t)I(t) - 2F(t)I(t) + 2k(t)F(t) = 2I(t)B^* \quad (3)$$

In Equation (3), the product has been expressed using $I(t)$, $k(t)$ and $F(t)$ eliminating the user-defined parameter B^*. Considering Equation (3), an error term e can be outlined from Equation (2) such that, $e = e(t) = k(t)^2 + F(t)^2 - 2k(t)I(t) - 2F(t)I(t) + 2k(t)F(t)$. Depending upon the interlaced relationship of the parameters ($F(t)$, $k(t)$ and $I(t)$) in the error term, it can be defined as e where, $F(t)$ and $k(t)$ is far less than $I(t)$; $k(t)I(t)$ and $F(t)I(t)$ are greater than. $k(t)^2 + F(t)^2 + 2k(t)F(t)$

$$e = \begin{cases} 0, if\ I(t) = B^* \\ <0, if\ I(t) \neq B^* \end{cases}$$

Therefore, Equation (3) can be rewritten as,

$$\sqrt{I(t)B^*} = I(t)\sqrt{1 + \frac{e}{2I(t)^2}} = I(t)\sqrt{1 - \frac{|e|}{2I(t)^2}} \quad (4)$$

Considering a factor α, ($\alpha = \sqrt{1 - \frac{1}{2}\frac{|e|}{I(t)^2}}$) termed as transparency factor, Equation (4) is transformed as,

$$\sqrt{I(t)B^*} = \alpha I(t) \quad (5)$$

Experimental tests show that, the value of α for an entire 2-dimensional frame varies from 1 to 1.154. So the value of α can be taken as 1. Thus, the Equation becomes $I(t) \approx \sqrt{I(t)B^*}$, which gives rise to a new frame equivalent to the actual frame with lower noise intensity. Consequently, when this equivalent frame is used instead of the actual frame, noise is minimized. Subsequently, minimum threshold value is achieved. In terms of operation and outcome, Equation (5) is referred to as current frame correction since it only applies correction over the frame while recording all the

traffic details. Thus, the induced transparency of vehicles in the field of view is termed as 'Transparency Effect' as detailed in Equation (5).

2.5. Methodology

Particular methodology of this study is outlined in Figure 2.1, which contains the important steps for the developed algorithm. Firstly, a background is selected from the video sequence without any traffic. Then, each video frame is passed through the frame correction technique according to Equation (5) and the differential image is obtained by subtracting the background from the corrected frame. After this, a vehicle image is obtained using a threshold. This image is then converted to a binary image using the same threshold to obtain a machine-readable content. Binary image, $b(t)$ means that if the pixel intensity in differential image is greater than a particular threshold, then the value in the binary image corresponding to that pixel is one and otherwise zero.

$$\left.\begin{aligned} b(t) &= 1,\ if\ \ d(t) \geq \tau(t) \\ &= 0,\ otherwise \end{aligned}\right\} \tag{6}$$

For the proposed algorithm, there are two parameter inputs: (1) static background; and (2) threshold value. Static background represents a frame without any vehicle in the field of view (FOV). Threshold value represents the intensity above which the difference is to be considered as traffic and has a range between 0 to 1. Otherwise, vehicles in the FOV will be eliminated. For this method, a threshold value of 0 to 0.15 is recommended.

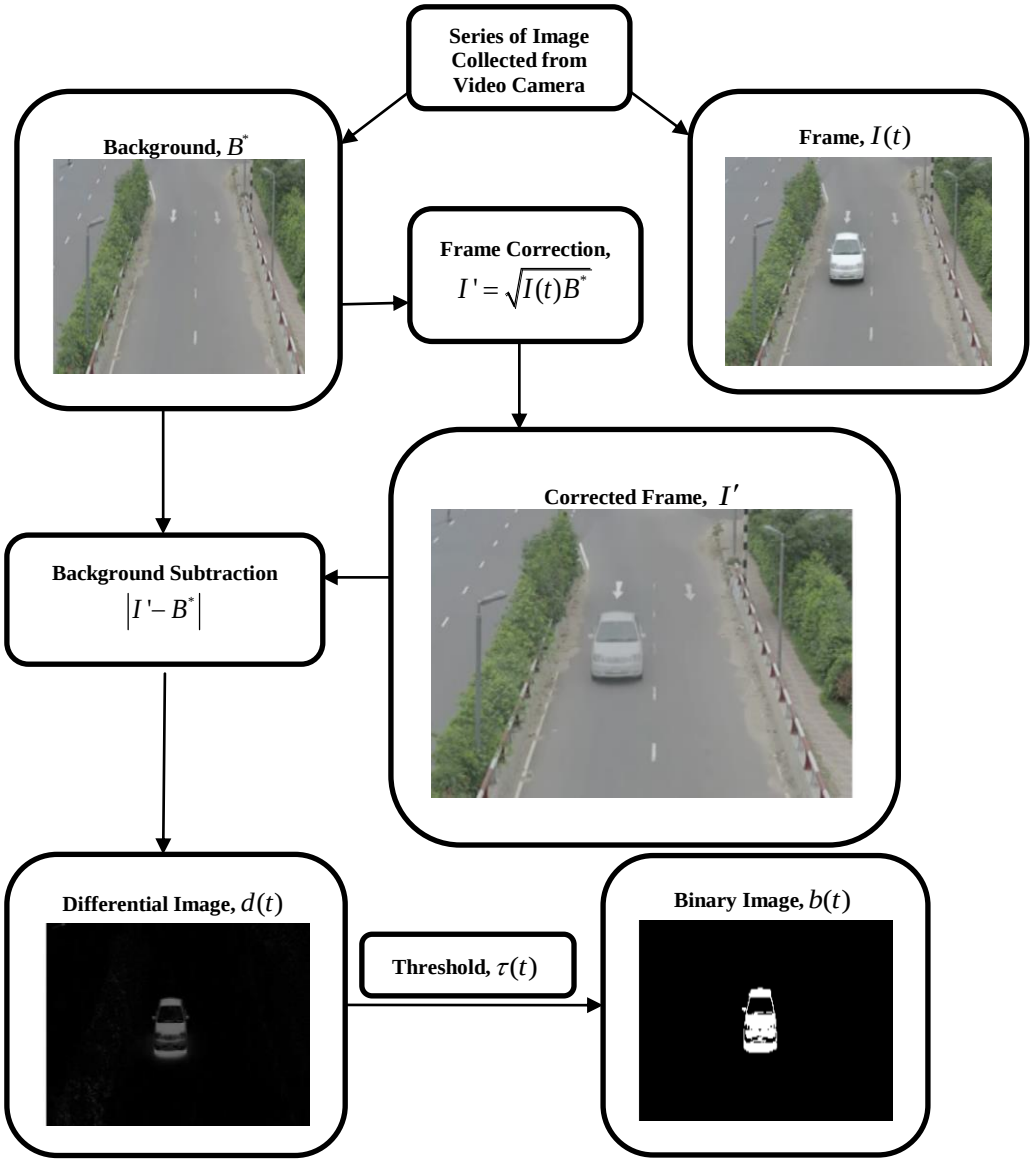

Figure 2.1: Synthesis of frame correction, static background and threshold steps of the proposed algorithm.

2.6. Data Collection

2.6.1. Field Data

2.6.1.1. The study site

The study area is located in the Tongi Diversion Road, a section of the Dhaka-Mymensingh Highway (N3) (Figure 2 .2). It is an 8-lane major arterial road in Dhaka city. The selected 3.26 km long uninterrupted section has one off-ramp, closely followed by an on-ramp. These form one diverge and one merge sections along the

corridor. There are exactly 4 through lanes on each direction of the test site totaling up to a width of 14.48 m to 14.94 m in different links. The on and off ramps have two lanes each, though lane discipline is absent in the main stream flow and in the ramp flows. The test section experiences a directional average annual daily traffic (AADT) of about 11451 vehicles. The traffic stream consists of 40% cars, 12% microbuses or jeeps, 10% motorcycles, 8% buses, 10% utility vehicles and 20% auto-rickshaws. Such geometric and traffic characteristics make the test site an ideal study location for non-lane-based heterogeneous uninterrupted traffic condition.

2.6.1.2. Methodology for data collection

The study site is divided into five links with the lengths varying from 320 m to 920 m as shown in Figure 2.2. The off-ramp is located at the end of link 2 and the on-ramp is located at the beginning of link 3. Five video cameras are installed along the mainline, one at approximately mid-length of each link. The data obtained from each camera is considered representative of the traffic condition of the whole link. The ramps are also equipped with video cameras for collecting data of the merging and diverging traffic. The approximate locations of the cameras are also indicated in Figure 2.2 whereas the details of each camera location can be found in Figure 2.3.

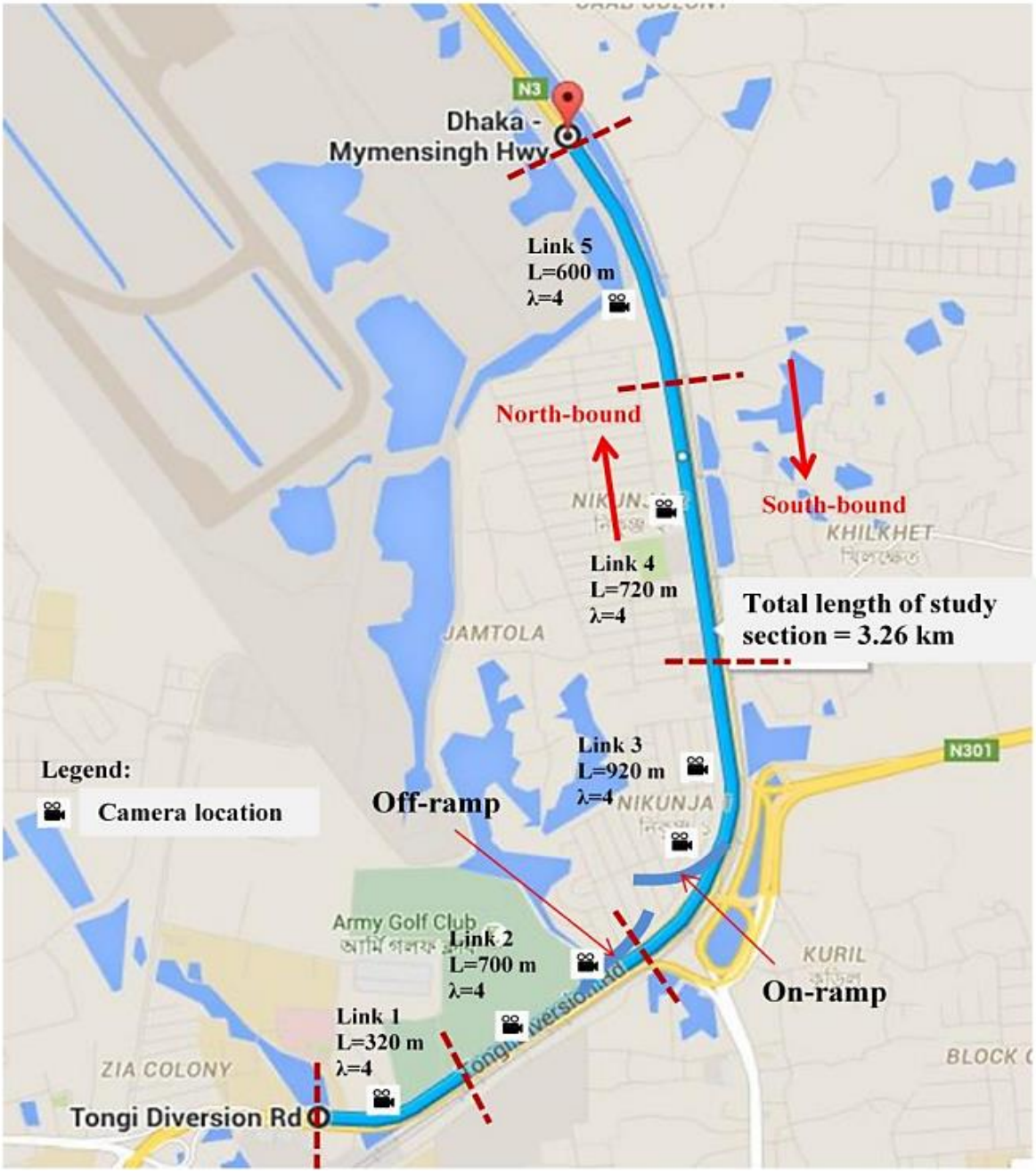

Figure 2.2: Detail layout of the study area.

Although the non-lane-based heterogeneous behavior becomes more acute with the increase of traffic volume in the roadway, the test site was videoed from 3:00 PM to 6:00 PM covering both peak and off-peak periods. Two sets of videos were collected for the same time period on 15th and 16th April, 2015. These videos were processed

and the extracted data was filtered for anomalies. To ensure better quality of the collected data, the camera height and angle of projection were strictly maintained.

(a) Camera location on Link 1

(b) Camera location on Link 2

(c) Camera location on Link 3

(d) Camera location on Link 3 (close-up)

(e) Camera location on Link 4

(f) Camera location on Link 5

(g) Camera on off-ramp (above); Field of vision of the camera (below)

(h) Camera location on on-ramp showing details of the data collection process

Figure 2.3: Cameral location on various spots.

As shown in Figure 2.3 (h), the mounting heights of the cameras were at least 20ft to reduce the object details detected by the image processing algorithm and the camera angle was less than 45 degrees to avoid perception problem. However, the angle was not so small as to cause restriction in vision. Due to the absence of suitable vantage points meeting such requirements in links 1, 2, 4 and the on-ramp location, cranes were used for mounting the cameras at the required height for a period of 3 consecutive hours each day. The presence of foot over bridges of sufficient height in

links 3 and 5 and on the off-ramp location allowed the data collection process to be carried out without the use of cranes.

2.6.2. Video Sequence

In order to evaluate the developed detection algorithms for free-flow and stop-and-go situation, two types of video sequence is considered: (1) synthetic, and (2) real-time.

- The synthetic video sequence is generated considering illumination variation, and camera displacement analogous to urban condition. For illumination variation, gradual and irregular sudden variation is adopted to simulate daylight variation and cloudy/rainy weather, respectively. Camera displacement is simulated by contrasting the pixel positions by 10% of the frame size in horizontal direction. It is done by replacing the coordinates of the pixel (x_t, y_t) with the $(x_t + \frac{B}{10}, y_t)$ at a certain time t, where B indicates the width of the frame.
- The real-time video sequence represents actual detection challenges, such as shadow interference, illumination variation and camera displacement. Moreover, high quality video data set is collected to determine the accuracy of different techniques in actual condition.

In this study, ground truth relates to actual data measured from both type of video sequences. Particularly for the synthetic video, one ground-truth frame for each frame is considered, which corresponds to a sampling rate of 25-frames/second. Following this step, 1400 frames are labeled manually for ground truth extraction task. This task involves two important operations: (1) removal of noise, and (2) filling up of voids. For instance, in the synthetic video, background is considered as a frame with no object, a complete black frame to be particular. Then, this background is subtracted from the synthetic video. The noises and the voids generated from this subtraction process are removed and filled up, respectively.

2.7. Effect of Frame Correction

In this section, the effect of frame correction is outlined in detail. Frame correction is applied for noise reduction. It should be noted that a large set of frames is a prerequisite to observe the effect of the frame correction. For this reason, the analysis is performed over a sample containing 9000 frames from the real video dataset. The actual condition is represented in Figure 2.4 (a-b) where, (a) represents an arbitrary frame from the sample and (b) shows the effect after the application of frame correction. Interestingly, the vehicles over the carriageway became transparent and other features such as lane markings achieved visibility through the vehicles. Such condition emphasize that noises have also gone through the same effect since they have smaller pixel intensity than the vehicles.

The effect of such correction is explained through a qualitative comparison between the application of frame correction and without frame correction. Figure 2.4(c) illustrates the threshold requirement in a static background with and without frame correction. This shows that the sample frames go through a scale down effect. Both curves are analogous in shape; curve has lower amplitude than the former one and shifts downward. This shift eliminates noises and the amplitude reduction makes the impact of noise smaller in the differential image.

2.8. Experimental Analysis

This section outlines the comparison of state of art algorithms namely KDE, GMM, PBAS and Sigma-Delta with our proposed algorithm in various test situations. The experimental analyses for the proposed algorithm are carried out in two ways: (1) qualitative analysis; and (b) quantitative analysis. Different parameter values involved in evaluation measures are elaborated in Table 2.2.

(a) (b)

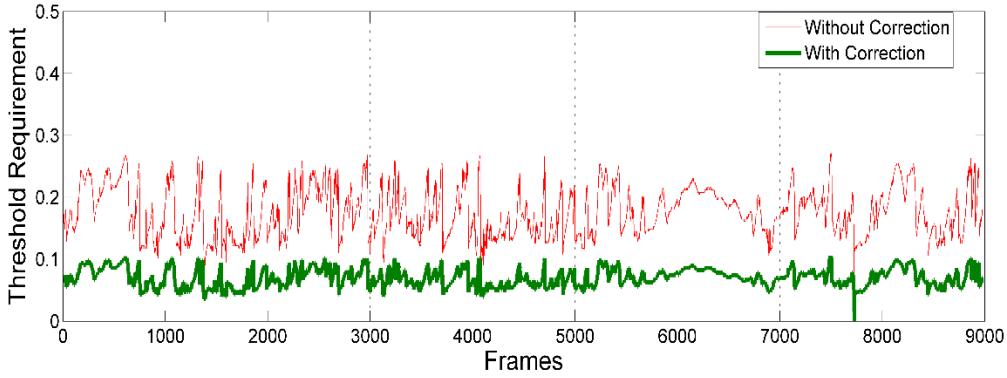

(c)

Figure 2.4: Frame correction technique; (a) real-time test frame; (b) real-time transparency effect; (c) threshold requirement with and without frame correction.

Table 2.2: Different parameter values involved in evaluation measures (Sobral, 2014)

Algorithm	
Parameter	**Value**
KDE	
Sequence Length	50
Time Window Size	100
SD Estimation Flag	Yes
Normalized RGB	Yes
Probability threshold	10e-8
suppress shadow rate	0.3
Binary threshold	0.15
GMM	
fading factor	0.05
Binary threshold	0.15
PBAS	
(default Parameter values)	
Sigma Delta	
(default Parameter values)	
Proposed Algorithm	
Static background	Located at 1st frame
Binary threshold	0

2.8.1. Qualitative analysis

In this subsection, the visual quality or perception of a binary image of the developed algorithm in comparison to other techniques is illustrated for different challenges such as illumination variation, camera displacement and shadow.

2.8.1.1. Illumination variation

In this experimental analysis a synthetic video data set is used to simulate the gradual and sudden illumination variation conditions. The actual frame of the synthetic dataset contains three yellow colored rectangular vehicles. The analysis illustrates that the proposed algorithm and PBAS outperforms KDE, GMM and Sigma-Delta. This particular result of KDE, GMM and Sigma-Delta can be attributed to noise surrounding the vehicle.

2.8.1.2. Camera displacement

The second experimental analysis sequence is based on the performance of several techniques in camera displacement condition. Interestingly, the road marking in the synthetic sequence is detected as an object due to camera displacement. Analysis of different algorithms shows that the lane markings are identified as individual objects, where the proposed algorithm performs better than others.

2.8.1.3. Shadow interference

In this experimental analysis, a synthetic video sequence is used to simulate the shadow condition. The qualitative analysis of different techniques shows the performance on eliminating shadow. For better representation, frame from real video dataset is used, where only the sigma delta algorithm failed to eliminate the shadow.

2.8.1.4. Stationary vehicle detection

In this experimental analysis, the ‘stationary vehicle’ sequence has been used to see the effect of stationary vehicle over the different algorithm. Figure 2.5 illustrates the

binary image produced by different algorithms for a stationary vehicle. The result shows that only KDE and proposed algorithm have successfully detected the vehicle.

2.8.1.5. Real-time video dataset

The previous analysis was done over the synthetic videos to see the performance in various controlled situations. This subsection outlines the performance analysis of different algorithms over the real-time video dataset. To see the performance, three types of situation are selected: 'Empty road', 'Slowly moving traffic' and 'Congestion'.

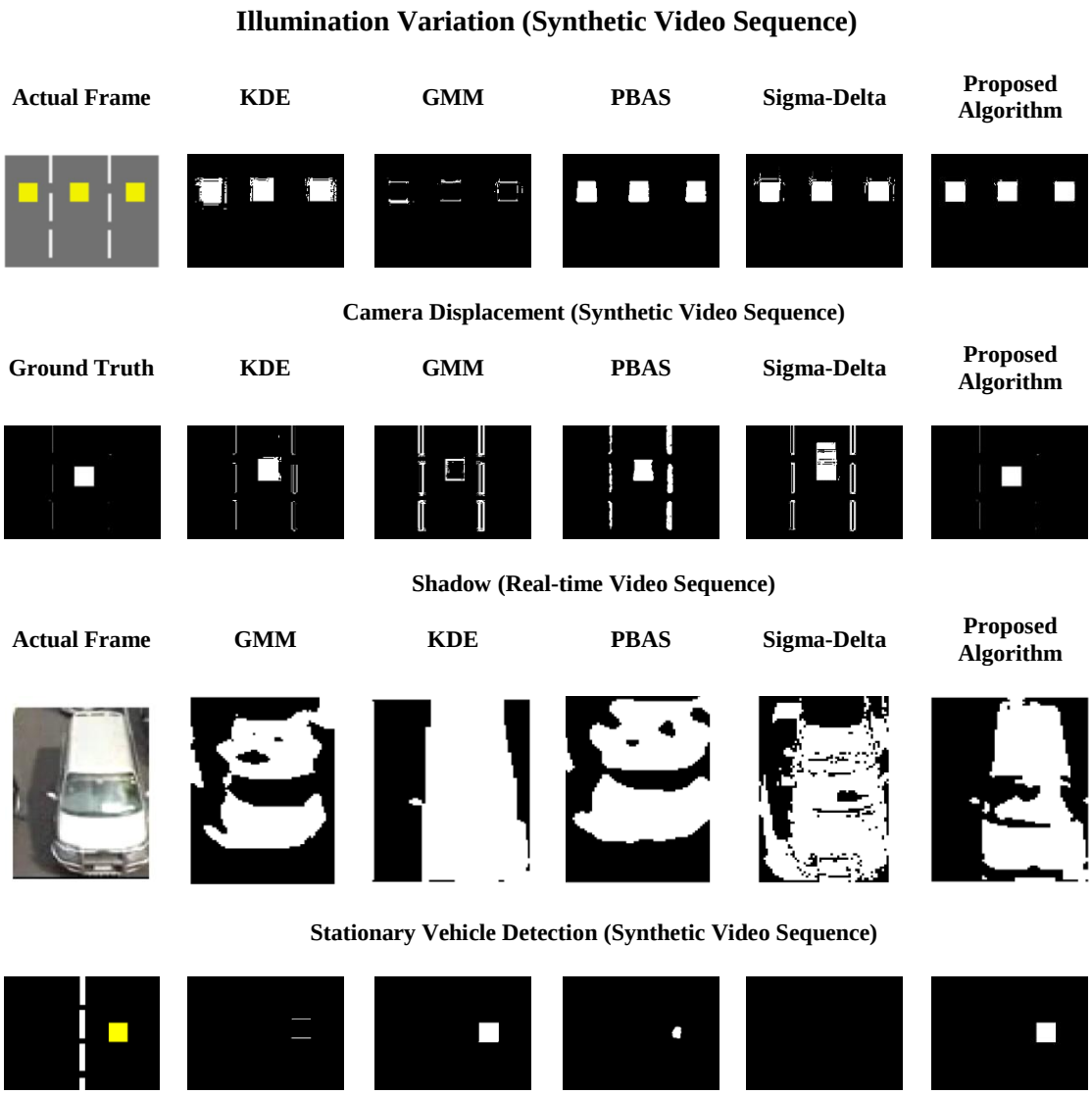

Figure 2.5: Qualitative comparisons of video frames in illumination variation, camera displacement, shadow, and stationary vehicle detection.

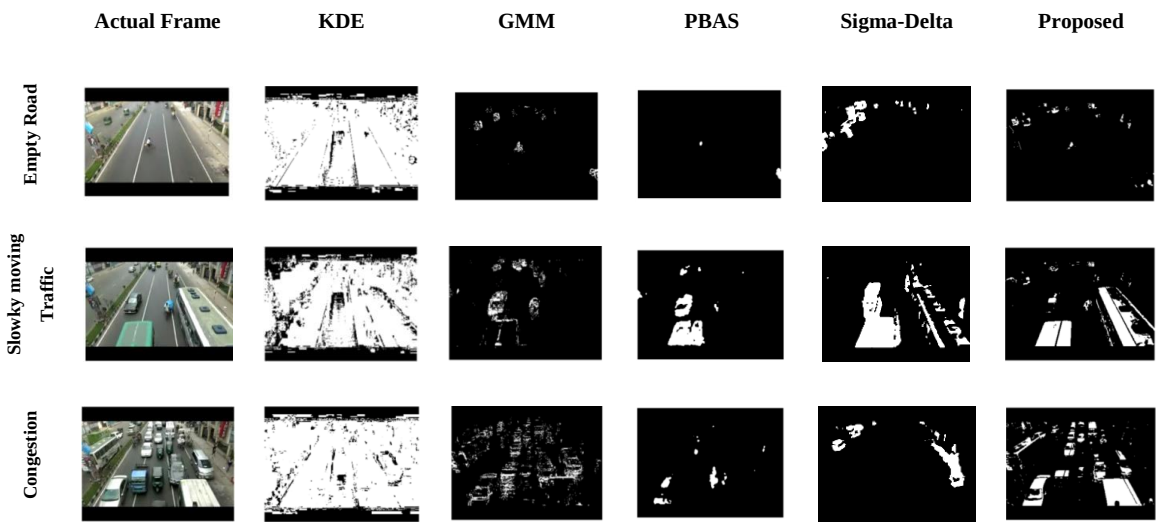

Figure 2.6: Qualitative comparisons of real video frames in empty road, slowly moving traffic and congestion situation.

Figure 2.6 illustrates qualitative comparison of real video Frames for different algorithms. Table 2.3 explains the performance of different algorithms over these situations. The result shows that the proposed algorithm outperforms other methods.

2.8.2. Quantitative analysis

In this subsection, the quantitative analysis of different algorithms (GMM, PBAS, KDE and Sigma-Delta) with respect to the proposed algorithm is outlined in detail. Generally, an algorithm labels sample frame as either positive or negative in a binary decision problem. In this study, samples are considered as pixel values in binary image, where “positive” represents foreground object pixel, and “negative” represents background pixel. In this study two classes of image (foreground and background) are used for analysis. For a given frame in a video sequence a comparison can be drawn between the resultant image and the ground truth image. A pixel is denoted as white when it is a part of an object in the foreground, and black when it actually belongs to the background. To quantify the classification performance, with respect to ground-truth, four basic measures are used, such as (1) true positives (TP): correctly classified

foreground pixels; (2) true negatives (TN): correctly classified background pixels; (3) false positives (FP): incorrectly classified foreground pixels; and (4) false negatives (FN): incorrectly classified background pixels.

Table 2.3: Description of qualitative evaluation of real video frames

Method	Empty Road	Slowly Moving Vehicle	Congestion
KDE	Frame is filled with FP pixels resulting in overestimation.	Accuracy is highly reduced as the frame is filled with FP pixels causing overestimation.	Accuracy is highly reduced for FP pixels in the frame, causing overestimation.
GMM	Can detect small vehicles and there is no impression of FP. FN is higher as the algorithm is unable to detect full details of a vehicle.	Can detect slowly moving traffic and there is no impression of FP. However, the detection accuracy is highly affected by FN since the vehicle is absorbed into the background for stop-and-go situation.	Can detect moving vehicles. However, unable to detect stationary vehicles.
PBAS	Cannot detect small vehicles and there is no impression of FP. However, FN is higher as the algorithm cannot detect the full details of the vehicle accurately.	Can detect slowly moving traffic and there is no impression of FP. However, the detection accuracy is highly affected by FN since vehicles are absorbed in the background for stop-and-go situation.	Cannot detect stationary vehicles as well as moving vehicles.
Sigma-Delta	Can detect small vehicles and suffers least amount of FP and FN. Whereas the detected vehicles are well-defined binary object.	Can detect slowly moving traffic and there is no impression of FP. However, the detection accuracy is highly affected by FN since vehicles are absorbed into the background for stop-and-go situation.	Cannot detect stationary vehicles as well as moving vehicles.
Proposed Algorithm	Can detect large as well as small vehicles and suffers least amount of FP and FN. The detected traffics are well-defined binary object.	Can detect slowly moving vehicles.	Can detect stationary vehicles. However, few vehicles are absorbed into the background due to presence of FN.

FP – False Positive (Overestimation)
FN – False Negative (Underestimation)
GMM – Gaussian Mixture Model

ROC curves represent the variation of the number of incorrectly classified examples with the number of correctly classified positive examples (TPR versus FPR) as given by,

$$TPR = \frac{TP}{TP + FN}\ ;\ FPR = \frac{FP}{FP + TN}\ ;\ \text{and}\ \ FNR = \frac{FN}{FN + TP}$$

However, PR curves are a good alternative since ROC curves have the risk of providing an optimistic appraisal of the classifier's performance when there is a significant skew in the class distribution (Davis and Goadrich, 2006). Moreover, PR curves may display differences between the algorithms behavior that are not visible in the ROC curves. PR curves are assembled from the following metrics:

$$\text{Precision} = \frac{TP}{TP + FP}\ ;\ \text{Recall} = \frac{TP}{TP + FN}\ ;\ \text{and}\ \ \text{Specificity} = \frac{TN}{FP + TN}$$

With a goal to obtain more handy metrics, particularly in the form of scalar measures, the area under the ROC or PR curves can be utilized. Other measures for fitness quantification, in the context of background subtraction techniques, have been proposed in the literature (Ilyas et al., 2009; Rosin and Ioannidis, 2003; White and Shah, 2007) such as F-measure (F), Percentage of Correct Classification (PCC), Jaccard Coefficient (J), etc.

$$\left.\begin{aligned} F &= 2\left(\frac{PR.RE}{PR + RE}\right),\ (0 \le F \le 1) \\ PCC &= \frac{TP + TN}{TP + FN + FP + TN} \\ J &= \frac{TP}{TP + FN + FP};\ (0 \le J \le 1) \\ Y &= \frac{TP}{TP + FP} + \frac{TN}{TN + FN} - 1;\quad (-1 \le Y \le 1) \end{aligned}\right\} \tag{7}$$

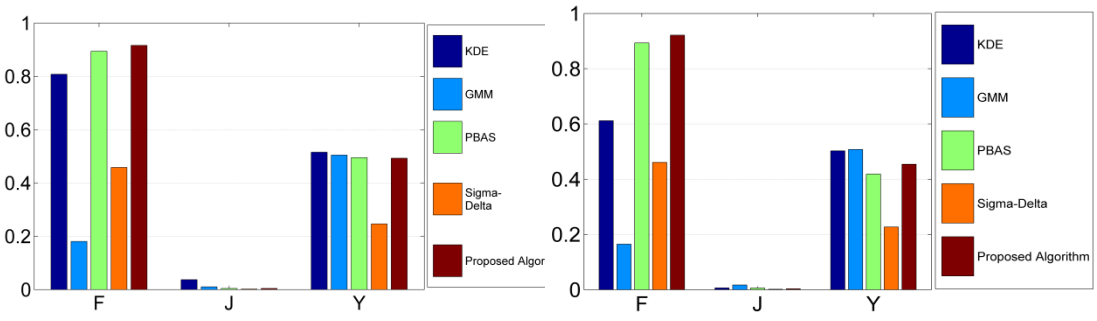

(a) (b)

Figure 2.7: Evaluation measures for moving (a) and stationary (b) vehicle sequence.

F-measure (*F*) combines precision and recall in the form of their harmonic mean, providing an index that is more representative than the pure PR and RE measures themselves. PCC is the percentage of correct classification alone, commonly used for assessing a classifier's performance. However, it can also give misleading estimates for a significant skew in the class distribution (Rosin and Ioannidis, 2003).

Yule coefficient (*Y*) is particularly defined on the interval [-1, 1]. The lower limit of this interval occurs when there are no matching pixels, whereas the coefficient would hit the upper bound for a perfect match. The following index set is considered as a valuable quantification of relative performance of each algorithm: $S = \{F, J, 0.5\,(1+Y)\}$. The set includes fitness coefficients with an ideal value equal to 1. Evaluation measures for moving and stationary vehicle sequence are presented in Figure 2.7. In Table 2.4, quantitative results for moving and stationary vehicle sequence are discussed in detail.

The main concept of evaluating algorithms using a constant threshold is to illustrate the stability of each algorithm. In this context, the clustering of points in one position represents more stability whereas scattered points represent that a particular algorithm fails to maintain its stability for a constant threshold. Furthermore, clustering of points at the upper right corner of Precision-Recall plot represent that algorithm is efficient in detection. Precision-recall relationship is illustrated in the Figure 2.8. Results of

false negative rate against time are presented in Figure 2.9. Figure 2.9(f) illustrates the applied speed variation in the synthetic video to see the behavior of various algorithms in stop-and-go situation. The upward shift of the FNR curve represents the inability of traffic detection at stationary condition. Table 2.5 outlines the description of quantitative analysis of different algorithms.

Table 2.4: Quantitative result for moving and stationary vehicle sequence

Evaluation Measures		KDE	GMM	PBAS	Sigma-Delta	Proposed
Moving Vehicle Sequence						
Precision	μ	0.673	0.584	0.924	0.719	0.935
	σ	0.016	0.014	0.021	0.016	0.01
Recall	μ	0.966	0.113	0.86	0.885	0.906
	σ	0.001	0.007	0.005	0.001	0.004
Specificity	μ	0.973	0.99	0.996	0.983	0.995
	σ	0.0005	0.0002	0.0001	0.0003	0.0001
PCC	μ	0.974	0.94	0.988	0.978	0.992
	σ	0.0005	0.0013	0.0002	0.0005	0.0001
F	μ	0.789	0.18	0.893	0.38	0.916
	σ	0.007	0.006	0.009	0.013	0.008
J	μ	0.027	0.01	0.004	0.01	0.004
	σ	0.0001	0.0002	0.0001	0.016	0
Y	μ	-0.056	0.009	-0.009	0.0.42	-0.014
	σ	0.022	0.0004	0	0.017	0
Stationary Vehicle Sequence						
Precision	μ	0.539	0.571	0.85	0.526	0.884
	σ	0.017	0.013	0.022	0.015	0.023
Recall	μ	0.08	0.51	0.949	0.61	0.952
	σ	0.01	0.004	0.0003	0.0063	0.001
Specificity	μ	0.991	0.993	0.995	0.989	0.998
	σ	0.0002	0.0002	0.0001	0.0003	0.00005
PCC	μ	0.975	0.978	0.995	0.983	0.997
	σ	0.0006	0.0005	0.0001	0.0004	0.00007
F	μ	0.164	0.597	0.893	0.583	0.921
	σ	0.01	0.003	0.003	0.01	0.002
J	μ	0.017	0.006	0.006	0.0015	0.003
	σ	0.0008	0.0001	0.001	0.0004	0
Y	μ	0.014	0.007	-0.163	-0.006	-0.092
	σ	0.0006	0.0002	0.0005	0.0003	0.024

μ = mean

σ = **standard deviation**

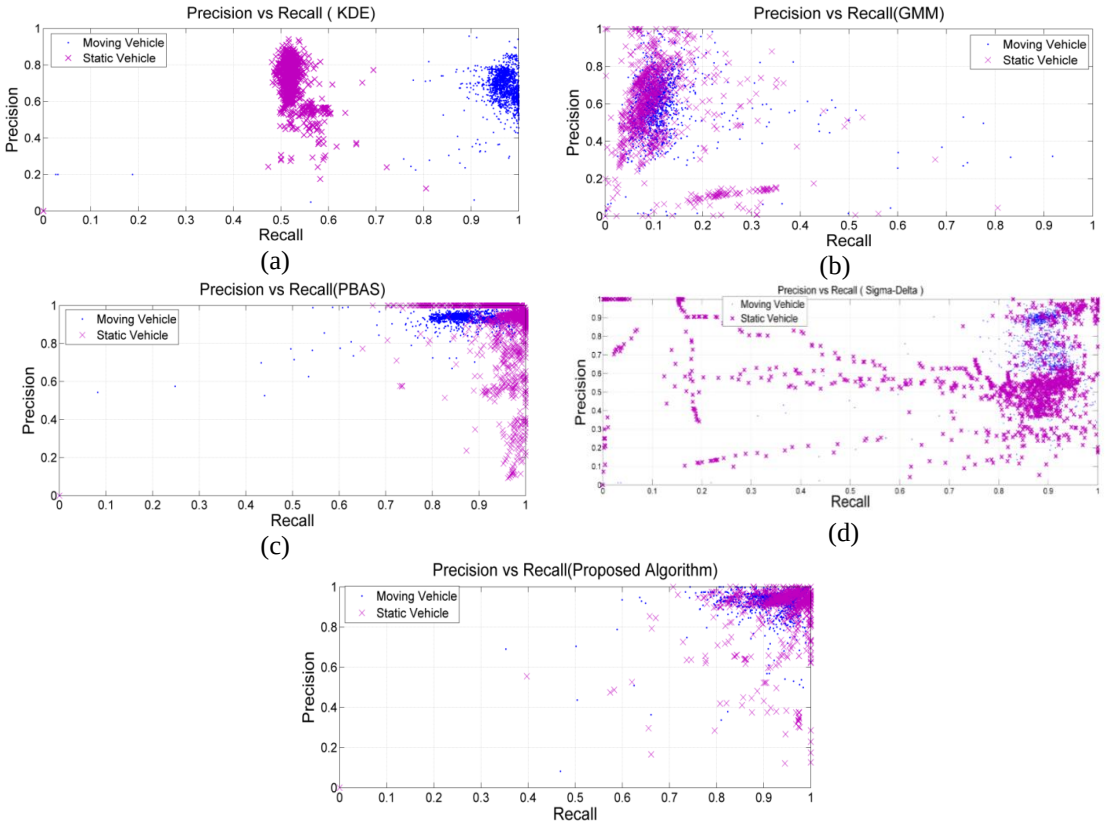

Figure 2.8: Precision-Recall Measure for Different Algorithms.

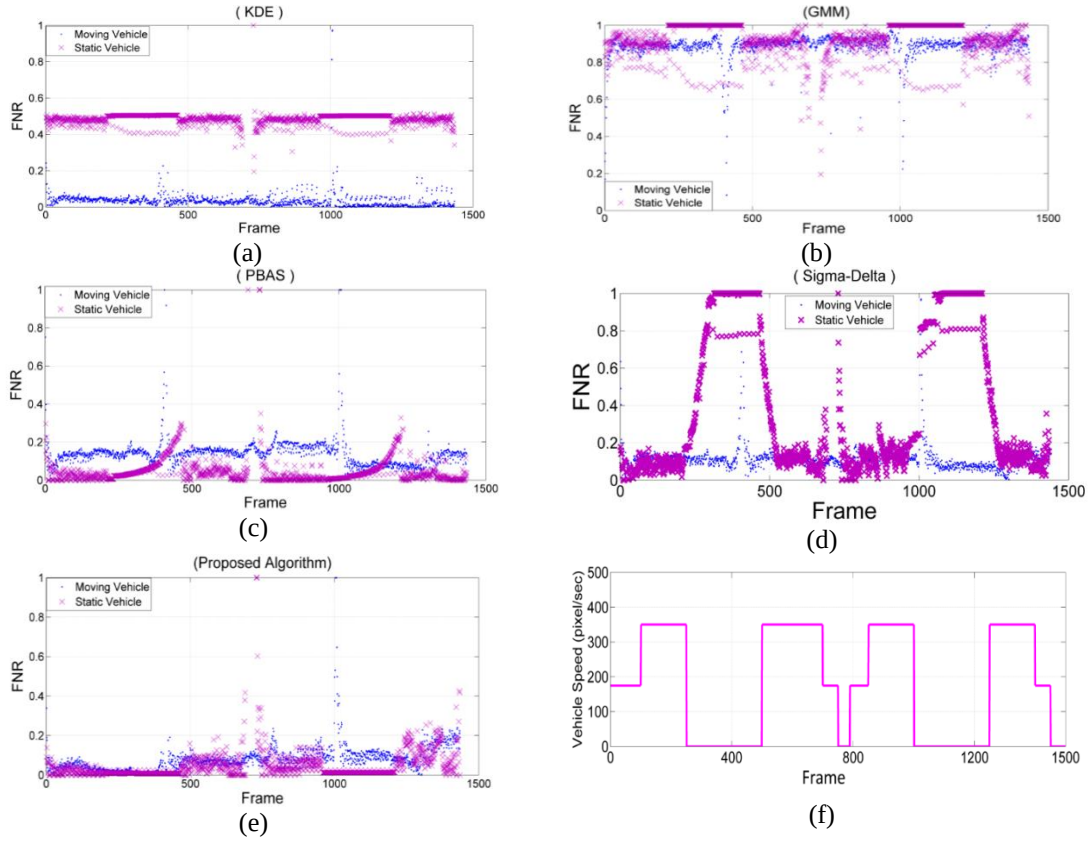

Figure 2.9: (a)-(e) Detection of moving and stationary vehicles by different algorithms; and (f) Applied speed variation in ‘static vehicle’ sequence.

Table 2.5: Description of quantitative analysis of different algorithms

Method	Precision-Recall Curve	FNR vs. Time Curve
KDE	• Shows good Precision-Recall relationship for 'Moving Vehicle' video sequences. • Recall decreases for 'Stationary Vehicle' sequence due to increase in FN values. • Shows good stability in both moving and stationary sequence as the points are clustered in a spot. It represents that the algorithm gives stable result for a single threshold value.	• Shows less amount of FNR for 'Moving Vehicle' sequence. • Shows increased amount of FNR for 'Static Vehicle' sequence. • The FNR remains almost constant with the time. Whereas for stationary condition it shifts upward a little. The speed of the vehicle in different frames is illustrated in Figure 2.8(f).
GMM	• Shows higher precision value and lower recall value for both 'Moving Vehicle' and 'Stationary Vehicle' video sequences. • Shows poor stability in PR relationship. The PR points are scattered, which means that the precision can vary for attaining a certain recall and vice versa. Therefore, for a single threshold value the algorithm will not give a stable result.	• It shows similar high FNR for both video sequences. • The FNR increases to maximum when the object comes to a rest condition.
PBAS	• Shows good Precision-Recall relationship for both 'Moving Vehicle' and 'Stationary Vehicle' video sequences. • Shows good stability in relationship.	• For both moving and stationary sequence the FNR is lower. • The FNR increases in a parabolic shape for the frames where the vehicles are static condition. Zero vehicle speed in Figure 2.8(f) represents the stationary condition.
Sigma-Delta	• Shows good precision-recall relationship for 'Moving Vehicle' sequence. • The precision value decreases for 'Static Vehicle' condition. • Shows poor stability in PR relationship as the points are scattered.	• For both condition the FNR is lower. • However, the FNR increase exponentially with time when the vehicle remains in stationary condition (Figure 2.8(f)).
Proposed Algorithm	• Shows good PR Relationship for both 'Moving Vehicle' and 'Stationary Vehicle' video sequences. • Shows stable Precision-Recall relationship as the points are dense in a certain area.	• FNR is low for both the video sequence. • No increase in FNR when the vehicle remains in stationary condition (Figure 2.8(f)).

2.8.2.1. Computational complexity

The computational speed is observed on 320 x 232 size of frame having 3 color channels. Table 2.6 shows the performance of several algorithms on a similar platform (3.60GHz Core i7 CPU, 8GB of RAM, C++ implementation).

Table 2.6: Computational complexity of different algorithms

Method	Average Time/frame	FPS	CPU (%)
GMM (RGB)	4ms, 8ms at congestion	125	6.27
KDE (RGB)	13ms, 30ms at congestion	33	6.3
PBAS (RGB)	14ms (also constant in congestion)	70	6.2
Sigma-Delta (RGB)	2.5 ms	400	0.5
Proposed Algorithm (RGB)	2 ms (constant in congestion)	500	1.1

ms – Millisecond
RGB – Red, Green, Blue

Figure 2.10 shows that the average CPU time for the proposed algorithm is less than KDE, GMM, and PBAS, whereas a bit more than Sigma-Delta. For private memory, PBAS requirement is the highest. However, the proposed method consumes memory at a rate equivalent to Sigma-Delta, and GMM. The performance on average execution time shows that the proposed algorithm requires the least amount of time and the PBAS method requires the highest time.

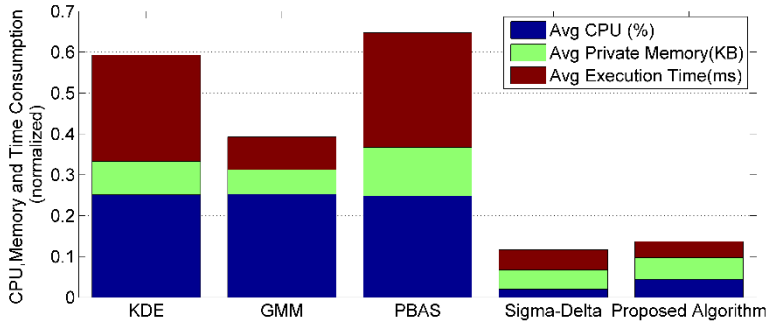

Figure 2.10: Computational complexity of different algorithms.

2.8.3. Estimation of traffic parameters

2.8.3.1. Flow estimation

Dimension of the analysis frame is an important element for fast processing as reduction in this feature reduces the processing effort significantly. In this regard,

strip analysis technique is more fathomable and favorable over frame based or regional approach. Moreover, magnitude of error or noise arising from camera vibration is considerably lower for smaller strips in contrast to entire frame. As a result, careful selection of the strip in the field of view contains vehicle pixel data and acts as a catalyst to accelerate the process. In this study, a single strip is selected in the frame and pixel by pixel processing is adopted for vehicle counting or traffic flow measurement. This method provides a count of one for a vehicle present in the strip, whereas zero without a vehicle, thereby forming a strip matrix. Summation of binary ones in the strip matrix represents the total width of an object occupying the strip. Considering the width of a representative vehicle (e.g. passenger car), vehicles present in the frame at time t, $P(t)$ is outlined where, w relates to strip width, C_w expresses car width, and $b(t)$ is the binary image which is extracted by the proposed algorithm.

$$\left.\begin{aligned} P(t) &= \frac{\sum_{i=1}^{m}\sum_{j=1}^{n} b(t)}{w \times C_w} \\ n(t) &= \begin{cases} \left(\frac{dP}{dt}\right)_t, & if\ \ dP>0 \\ 0 \end{cases} \\ N(t) &= \int_0^t n(t)dt \\ q(t) &= \left(\frac{dN}{dt}\right)_t \end{aligned}\right\} \qquad (8)$$

The value of $P(t)$ largely depends on the vehicle width w. Large vehicle width tends to underestimate small vehicle counts, whereas small vehicle width when selected tends to overestimate. For this, the weighted mean of the observed composition is more suitable. The number of vehicle within the frame at time t, is represented as $n(t)$. When a vehicle enters the FOV, $n(t)$ will be non-negative, whereas $n(t)$ will return zero for a vehicle leaving the frame. In fact, the function responds to the increment of vehicles. Vehicle count is represented as $N(t)$, sum of the all vehicles that passed the

field of view at up to time *t*. The flow $q(t)$ is obtained, differentiating the counting function in Equation (8).

2.8.3.2. Density estimation

Density is estimated employing the area of standard vehicle in the current frame or foreground. The technique operates through facilitating a larger and wider strip, positioned on the frame over which the density is analyzed rather than the entire frame region. To avoid overestimation or underestimation, mid-section is preferred over upstream and downstream location of the strip. Density $k(t)$ is calculated using the Equation (9) where, A relates to standard vehicle area, L represents the strip length.

$$k(t) = \frac{\sum_{i=1}^{m}\sum_{j=1}^{n} b(t)}{A \times L} \tag{9}$$

The Equation is also sensitive to vehicle area A. The area of a vehicle changes in the field of view. On the contrary, the area also changes with the vehicle type. As a result, for practical purpose the midrange weighted average area is more suitable for this computation. Another parameter L also affects the result significantly. Small length vehicles when selected as reference, tends to overestimate density over a link. Moreover, L depends on the camera height and angle. An aerial view of a link can provide a conducive view for density computation.

2.8.3.3. Speed estimation

The speed of the vehicles in the field of view is computed at blob level. The frame is divided into several segments to determine the aggregated speed. This method is adopted to avoid excess utilization of computational resources like pattern recognition within consecutive frames. The instantaneous and mean speed of all the vehicles present in a frame can be determined by Equation (10), where, v_j denotes to

instantaneous speed at frame j, $\bar{v}$ relates to time mean speed at frame j; s_i relates to the change in position of object at segment i within time t' from frame $(j-1)$ to frame j; N expresses number of vehicles present in frame; n represents the number of user defined segments; N_j expresses number of objects present in frame j; and m corresponds to number of frames. The value of n is selected carefully depending upon the size of vehicles within the binary image, not in the field.

$$\left.\begin{aligned} v_j &= \frac{\sum_{i=1}^{n} s_i}{N \times t'} \\ \bar{v} &= \frac{\sum_{j=1}^{m}\sum_{i=1}^{n} s_i}{N_j \times t' \times m} \end{aligned}\right\} \quad (10)$$

2.8.3.4. Estimated traffic parameters

Using Equation (8)-(10) traffic state parameters are estimated for different detection algorithms. Figure 2.11 compares the estimated parameters with the actual one, which shows that the algorithm performs with much accuracy in flow and speed. Figure 2.11 shows scatter plots of the algorithm output versus manually extracted ground truth data for velocity and flow. Figure 2.11(c) summarizes the RMSE for speed, flow and density. Output of the detection algorithms show that the estimated speed is accurate. Even if the vehicles suffer from occlusion or splitting, the imperfect blobs still move at the normal speed. The errors in flow and density are primarily due to missed or divided vehicles at their windshield. Often, an error of two or three vehicles in one sample can be very significant. For example, one missed vehicle in a 1 min sample can cause 60 veh/hour differences. At 2500veh/h less error is projected in the output whereas for 1500 veh/h and 4500 veh/h, the error per missed vehicle is slightly higher. The greatest source of error appears to be from the selection of appropriate background that ultimately yields noise to the frames. As a result, the detection

algorithm underestimates some vehicles, having same color as the pavement. The results are promising nonetheless and the error shown in Figure 2.11(c) (RMSE) should be taken in context.

These experiments underscore difficult conditions where earlier many image processing algorithms ceases: congestion, shadows linking vehicles together, and camera movement. The real video sequence includes shadows, both from vehicles and from wayside objects like building. Approximately 25% of the samples included shadow and 15% of the segments included camera movement due to high winds. Performance does not show any significant changes under different conditions. The performance of the algorithms in traffic state estimation is featured in Figure 2.10, under two challenging conditions: (1) illumination variation with long shadows during daytime and (2) camera displacement. There are 60 sample video datasets, each being 1 minute in time, containing 6800 vehicles. Note that the evening peak starts during the video sequence and approximately 50% of data are under light to severe congestion, and thus, frequent occlusions. Occlusion results from the variety of traffic composition or from the position of the video sensor. For traffic composition, smaller vehicles remain undetected in the FOV due to the presence of large truck or other vehicles. For solution, a minimum height of 40 feet and an angle around 45 degree with the vertical would resolve this problem for the video sensor, as view will increase at higher level and angle. Table 2.7 elaborates on the performance of different algorithms in traffic state measurement.

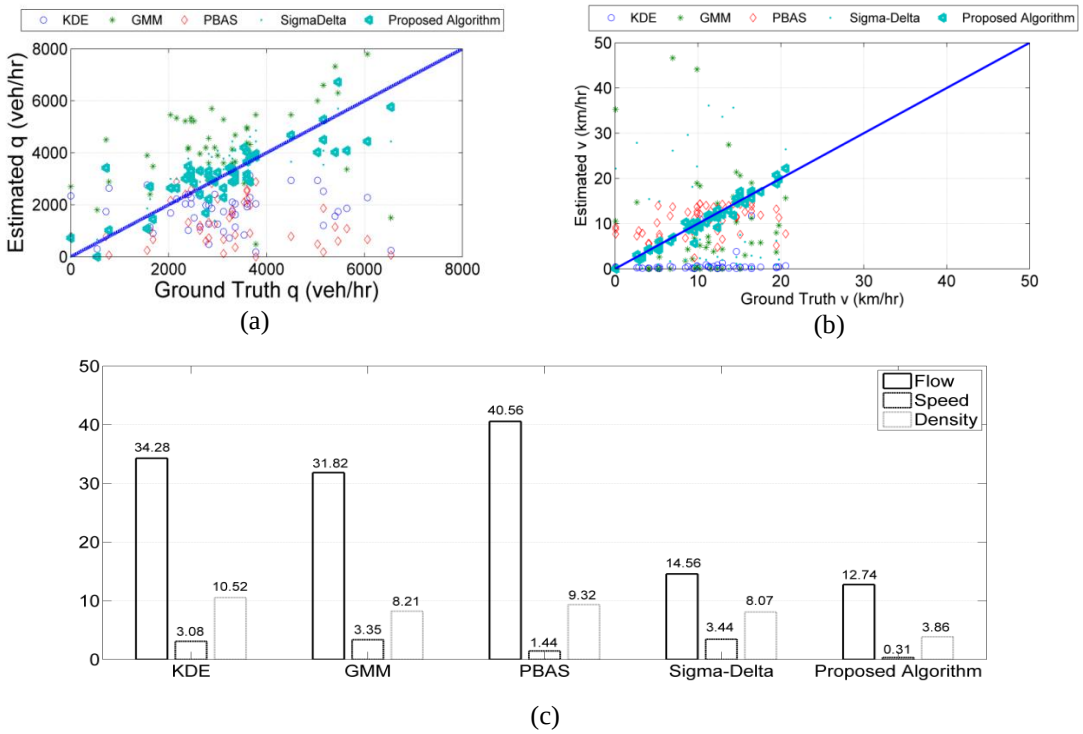

Figure 2.11: Scatter plot of the algorithm output versus manually extracted ground truth data for all the algorithms for speed (a) and flow (b); and RMSE value for speed, flow and density (c).

Table 2.7: Performance description for traffic state measurement

Method	Flow	Speed	Density
KDE	Exhibits high RMSE value	Exhibits better performance compared to Sigma-Delta	Exhibits very high RMSE value
GMM	Exhibits better performance compared to KDE	Exhibits very high RMSE value compared to other methods	Exhibits better performance compared to KDE
PBAS	Exhibits very high RMSE value compared to other methods	Shows comparatively better result than KDE	Exhibits better performance compared to KDE
Sigma-Delta	Exhibits better performance compared to GMM	Exhibits very high RMSE value	Exhibits better performance compared to KDE,GMM, and PBAS
Proposed Algorithm	Exhibits better performance compared to all other methods	Exhibits better performance compared to all other methods	Exhibits better performance compared to all other methods

2.8.3.5. Relationship of traffic state parameters and evaluation parameters

The relationship between traffic state parameters and evaluation parameters is established to provide a guideline to nominate a particular image-processing algorithm suitable for traffic application. Two particular parameters such as False Positive Rate (FPR), and False Negative Rate (FNR) are selected to establish the relationship because they form the basic measure of evaluation for any image processing algorithm. FPR and FNR both affects flow measurement. When FPR increases, the estimated flow will also increase from the actual flow. Whereas, the flow will decrease from the actual flow when FNR increases. Table 2.8 underscores the relationship between traffic state parameters and evaluation parameters.

Table 2.8: Relationship between traffic state parameters and evaluation parameters

Traffic State Parameter	Evaluation Parameter	
	FPR	FNR
Flow	+	–
Density	+	–
Speed	–	–

+ = Increase
– = Decrease

The FPR and FNR have the same effect over density as flow. However, FNR and FPR have substantial effect on speed because the FNR rate increases non-linearly at stationary condition (Figure 2.9). This increase marks a phenomenon in which stationary traffic is absorbed into the background over time. Thus, the presence of traffic decreases with time. Conversely, when FPR increases the aggregate speed of the vehicles decreases. From the derived relationship between traffic state parameters and evaluation parameters it can be stated that an algorithm for which FPR and FNR are minimum, should be adopted for traffic detection.

2.9. Conclusion

This research emphasizes on a novel traffic detection algorithm. The developed algorithm follows deterministic approach rather being probabilistic. The deterministic relationship among the algorithm parameters aids in defining the problem and developing the exact solution. Moreover, such approach also reduces the number of parameters involved in the application process, thus making it simple to deal with variety of challenges. The developed algorithm uses only two different parameters: (1) static background; and (2) threshold parameter. The first one initializes the background for background subtraction model and applies correction over the frames to be analyzed. The latter parameter decides whether the pixel belongs to traffic.

The algorithm achieves high accuracy of detection through small computational effort. Specifically, it achieves overall classification accuracy (>95%) with very small computational resource (500 frames per second) as compared to the most efficient algorithms identified in the recent study by (Sobral and Vacavant, 2014). Another important feature of the algorithm is that it detects traffic in three prevalent conditions such as stationary, slowly moving, and fast moving, having very little setbacks compared to Vargaset et al. (2010).

The innovation of the algorithm involves the use of transparency effect for frame correction to deal with challenges affecting the accuracy of traffic detection such as illumination variation, shadow, and camera displacement. The qualitative analysis shows that compared to others the proposed algorithm can detect vehicles accurately and suffers least amount of false positive and false negative, under different traffic conditions. The quantitative analysis of the algorithm shows stable Precision-Recall Relationship for both moving and stationary vehicle. The precision, recall, and percent correct classification values are 0.935, 0.906, and 0.992 respectively.

The RMSE values computed from ground truth and estimated traffic parameters show that the proposed algorithm outperforms others. While estimating the traffic parameters, a set of equations were developed which can be readily adopted with other detection algorithms. Most of the algorithms elaborated in literature focuses only on the image processing for object detection, making it difficult to select a particular algorithm to be useful in traffic application. Such application although in highlighted in a survey approach by Buch et al. (2011), does not provide a generic guideline based on which an algorithm can be selected. Thus, correlations between traffic parameters and algorithm evaluation parameters (False Positive Rate, and False Negative Rate) are established to determine the applicability of any image-processing algorithm for traffic state estimation. The increment or decrement of evaluation parameters marks the characteristics of an algorithm, which dictates whether the algorithm is suitable for traffic state estimation.

For background changing with time, the proposed algorithm can be adjusted for day to night transition sequence by replacing the static background parameter. Moreover, there is a certain research scope to estimate the traffic parameters at night time situation by extending state estimation equations developed in this study.

2.10. Reference

1. Bouwmans, T., 2014. Traditional and recent approaches in background modeling for foreground detection: An overview. *Computer Science Review, 11*, 31-66.
2. Buch, N., Velastin, S., Orwell, J., 2011. A review of computer vision techniques for the analysis of urban traffic. *Intelligent Transportation Systems, IEEE Transactions on, 12*(3), 920-939.
3. Coifman, B., Beymer, D., McLauchlan, P., Malik, J., 1998. A real-time computer vision system for vehicle tracking and traffic surveillance. Transportation Research Part C: Emerging Technologies, 6(4), 271-288.

4. Davis, J., Goadrich, M., 2006. The relationship between Precision-Recall and ROC curves. In *Proceedings of the 23rd international conference on Machine learning*, ACM. (pp. 233-240).
5. Elgammal, A., Harwood, D., Davis, L., 2000. Non-parametric model for background subtraction. In *Computer Vision—ECCV 2000*, Springer Berlin Heidelberg. (pp. 751-767).
6. Guo, L., Ge, P. S., Zhang, M. H., Li, L. H., Zhao, Y. B., 2012. Pedestrian detection for intelligent transportation systems combining AdaBoost algorithm and support vector machine. *Expert Systems with Applications*, *39*(4), 4274-4286.
7. Gupte, S., Masoud, O., Martin, R. F., Papanikolopoulos, N. P., 2002. Detection and classification of vehicles. *Intelligent Transportation Systems, IEEE Transactions on*, *3*(1), 37-47.
8. Hsu, W. L., Liao, H. Y., Jeng, B. S., Fan, K. C. (2004). Real-time traffic parameter extraction using entropy. *IEE Proceedings-Vision, Image and Signal Processing*, *151*(3), 194-202.
9. Ilyas, A., Scuturici, M., Miguet, S., 2009. Real time foreground-background segmentation using a modified codebook model. In *Advanced Video and Signal Based Surveillance, 2009. AVSS'09. Sixth International Conference on IEEE*, (pp. 454-459).
10. Karasulu, B., Korukoglu, S., 2012. Moving object detection and tracking by using annealed background subtraction method in videos: Performance optimization. *Expert systems with applications*, *39*(1), 33-43.
11. Lai, J. C., Huang, S. S., Tseng, C. C., 2010. Image-based vehicle tracking and classification on the highway. In *Green Circuits and Systems (ICGCS), 2010 International Conference on* IEEE, (pp. 666-670).
12. Mandellos, N. A., Keramitsoglou, I., Kiranoudis, C. T., 2011. A background subtraction algorithm for detecting and tracking vehicles. *Expert Systems with Applications*, *38*(3), 1619-1631.
13. Manzanera, A., Richefeu, J. C., 2007. A new motion detection algorithm based on Σ–Δ background estimation. *Pattern Recognition Letters*, *28*(3), 320-328.
14. Mao, H., Ye, C., Song, M., Bu, J., Li, N. (2009, October). Viewpoint independent vehicle speed estimation from uncalibrated traffic surveillance

cameras. In *Systems, Man and Cybernetics, 2009. SMC 2009. IEEE International Conference on* IEEE, (pp. 4920-4925).

15. Pan, X., Guo, Y., Men, A., 2010. Traffic surveillance system for vehicle flow detection. In *Computer Modeling and Simulation, 2010. ICCMS'10. Second International Conference on* IEEE, (Vol. 1, pp. 314-318).
16. Pletzer, F., Tusch, R., Böszörmenyi, L., Rinner, B., 2012. Robust traffic state estimation on smart cameras. In *Advanced Video and Signal-Based Surveillance (AVSS), 2012 IEEE Ninth International Conference on* IEEE, (pp. 434-439).
17. Rosin, P. L., Ioannidis, E., 2003. Evaluation of global image thresholding for change detection. *Pattern Recognition Letters*, *24*(14), 2345-2356.
18. Shen, Y., 2008. The research and applications of visual tracking based on mean shift (Ph.D. thesis). Jiangsu University of Science and Technology.
19. Sobral, A., 2014. BGS Library. Available at: https://github.com/andrewssobral/bgslibrary. Accessed June., 2015.
20. Sobral, A., Vacavant, A., 2014. A comprehensive review of background subtraction algorithms evaluated with synthetic and real videos. *Computer Vision and Image Understanding*, *122*, 4-21.
21. Stauffer, C., Grimson, W. E. L., 1999. Adaptive background mixture models for real-time tracking. In *Computer Vision and Pattern Recognition, 1999. Computer Society Conference on IEEE*, (Vol. 2).
22. Takeuchi, A., Mita, S., McAllester, D. (2010, June). On-road vehicle tracking using deformable object model and particle filter with integrated likelihoods. In *Intelligent VehiclesSymposium (IV), 2010 IEEE*, (pp. 1014-1021).
23. Vargas, M., Milla, J. M., Toral, S. L., Barrero, F., (2010). An enhanced background estimation algorithm for vehicle detection in urban traffic scenes.*Vehicular Technology, IEEE Transactions on, 59*(8), 3694-3709.
24. Wan, Y., Huang, Y., Buckles, B., 2014. Camera calibration and vehicle tracking: Highway traffic video analytics. Transportation Research Part C: Emerging Technologies, 44, 202-213.
25. White, B., Shah, M., 2007. Automatically tuning background subtraction parameters using particle swarm optimization. In *Multimedia and Expo, 2007 IEEE International Conference on* IEEE, (pp. 1826-1829).

26. Zivkovic, Z., van der Heijden, F., 2006. Efficient adaptive density estimation per image pixel for the task of background subtraction. *Pattern recognition letters*, *27*(7), 773-780.
27. Zou, Y., Shi, G., Shi, H., Wang, Y., 2009. Image sequences based traffic incident detection for signaled intersections using HMM. In Hybrid Intelligent Systems, 2009. HIS'09. Ninth International Conference on IEEE. (Vol. 1, pp. 257-261).

CHAPTER 3: VISCAL: TO CALIBRATE MICROSCOPIC SIMULATION PARAMETERS[†]

3.1. Introduction

Microscopic traffic simulation tools (e.g. VISSIM, PARAMICS, MITSIM, AIMSUM, etc.) have gained popularity due to extensive features that enable network design and evaluation, planning and analysis, etc. These features include flexible representation of spatial and temporal demand patterns, modeling of complex interaction between vehicles and driving behavior, replicating driving decisions (e.g. route choice), and simulating operations of traffic management strategies. However, the developed micro-simulation model is a complex constitution of several components based on a large number of inputs and parameters to best represent observed local traffic condition. Therefore, model calibration that ensures the accurate reflection of the local driving environment by matching model output with measured field values is a crucial step in building a reliable microscopic traffic simulation model.

Complexity of the calibration problem calls for an adequate optimization technique that can produce an optimal parameter set, saving both time and effort. Researchers widely use heuristic methods due to its ability to continuously adapt search in response to intermediate trial results. For example, genetic algorithm (Park and Qi, 2005; Kim et al., 2005; Ma et al. 2007; Ma and Abdulhai, 2002) simulated annealing (Park and Yun, 2006), Simultaneous Perturbation Stochastic Approximation (SPSA)

[†] This chapter is a modified version of a published article in the Journal of Built Environment, Technology and Engineering, Vol. 1 (Sept.), 2016. Muniruzzaman, S. M., Hadiuzzaman, M., Rahman, M. M., Hasnat, M. M., Haque, N., Rahman, F., Hasan, T. "Calibration and Validation of Microscopic Simulation Model for Non-lane Based Heterogeneous Traffic Stream of Developing Country" pp244-255. It also includes the accepted manuscript submitted in the Journal of Traffic and Transportation Engineering (English Edition). Hadiuzzaman, M., Siam, M., Nasrin, S., Muniruzzaman, S. M., Haque, N. "VISCAL: Heuristic Algorithm Based Application Tool to Calibrate Microscopic Simulation Parameters"

(Balakrishna et al., 2007; Paz et al., 2014) and complex algorithm (Toledo et al., 2004) have been used in different studies. These algorithms automate the calibration process to a certain degree and generally improve the simulation performance over default model parameter values for a particular study area. Many of the projects and research studies have investigated and proposed new techniques for the calibration process. However, to the authors' best knowledge very few has furnished a general application tool, offering flexibility and practicality for any real-world calibration problem, such as GENOSIM (Ma and Abdulhai, 2002), VISGAOST (Stevanovic et al., 2007). This is may be due to the complex inter-relationship among the large number of micro-model parameters, cost associated with the single or multi-criteria objective function replicating actual network characteristics, and underlying differences of the algorithm parameters of different optimization techniques.

Calibration of a micro-simulation model is a time-consuming task and even a medium sized network can take months to build, spending most of the time on calibrating the parameters. This is because much of the accuracy or satisfactory outcome of the simulation model is dependent on the appropriate selection of parameters. Most of the calibration studies focus on specific parameter set, such as, driving behavior parameters (Kim et al., 2005; Balakrishna et al., 2007; Toledo et al., 2014), mean target headway and mean reaction time (Gardes et al., 2002; Lee et al., 2001), car following factors (Kim and Rilette, 2003; Schultz and Rilette, 2004), Origin-Destination (O-D) flow (Toledo et al., 2004; Jha et al., 2004) etc. Others identify the significant parameters that have a definite effect on the driving behavior and performance of the network and then calibrate those parameters (Park and Qi, 2005; Ma and Abdulhai, 2002; Kim and Rilette, 2003; Jha et al., 2004; Dowling et al., 2004). Thus, choice of decision parameters for a particular micro-model either appropriate or inappropriate will have a positive or negative impact on the network

performance as measured by a relevant objective function. This process of appropriate parameter selection when automated will definitely provide a time-effective solution to the user.

Objective function plays a critical role in expressing the network characteristics and adds to the complexity of the calibration process. Mostly objective function is based on either single criterion (speed, or flow, or delay) or, multi-objective criteria (speed-flow, density-flow, etc.). However, it should be noted that each single evaluation of the objective function is very costly, depending on the scale (small or large) of the built network, and the number of simulated vehicles. From practical cost consideration, calibration process in most of the studies is based on single criteria objective function (e.g. speed, or flow). Based on this criteria, some studies showed good performance using speed (Toledo et al., 2004), some showed satisfactory result using flow (Kim et al., 2005; Ma and Abdulhai, 2002; Kim and Rilette, 2003). Very few studies have worked with multi-objective criteria, e.g. speed-flow (Paz et al., 2015). The limitation of using single criteria objective function is that the minimization of error based on only one criterion does not necessarily reflect likewise for other objective functions. All these studies represent one particular and important fact that the objective function is data-specific and network-specific. This implies that a particular objective function suitable for a particular study network may not bring representative outcome for another network. Thus, it is a primary concern to underscore the suitable objective function for a particular network emphasizing on the single or multi-objective criteria, otherwise the entire calibration process will generate unrealistic outcome. From practical considerations, an opportunity to select the best suitable objective function for a particular network through an automated process would greatly reduce the cost and increase the efficiency of the calibration process.

For heuristic optimization algorithms, the underlying parameters of different algorithms are significantly different from the other. These algorithms start with a feasible parameters set(s) and evaluate the closeness between the field measurements and simulation under the feasible set(s). Every algorithm possesses unique rules that are used to replace the unfit parameter sets by better ones iteratively until the gap is narrowed to a satisfactory level. For instances, Genetic Algorithm (GA) is a stochastic search method based on the principles and mechanisms of natural selection and survival of the fittest from natural evolution whereas the simultaneous perturbation stochastic approximation (SPSA) method preforms the search operation along the gradient approximation at every iteration. The operation of the simulated annealing (SA) is also significantly different from other algorithms, where SA escapes local optima by allowing hill-climbing moves (i.e., moves that worsen the objective function value). These differences make it difficult to decide on a generic optimization algorithm for the calibration process. For instance, a satisfactory outcome obtained from using GA for a particular network does not ensure that likewise outcome will be possible for a different network, with a different set of parameters. For this reason, there is a need to test the suitability of the available optimization algorithms for a particular network. A generic calibration tool featuring different heuristic optimization algorithms may offer such flexibility and ease the tedious process of calibration.

This study proposes a generic calibration tool VISCAL that is able to calibrate any type and extent of network for VISSIM. It includes three heuristic optimization algorithms: (1) GA; (2) SPSA; and (3) SA. It also includes four objective function choices: (1) speed; (2) flow; (3) delay; and (4) multi-objective criteria. VISCAL has the ability: (1) to test the significance of the appropriate decision parameter set for a particular network; (2) to determine the most suitable objective function to reflect

network characteristics; and (3) to check the suitability of any of the three heuristic optimization algorithms for a particular network. VISCAL offers greater flexibility to the user by providing control on every aspect of the calibration process, specifically over the run time, number of trials, and the trial values themselves. The operation of the proposed calibration tool is tested for a freeway scenario.

The remainder of the chapter is organized as follows. The methodology of the developed calibration tool including the configuration of the optimization algorithms, selection of objective function, sensitivity analysis of micro-simulation parameters, and data input system is discussed in detail. A freeway scenario of Dhaka, Bangladesh is used to test the calibration processes of VISCAL. For evaluation, three objective functions (speed, flow, and speed-flow) from the four options coded in VISCAL are considered. A comparative analysis is drawn among the optimization algorithms (GA, SA, and SPSA) and a sensitivity analysis of the objective function results is carried out to find the most suitable combination of an objective function and optimization algorithm (e.g. multi-objective criteria and GA for this study) that provides the best estimates for field measured values. Finally, conclusion and further scopes are drawn.

3.2. VISCAL Methodology

Note that the calibration process is substantially affected by the extent of the network (small or large network) since the more the size of the network increases the more complex and tedious the calibration process becomes, involving greater number of links, simulated vehicles, and traffic decisions (route choice, control options, etc.). The intensive computational effort required to find an optimized set of parameters for a micro-model considering all the difficulties associated with calibration, has been the motivation for this study to develop an automated and robust calibration tool, VISCAL for widespread microscopic simulation software, VISSIM. The developed tool provides total control over the run time, number of trials, and the trial values

themselves during the calibration operation. For this purpose, four-candidate objective functions (speed, flow, density, and multi-objective criteria) are coded to offer greater flexibility to optimize the network. VISCAL generates charts, which can be used to draw comparison between distinct optimal simulation outputs and observed data, and then the user can decide on the most suitable objective function for a particular network.

Basic environment is preferred due to its capability to handle complex data structures and implementing complex mathematical functions. Figure 3.1 shows the flow chart of the VISCAL, and Figure 3.2(a) shows each of the program features integrated in the VISCAL. Steps involved with the calibration process of VISCAL are explained in details in the following subsections.

3.2.1. Algorithm configuration

Since the underlying parameters of different optimization algorithms are significantly different from the other, VISCAL includes an option to configure these parameters, specific to each algorithm as shown in Figure 3.2(b). Likewise, a preliminary analysis is a prerequisite for selection of appropriate algorithmic parameters such as a, c, α, γ and A in SPSA. VISCAL receives user defined algorithmic operators (i.e. for GA crossover rate, selection rate, number of generation, population size etc.) and then carry out various calibration tests using different values for the algorithms' operators to choose only the best outcome. This feature also enables user to control the run time for heuristic algorithms with small annealing schedules or numbers of generations.

3.2.2. Objective function selection

VISCAL offers flexibility to the user by coding four objective function choices into the system: (1) speed, (2) flow, (3) delay, and (4) multi-objective criteria. These options can be selected for calibration through the developed user-interface (Figure 3.2(b)).The set of equations (1), (2), and (3) constitute the objective function used for

single-criteria (e.g., flow, speed, and delay) calibration approach. In this study, Mean Absolute Percentage Error (MAPE) is used as speed and flow based objective function. As for delay, absolute error is computed. For multi-criteria (e.g. speed-delay, speed-flow) calibration approach, weighted sum method (Equation 4) is used to ensure that each individual objective function has equal contribution in obtaining the combined fitness result.

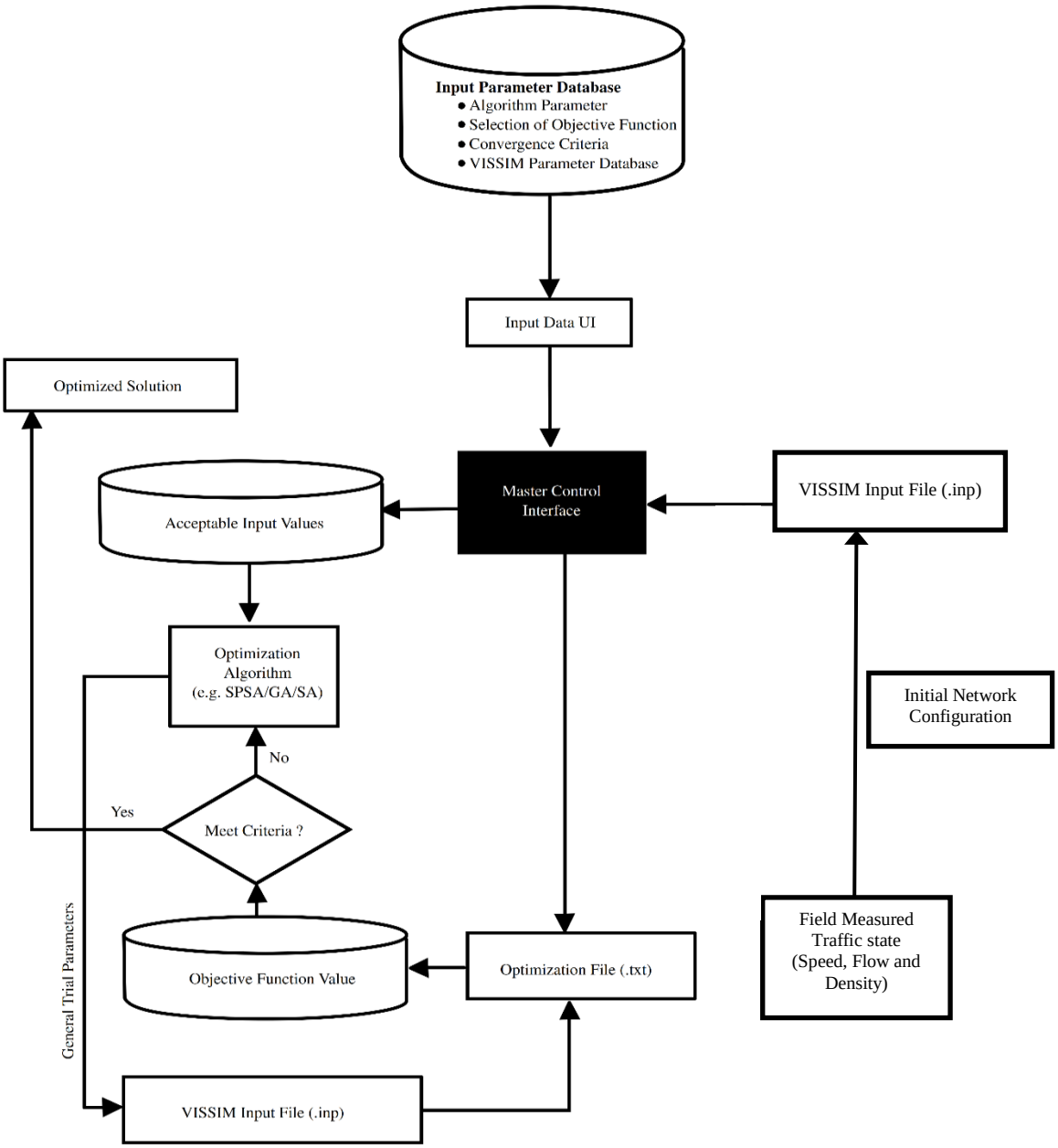

Figure 3.1: Flow chart of VISCAL.

The calibration of the simulation model parameters, θ is formulated using a mathematical programing approach. Usually values of speed vary within 100 km/hour whereas the values of flow vary from hundreds to thousands vehicles/hour. Therefore an objective function combining simple values of both the criteria (speed and flow) will invariably be influenced by flow only due its numerical superiority, rendering biased fitness value for a particular objective function. To solve this conflict, a scalar positive weightage is assigned to each criterion centering on its relative importance.

$$\text{Minimize MAPE for flow (\%)} = \frac{1}{N}\times\frac{1}{T}\times\sum_{t=1}^{T}\left(\sum_{i=1}^{N}\left|\frac{V_{i,t}-\tilde{V}(\theta)_{i,t}}{V_{i,t}}\right|\right)\times 100 \quad (1)$$

$$\text{Minimize MAPE for speed (\%)} = \frac{1}{N}\times\frac{1}{T}\times\sum_{t=1}^{T}\left(\sum_{i=1}^{N}\left|\frac{S_{i,t}-S(\theta)_{i,t}}{S_{i,t}}\right|\right)\times 100 \quad (2)$$

$$\text{Minimize absolute error for delay} = \sum_{i=1}^{n}\left|d_s^j(\theta)-d_o^i\right| \quad (3)$$

Minimize MAPE (%) =

$$\frac{1}{N}\times\frac{1}{T}\times\sum_{t=1}^{T}\left(w_1\times\sum_{i=1}^{N}\left|\frac{V_{i,t}-\tilde{V}(\theta)_{i,t}}{V_{i,t}}\right|+w_2\times\sum_{i=1}^{N}\left|\frac{S_{i,t}-S(\theta)_{i,t}}{S_{i,t}}\right|\right)\times 100 \quad (4)$$

Lower bound $\leq \theta \leq$ Upper bound

Where: $V_{i,t}$ = actual link flow for link i and time t,

$\tilde{V}(\theta)_{i,t}$ = simulated link flow for link i and time t,

$S_{i,t}$ = actual speeds for link i and time t,

$S(\theta)_{i,t}$ = simulated speeds for link i and time t,

N = total number of links in the model,

T = total number of time periods t,

w_1 = weight used to assign more or less value to flows,

w_2 = weight used to assign more or less value to speeds,

d_s^j = average delay obtained from the simulation model for intersection j,

d_o^j = observed field delay for intersection j, and

n = number of intersections under consideration.

3.2.3. Field measured traffic data input

The primary goal of calibration is to narrow the gap between field measured data and simulated data by allowing the optimization technique to gradually converge to an optimal parameter set through an iterative process. The field data is obtained employing various sensors (e.g. video sensor, loop detector, etc.) in the field. VISCAL has an input interface (Figure 3.2(c)) to record these data through an automated or manual way, to be used in the successive steps of the calibration process. The user provides three types of information in the interface: (1) number of link, (2) number of data in each link, and (3) time interval between each data (in minutes). VISCAL has the flexibility to handle ones, tens, or thousands of field measured values for a particular objective function provided by the user. VISCAL will generate a spreadsheet provided that the user has successfully recorded all the field data through input-interface, otherwise for any discrepancy error messages will pop-out. Since the input data can be large and may not simultaneously viewable on screen, tool controls (e.g., scrollbars, combo boxes, and radio buttons) is provided to allow seamless browsing. Moreover, VISCAL interface is designed in a way that it can load values consistent with the active choices on-screen from thousands of values.

3.2.4. Sensitivity analysis and VISSIM parameter selection

VISCAL performs a one-way ANOVA sensitivity analysis to determine significant parameters that has a definite effect on the developed network. This feature allows the

sensitivity analysis to be performed on user-defined parameters and automatically triggers the calibration process.

The calibration settings defined by the user are saved into an optimization file (e.g., ‘‘*. txt’’); for future reference, and to prevent any need for re-typing or to avoid redundancy.

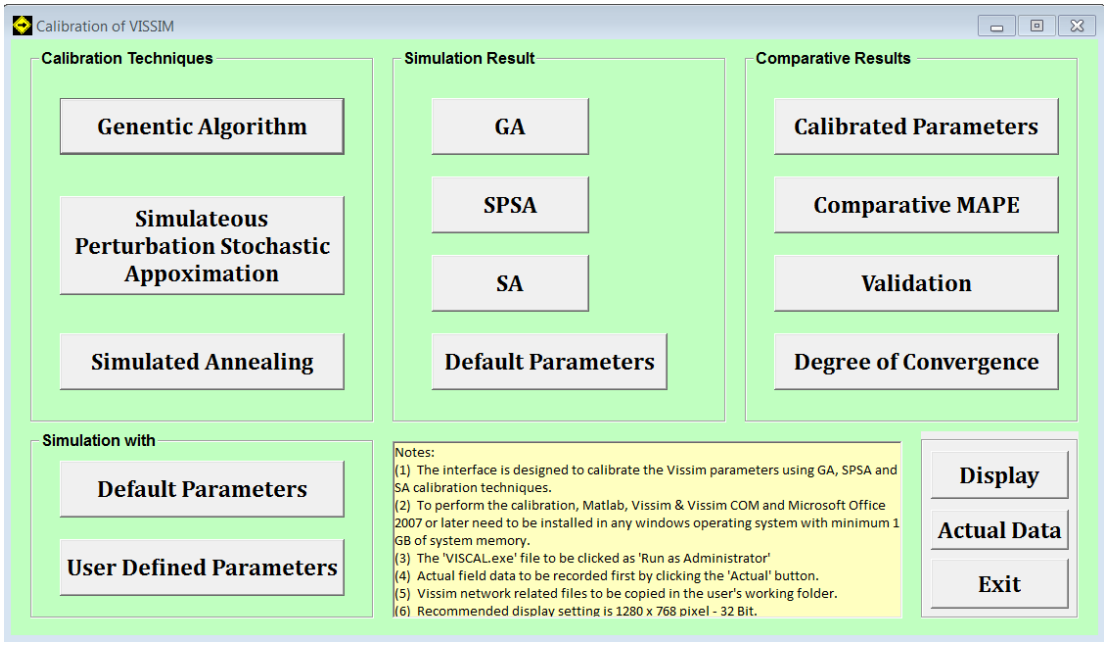

(a)

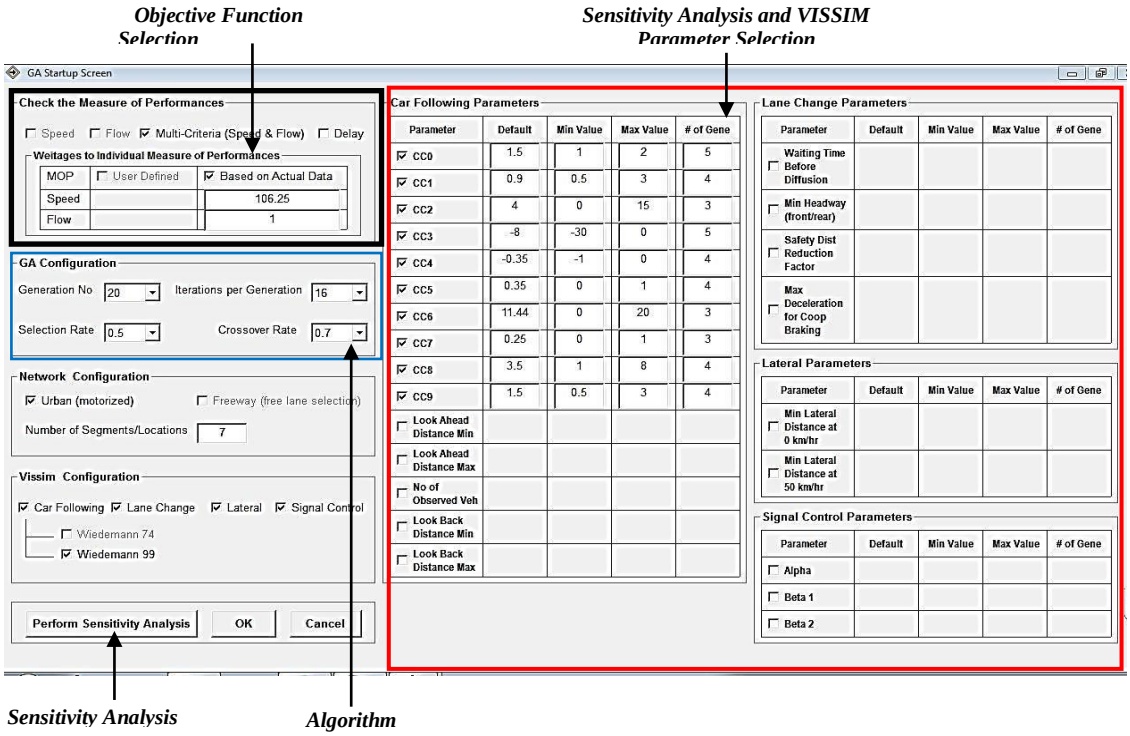

(b)

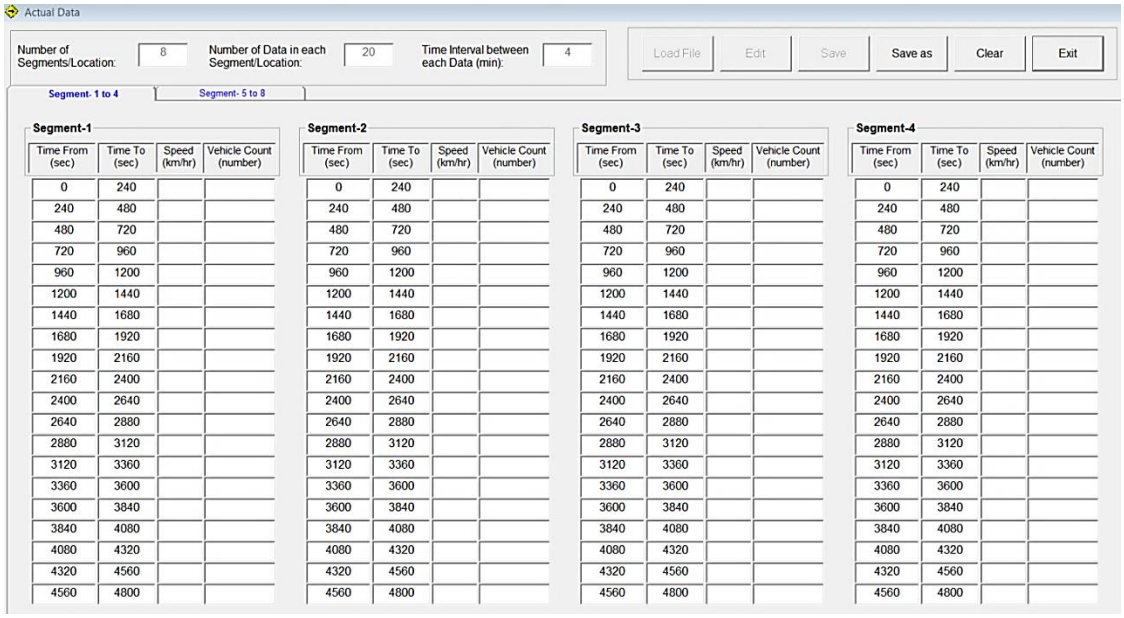

(c)

Figure 3.2: (a) Primary interface of VISCAL; (b) master control interface of GA for VISCAL; and(c) field measured traffic data input interface of the VISCAL.

3.2.5. Optimization algorithm

VISCAL is designed to perform the optimization operation based on three heuristic algorithms: (1) SPSA; (2) GA; and (3) SA. This operation starts by initializing a vector of feasible parameters, which is then forwarded to the VISSIM model via a text configuration file. Based on that configuration, a simulation run is triggered automatically. This process is continued via iteration loop until the simulation stops, and results are generated. The outcome of the simulation run is read into selective objective function from the results generated in the output text files. This result is then converted to fitness value (e.g. MAPE), corresponding to the feasible parameter set initiated at the start. Thus, one simulation run is necessary to evaluate each parameter set. Note that the total number of simulation runs is determined by initialized algorithm parameter, unique for each algorithm. For example, it is determined by the population size, and the total number of new chromosomes produced through all generations for GA.

Fitness value is calculated based on the difference between model output from various configurations and the corresponding observed data. Based on this fitness value of each parameter set, each algorithm performs its own mechanisms, i.e., the GA conducts genetic operations (e.g. selection, crossover, mutation, and replacement) to produce a new generation of solutions. The calibration process continues until a stopping rule is met, which is usually determined by either convergence or by reaching a pre-specified maximum number of generations. In VISCAL, the stopping rule is simply coded as the maximum number of generations set by the user.

3.2.5.1. Simultaneous perturbation stochastic approximation (SPSA)

Simultaneous Perturbation Stochastic Approximation (SPSA) is well known for its application to tackle optimization problems where the direct measurement of gradient $g(\theta)$ is impossible, such as in the case of micro simulation calibration. For a system, $L(\theta)$ is a scalar-valued performance measure, and θ is a continuous-valued p-dimensional vector of the system parameters that can be manipulated to achieve a better system performance. It is common that a noise ε could occur when observing $L(\theta)$ and then the observation $z(\theta)$ would be:

$$z(\theta) = L(\theta) + \varepsilon \tag{5}$$

It is assumed that $L(\theta)$ is differentiable over θ and that the minimum θ^* is obtained at a zero point of the gradient, i.e.

$$g(\theta) = \left|\frac{\delta L}{\delta \theta}\right|_{\theta=\theta^*} = 0 \tag{6}$$

SPSA algorithm starts with an initial guess θ_0 (e.g., the default parameter values in the simulation software). It then applies a series of "simultaneous perturbation" over the successive steps until the approximation of the gradient $g(\theta)$ converges to zero. Along

the successive steps, default parameters in simulation will get replaced with the estimated parameters θ_k. θ_k is updated recursively in the standard form:

$$\hat{\theta}_{k+1} = \hat{\theta}_k - a_k \hat{g}_k(\hat{\theta}_k) \tag{7}$$

Where the gain sequence $\{a_k\}$ needs to satisfy the regularity conditions, and $\hat{g}_k(\hat{\theta}_k)$ is the estimated gradient at $\theta = \theta_k$ at k^{th} iteration.

The perturbation is performed upon deriving $\hat{g}_k(\hat{\theta}_k)$. At iteration step k, a p-dimensional random perturbation vector Δ_k is generated. Each of the p components of Δ_k are independently generated form a zero mean probability satisfying certain conditions (Spall, 1992). Each component of Δ_k is usually generated from the Bernoulli (± 1) distribution. Let,

$$z_k^{(+)}(\theta_k) = L\left(\theta_k + c_k\Delta_k\right) + \varepsilon_k^{(+)} \tag{8}$$

$$z_k^{(-)}(\theta_k) = L\left(\theta_k - c_k\Delta_k\right) + \varepsilon_k^{(-)} \tag{9}$$

Where c_k is a positive scalar, and $z_k^{(+)}(\theta_k)$, $z_k^{(-)}(\theta_k)$ are the measurements of the system under the perturbation $\hat{\theta}_k + c_k\Delta_k$, $\hat{\theta}_k - c_k\Delta_k$, respectively.

According to Spall (1998), SPSA uses the following formula to obtain the approximation of $\hat{g}_k(\hat{\theta}_k)$.

$$\hat{g}_k(\hat{\theta}_k) = \frac{z_k^{(+)} - z_k^{(+)}}{2c_k}\begin{bmatrix} \Delta_k^{-1} \\ \Delta_k^{-2} \\ .... \\ \Delta_{kp}^{-1} \end{bmatrix} \tag{10}$$

The gain sequences of a_k and c_k is used to balance the algorithm stability and the desired form of the gain sequence is shown below:

$$a_k = \frac{a}{(1+A+k)^{\alpha}} ; c_k = \frac{c}{(1+k)^{\gamma}} \quad (11)$$

Spall (1998) recommended some general guidelines regarding the choices of a_k and c_k . If *a* is small, the calculations are stable initially; however, this may result in sluggish performance for large calculations. On the other hand, a large numerator, $a_k > 0$, which is used to produce non-negligible step sizes, leads to instability early in the calculation. It is most effective to set the numerator c to a small positive number.

3.2.5.2. Genetic algorithm (GA)

Genetic algorithm (Goldberg, 1989; Holland, 1975) is a heuristic search method that belongs to the larger class of evolutionary algorithms. GA optimization is a stochastic search process that mimics the natural process of the survival of the fittest through the manipulation of a population of chromosome. GA starts with a population with random 'chromosomes' (initial population of parameter values), where each chromosome represents a vector of parameters containing a solution for the optimization problem. A fitness value (e.g. MAPE of speed) is assigned to each chromosomes according to the quality of the solution. Based on the fitness value of individuals that contribute to the population of the next generation, selection rules select individuals with probabilities. Afterwards, a random decision to either 'mutate' or 'crossover' is executed. In case of mutation decision, a random 'chromosome' is elected from the current population and the parameter values are then changed to create an 'offspring' chromosome by random process. For crossover decision, two random 'chromosomes' are elected and random information (parameter values) are swapped to create an offspring chromosome. The chromosome (parameter set) that yields the worse fitness results (e.g. higher MAPE) from either 'mutation' or 'crossover' operation is then dropped. This process is continued until the maximum

number of iterations is achieved or there are no changes in parameter sets between iterations.

3.2.5.3. Simulated annealing (SA)

Simulated annealing (SA) employs a stochastic approach in the search of global optima. In contrast to GA's stochastic manipulation of a whole pool of candidate solutions, the SA algorithm avoids being trapped in the neighborhood of local optima by allowing for temporary increases in the "cost", namely the difference between the simulated outputs and their corresponding field measurements in the case of calibrating a micro-simulation model.

Simulated annealing (SA) was first introduced by Metropolis et al. (1953). It imitates the annealing process used in metallurgic, specifically where a solid that has been brought into liquid phase by increasing its temperature is brought back to the solid phase by slowly reducing the temperature. This conversion is carried out in such a way that all the particles are allowed to arrange themselves in a perfect crystallized state, resembling the global minimum of certain energy function. Kirkpatrick et al. (1983) introduced the application of SA for deterministic optimization problems as an analogy of the annealing process for a thermodynamic system. In emulating the physical annealing process, SA treats the feasible solutions as the possible energy states in a physical system, and the fitness value in the optimization problem as the energy of a physical system.

The parameters to be calibrated are denoted by vector θ_i, and $F(\theta_i)$ is the associated fitness value (e.g. MAPE of flow) and i is the iterative index. The current solution is randomly perturbed to obtain a new feasible solution θ_j. The new solution is accepted with a probability of p_k^j.

$$p_k^j = \begin{cases} 1 & \text{if } F(\theta_i) \le F(\theta_j) \\ \exp\left(\dfrac{F(\theta_i) - F(\theta_j)}{T_k}\right) & \text{otherwise} \end{cases} \quad (12)$$

Where, T_k is a monotonically decreasing scalar sequence, imitating the cooling of temperature in the physical annealing process. As the sequence number k increases, the probability of accepting an inferior solution (compared with the previous solution) will decrease.

Based on the above process, SA avoids being trapped at local minima to find the best fitness value by accepting not only the changes that decrease objective function, but also some changes that increase it. Generally, the escape from local minima in SA is dependent on the annealing schedule, the choice of initial temperature, and the number of perturbation at each temperature, and the amount of temperature reduction (Venkataraman, 2001).

3.3. Case Study: Freeway Scenario

VISCAL can be used to calibrate any type of micro-simulation network (e.g. urban, rural etc.). However, in this study, dataset from a freeway section of 3.26 km is used to test the operation of VISCAL. The study section is actually a part of the Dhaka-Mymensingh Highway (N3) in Bangladesh (Figure 3.3a) named as Tongi Diversion Road. Detail description of which including data collection process has been described in Chapter 2 (Section 2.6).

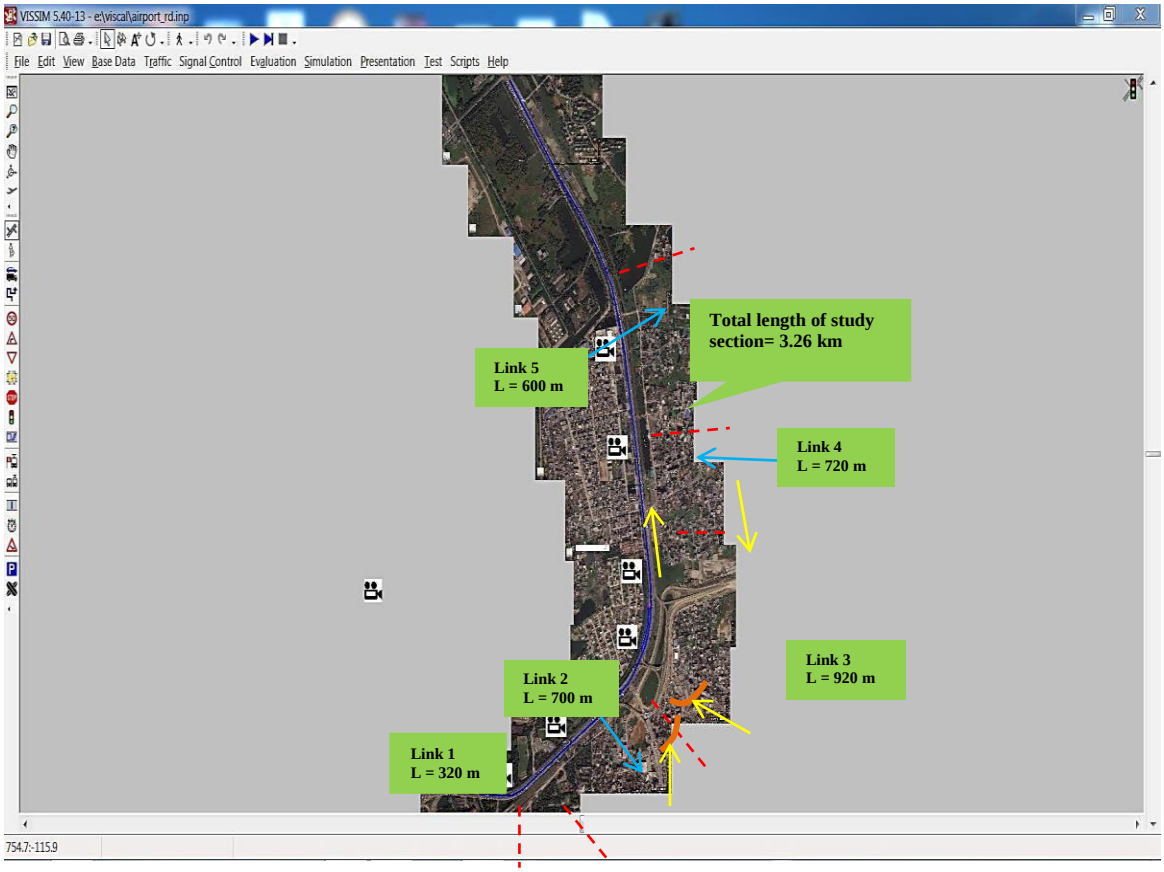

(a)

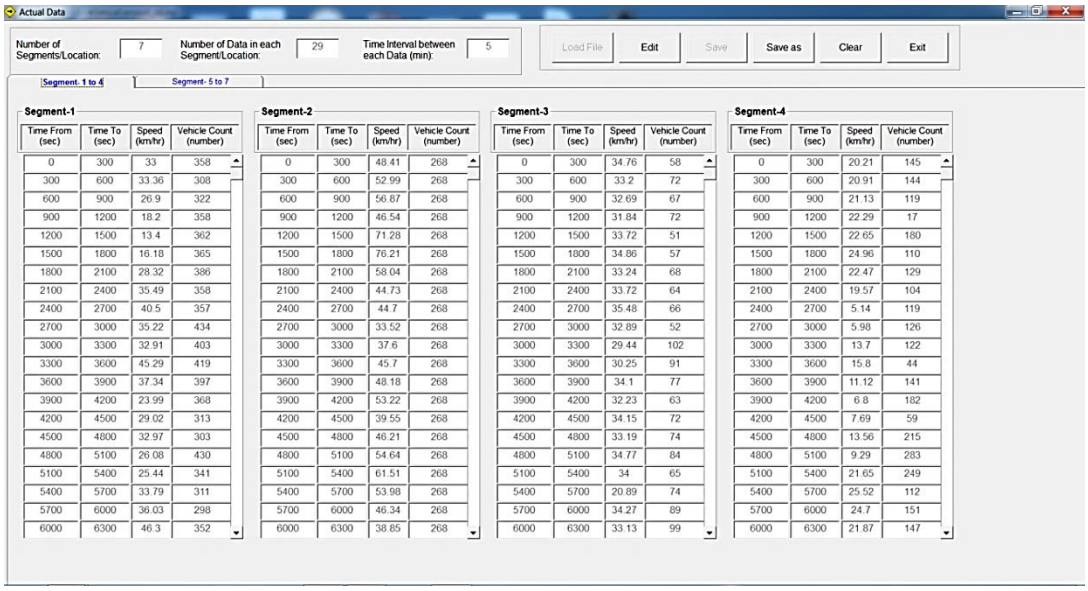

Segment-1				Segment-2				Segment-3				Segment-4			
Time From (sec)	Time To (sec)	Speed (km/hr)	Vehicle Count (number)	Time From (sec)	Time To (sec)	Speed (km/hr)	Vehicle Count (number)	Time From (sec)	Time To (sec)	Speed (km/hr)	Vehicle Count (number)	Time From (sec)	Time To (sec)	Speed (km/hr)	Vehicle Count (number)
0	300	33	358	0	300	48.41	268	0	300	34.76	58	0	300	20.21	145
300	600	33.36	308	300	600	52.99	268	300	600	33.2	72	300	600	20.91	144
600	900	26.9	322	600	900	56.87	268	600	900	32.69	67	600	900	21.13	119
900	1200	18.2	358	900	1200	46.54	268	900	1200	31.84	72	900	1200	22.29	17
1200	1500	13.4	362	1200	1500	71.28	268	1200	1500	33.72	51	1200	1500	22.65	180
1500	1800	16.18	365	1500	1800	76.21	268	1500	1800	34.86	57	1500	1800	24.96	110
1800	2100	28.32	386	1800	2100	58.04	268	1800	2100	33.24	68	1800	2100	22.47	129
2100	2400	35.49	358	2100	2400	44.73	268	2100	2400	33.72	64	2100	2400	19.57	104
2400	2700	40.5	357	2400	2700	44.7	268	2400	2700	35.48	66	2400	2700	5.14	119
2700	3000	35.22	434	2700	3000	33.52	268	2700	3000	32.89	52	2700	3000	5.98	126
3000	3300	32.91	403	3000	3300	37.6	268	3000	3300	29.44	102	3000	3300	13.7	122
3300	3600	45.29	419	3300	3600	45.7	268	3300	3600	30.25	91	3300	3600	15.8	44
3600	3900	37.34	397	3600	3900	48.18	268	3600	3900	34.1	77	3600	3900	11.12	141
3900	4200	23.99	368	3900	4200	53.22	268	3900	4200	32.23	63	3900	4200	6.8	182
4200	4500	29.02	313	4200	4500	39.55	268	4200	4500	34.15	72	4200	4500	7.69	59
4500	4800	32.97	303	4500	4800	46.21	268	4500	4800	33.19	74	4500	4800	13.56	215
4800	5100	26.08	430	4800	5100	54.64	268	4800	5100	34.77	84	4800	5100	9.29	283
5100	5400	25.44	341	5100	5400	61.51	268	5100	5400	34	65	5100	5400	21.65	249
5400	5700	33.79	311	5400	5700	53.98	268	5400	5700	20.89	74	5400	5700	25.52	112
5700	6000	36.03	298	5700	6000	46.34	268	5700	6000	34.27	89	5700	6000	24.7	151
6000	6300	46.3	352	6000	6300	38.85	268	6000	6300	33.13	99	6000	6300	21.87	147

(b)

Figure 3.3: (a) VISSIM snapshot of the 3.26 km study site and (b) Input for field measured.

3.3.1. Traffic data

Total seven video cameras are installed for data collection details of which have been explained in section 2.6 of Chapter 2. From practical considerations, a 2.5-hour dataset retrieved from the recorded database is used as the field measured value (Figure 3.3b) in the VISCAL system.

Note that, for each of the optimization algorithm in VISCAL, various calibration tests are carried out using different values for the algorithm parameters and only the best results are presented below (Figure 3.4). The parameter values in two algorithms (GA and SA) is kept identical to reduce the difference in error caused by randomness in the initial parameter selection, whereas for SPSA, optimal algorithm parameter set is used for individual objective function following the guidelines specified by Spall (1992).

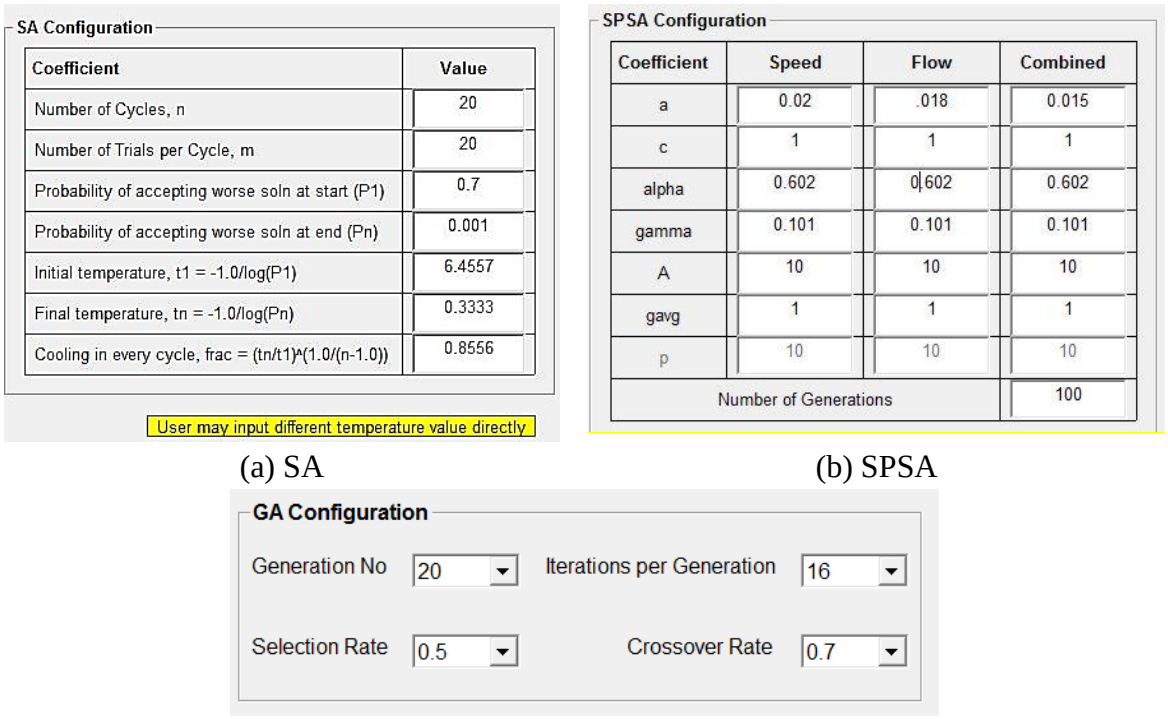

(a) SA (b) SPSA

(c) GA

Figure 3.4: VISCAL Input Windows for(a) SA (B) SPSA (C) GA Algorithm Operators.

3.3.2. Selection of sensitive VISSIM parameters

A sensitivity analysis is performed to find parameters that have significant effect on the VISSIM model outputs (e.g. speed, and flow). VISCAL automatically starts the calibration process after performing the sensitivity analysis.

Note that VISCAL has the capability to perform calibration operation on the driving behavior parameters including car following, lane changing, lateral, and signal control. However, for this study only the car following parameters are calibrated considering the Wiedemann 99 model recommended for freeway traffic operation. The values of CC0 to CC9, suggested for the freeway traffic, are obtained from Park and Qi (2006).

Table 3.1: VISSIM parameters affecting speed and flow

Parameter	Description	Unit	Default	Allowable Min.-Max
CC0	Defines the desired distance between stopped cars	m	1.50	1.0-2.0
CC1	The time (in seconds) that a driver wants to keep. The higher the value, the more cautious the driver is	s	0.90	0.5-3.0
CC2	Restricts the longitudinal oscillation or how much more distance than the desired safety distance a driver allows before he intentionally moves closer to the car in front	m	4.00	0~15.0
CC3	Threshold for entering Following, controls the start of the deceleration process	-	-8.00	-30.0-0
CC4	Negative Following Threshold	-	-0.35	-1.0~0
CC5	Positive Following Threshold	-	0.35	0~1
CC6	The Influence of distance on speed oscillation while in following process	-	11.44	0~20
CC7	Actual acceleration during the oscillation process	m/s^2	0.25	0~1.0
CC8	Desired acceleration when starting from standstill	m/s^2	3.50	1.0~8.0
CC9	Desired acceleration at 80 km/h	m/s^2	1.50	0.5~3.0

3.3.3. Objective functions

The calibration tool, VISCAL offers flexibility by coding four choices for objective function into the system. However, for this study three choices (speed, flow, and multi-objective criteria) are considered to evaluate the performance of the tool for freeway environment. Simulations runs are performed in a windows environment (Intel Xeon CPU E3-1220 v2, 3.1GHz, and 16.0 GB of memory). The calibration process, including the connectivity between the micro-model and the optimization algorithms, has been programmed in MATLAB.

3.3.3.1. Single criteria objective function

The optimization operation of SA, GA, and SPSA is performed on the same search space to draw a comparison between the outcomes. The improvement of the speed based objective function at each iteration of the calibration process is presented in Figure 3.5(a) and the results are summarized in Table 3.2. The value of the objective function for the default parameter set in this case is 81.82%. Results shows that SA reaches best fitness value (FV) of 36.34% after 356 iterations, GA displays a FV of 38.11% after 108 iterations, and SPSA shows the least FV of 39.32% for only 16 iterations.

The fitness value of SPSA shows a sudden drop during the first few iterations and then continues as a noisy trajectory on the graph (Figure 3.5a). This is because of the application of stochastic perturbation on all micro-model parameters over the next iterations to obtain the gradient approximation.

SA outperformed GA and SPSA for speed-based objective function. The evolution of model parameters during each iterations of SA is presented in Figure 3.5(b). SA represents the temperature deviation “hot from cold” sequence in the contour plot for the micro-simulation parameters. The progression of the parameters show numerous local optima marked by small “valleys”, indicating that the lowest FV is within the

close vicinity of the local minima. Presence of these small valleys proves that SA has a provision to accept a fraction of inferior solutions to escape local optima in search of global optima.

The improvement of the flow based objective function at each iteration of the calibration process is presented in Figure 3.5(c) and the results are summarized in Table 3.2. The value of the objective function for the default parameter set in this case is 35.04%. Detail analysis shows that GA achieves best FV of 29.93% after 110 iterations, SA displays a FV of 30.58% after 120 iterations, and SPSA shows the least FV of 31.72% for 85 iterations. GA outperformed other two techniques for flow based objective function.

Visualization of the fitness values shows that SPSA remains oscillatory and reflects a sharp fall of FV after approximately 60 iterations during the convergence process (Figure 3.5(c)). GA shows a gradual convergence with very little oscillation of the fitness value whereas SA shows sharp fall and rise after every 20 iterations before converging towards the optimal parameter set.

3.3.3.2. Multi-criteria objective function

Multi-criteria objective function based calibration is performed by VISCAL to test the FV with respect to two traffic attributes, specifically speed and flow. The value of the objective function for the default parameter set in this case is 49.31%. Detail analysis shows that GA achieves best FV of 31.72% after 122 iterations, SA displays a FV of 32.31% after 377 iterations, and SPSA shows the least FV of 32.63% for 42 iterations. Visualization of the fitness values shows that SPSA fall sharply at the beginning and reflect a noisy trajectory of FV after approximately 25 iterations during the convergence process (Figure 3.5d). GA shows a sudden rise at the beginning then gradually converges to the solution with very little oscillation of the fitness value

whereas SA shows sharp rise and fall after every 40 iterations approximately before converging.

For multi-criteria (speed-flow) based evaluation, GA outperformed SA and SPSA. The progression of micro-simulation parameters during each iterations of GA is presented in Figure 3.5(e). A close examination of the successive solutions indicates that, in the beginning of the calibration, the population includes randomly generated individuals; over the iterations, the population evolves towards better solutions and in the very last iteration, the majority of the population individuals are virtually identical.

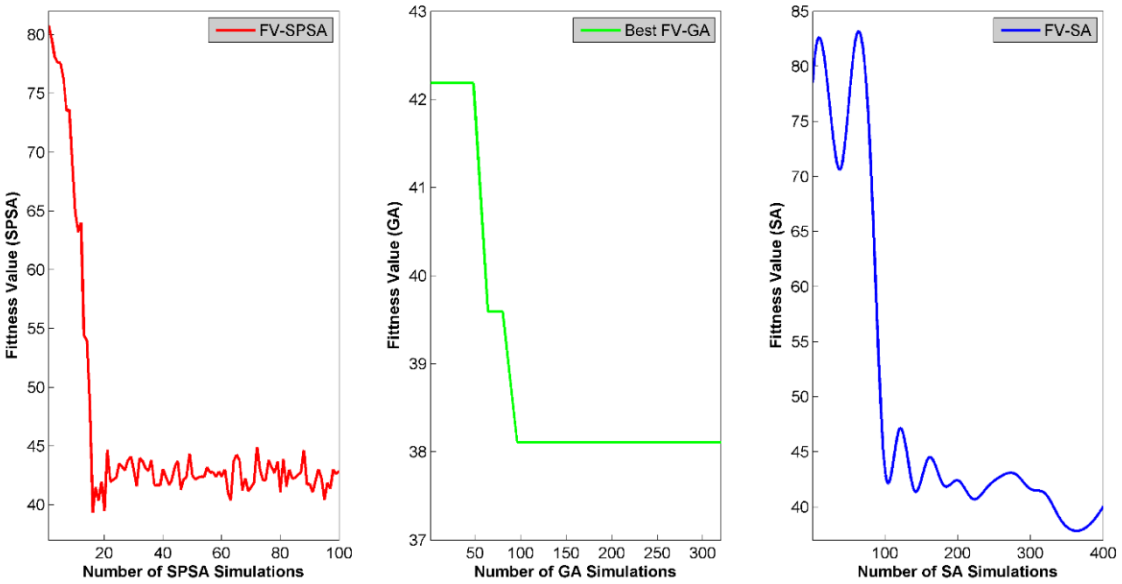

(a)

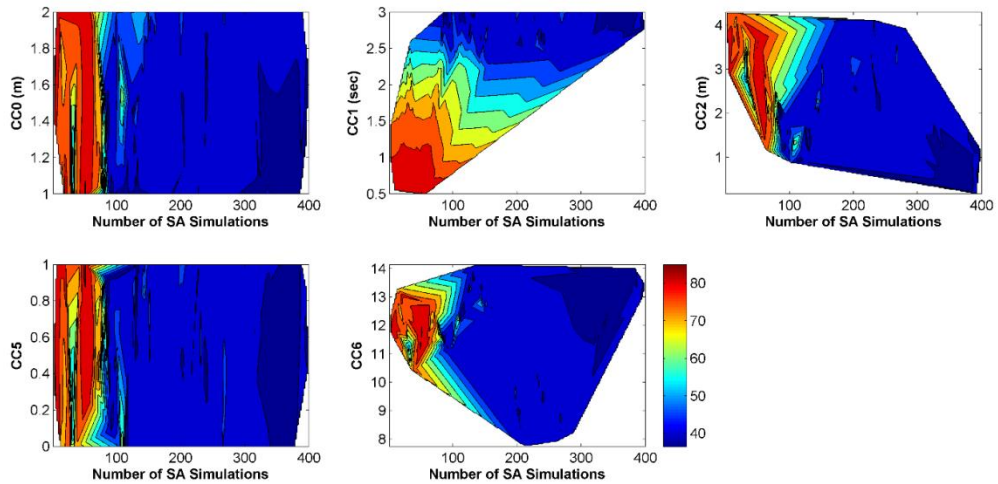

(b)

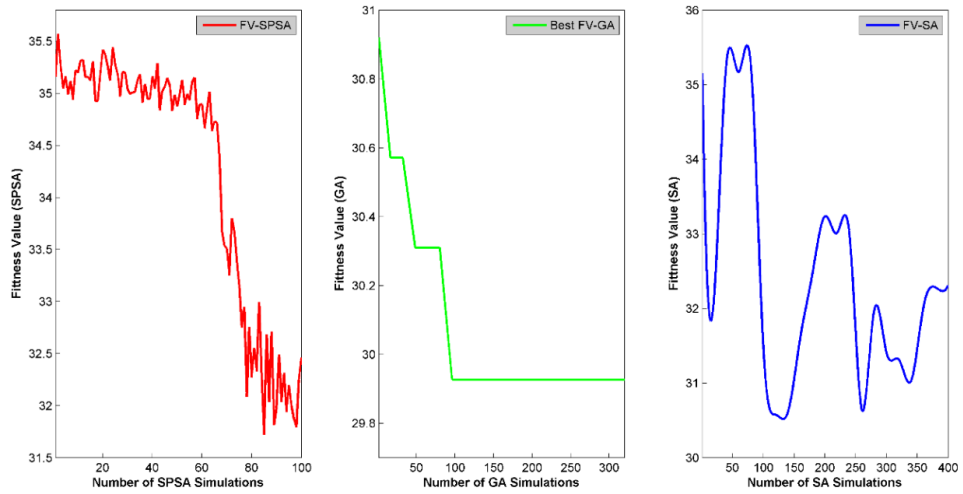

(c)

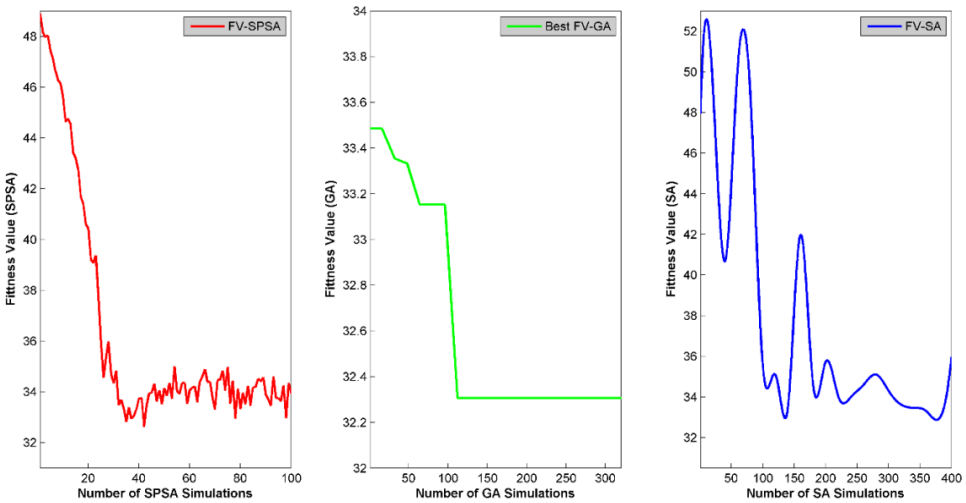

(d)

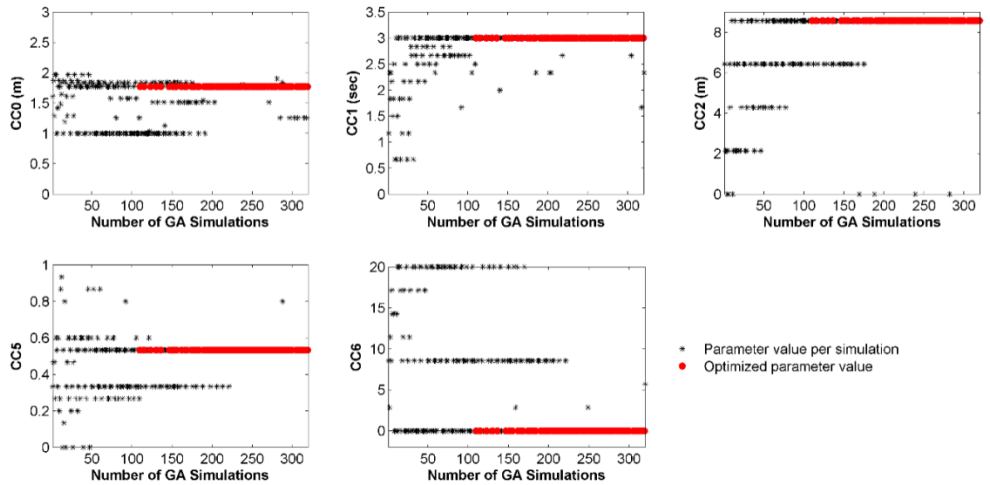

(e)

Figure 3.5: (a) Speed based parameter calibration convergence diagram; (b) evolution of micro-model parameters over iterations of SA; (c) flow based parameter calibration convergence diagram; (d) multi-objective criteria (speed-flow) based parameter calibration convergence diagram; (e) evolution of micro-model parameters over iterations of GA.

Table 3.2: Optimized parameter set

Objective Function	Algorithm	CC0	CC1	CC2	CC5	CC6
Speed	GA	1.77	2.50	4.29	0.60	3.00
	SPSA	1.53	2.49	4.57	0.25	12.16
	SA	1.01	2.93	0.71	0.06	13.51
Flow	GA	1.77	3.00	8.57	0.53	0
	SPSA	1.68	2.94	4.50	0.29	11.52
	SA	2.00	2.99	2.97	0.13	8.13
Multi-objective	GA	1.10	2.67	2.14	0.80	5.71
	SPSA	1.75	2.45	4.30	0.44	12.09
	SA	2.00	2.48	2.59	0.91	10.37

Generally, there is a trade-off between the quality of the solution and the time available for calibration. Often in research projects and studies there is a time limit that is directly related to cost from practical considerations. VISCAL gives the user such flexibility that the entire calibration process can be oriented towards quality of the solution while compromising time or vice-versa. This trade-off between time and quality is reflected in the case study of the freeway scenario.

For instance, Table 3.3 shows that SPSA converged to an optimal solution for speed-based evaluation by few iterations (only 16) compared to other two techniques (108, and 356 for GA and SA, respectively). However, the quality of the output, FV in this case is found to be least from others.

Table 3.3: Computational complexity of different algorithm

Objective Function	Algorithm	Total Number of FV Evaluation	Converge at	Optimal Fitness Value (%)	CPU Run-time (hr.)
Speed	GA	320	108	38.11	44.5
	SPSA	100	16	39.32	39
	SA	400	356	36.34	46
Flow	GA	320	110	29.93	53
	SPSA	100	85	31.72	40.5
	SA	400	120	30.58	55
Multi-objective	GA	320	122	32.31	49
	SPSA	100	42	32.63	44
	SA	400	377	32.92	55

Note that the complexity of the calibration process depends on the number of involved micro-simulation parameters. This implies that the increase in the number of parameters has a substantial effect on the computational time and outcome of the calibration process.

3.3.3.3. Sensitivity of objective function

VISCAL features allow a sensitivity test of the results obtained from different objective function options. Note that three objective function options are used to carry out the analysis of the freeway scenario: (1) speed; (2) flow; (3) multi-criteria (speed-flow). From the result, only the best heuristic algorithm for each objective function is selected. For instance, SA is selected for speed-based evaluation; whereas GA is selected for flow-based and multi-objective based evaluation.

Table 3.4: Sensitivity of the objective function

Optimization Criteria	**Algorithm**	**Sensitivity Criteria**	**MAPE (%)**	**Error compared to defaults observed**
VISSIM Defaults Observed	N.A.	Speed Sensitivity	81.82	N.A.
		Flow sensitivity	35.04	N.A.
Speed	SA	Speed Sensitivity	36.34	55.59%
		Flow sensitivity	52.74	*-50.51%*
Flow	GA	Speed Sensitivity	34.01	58.43%
		Flow sensitivity	29.93	14.60%
Multi-objective	GA	Speed Sensitivity	31.98	60.92%
		Flow sensitivity	29.77	15.07%

Note: In the table, the italic number refers to a deterioration in model performance compared to the VISSIM defaults observed. N.A. denotes non-applicable.

Table 3.4 shows that the combination of speed and SA provide good estimation for speed. However, show poor combination for flow estimation. Combination of flow and GA shows good estimates of speed as well as for flow. Interestingly, the

combination of multi-objective criteria and GA provides the best estimates for speed and flow in the freeway scenario.

3.4. Conclusions

Calibration is a complex and tedious process involving large set of micro-simulation parameters for a particular network. Previously several studies have added new techniques and automation to the calibration process (Ma and Abdulhai, 2002; Balakrishna et al., 2007; Paz et al., 2014). However, the use of generic calibration tool for any micro-simulation model is very limited in the literature that is particularly important and invaluable to any practitioner or researcher considering the complexity, cost, and time associated with the calibration process.

This study develops a generic calibration tool, VISCAL for microscopic simulation parameters in VISSIM environment. The optimization system of the tool is based on three heuristic algorithms: (a) GA; (b) SPSA; (c) SA. This tool offers greater flexibility to the user by providing control on every aspect of the calibration process. VISCAL includes significant features consisting of the ability to test the significance of the appropriate decision parameter set for a particular network, to determine the most suitable objective function to reflect network characteristics, and to check the suitability of any of the three heuristic optimization algorithms for a particular network. Note that VISCAL can be used to calibrate any type (rural, urban etc.) and extent (large, medium etc.) of network. However, in this study the operation of the tool is tested by a dataset obtained from a 3.26 km section of a freeway of Dhaka, Bangladesh.

Three objective functions (speed, flow, and speed-flow) from four options coded in the VISCAL system are considered for the freeway scenario. Results show that compared to GA and SA, SPSA generally obtained an acceptable set of parameters in

much less time (Table 3.3). However, it should be noted that one particular optimization algorithm would not be able to outperform the other two in all cases. For example, GA achieved best FV (MAPE) for flow based evaluation as well as multi-criteria (speed and flow) evaluation whereas; SA achieved best FV for speed evaluation of the same network.

The trade-off between time and quality is also reflected in the analysis of the freeway scenario (Table 3.3). For instance, the SPSA converged to an optimal solution for speed-based evaluation by few iterations (only 16) compared to other two techniques (108, and 356 for GA and SA, respectively). However, the quality of FV in this case is found to be least from others. The sensitivity analysis of the objective function results showed that the combination of multi-objective criteria and GA provides the best estimates for speed and flow in the freeway scenario.

For future research options, two-way ANOVA can be used to determine the significant parameters for a particular microscopic model. The existing features can be improved by using parallel processing to facilitate simultaneous run of all the three-optimization algorithms and four objective function options to reduce the computational time.

3.5. References

1. Park, B., and H. Qi. Development and Evaluation of a Procedure for the Calibration of Simulation Models. In Transportation Research Record: Journal of the Transportation Research Board, No. 1934, Transportation Research Board of the National Academies, Washington, D.C., 2005, pp. 208–217.
2. Kim, S. J., Kim, W., and Rilett, L. R. Calibration of Micro Simulation Models using Non Parametric Statistical Techniques. Transportation Research Record: Journal of Transportation Research Board, No.1935, Transportation Research Board of the National Academies, Washington, D.C., 2005,pp.111-119.

3. Ma, J., Dong, H., and Zhang, H. Calibration of micro-simulation with heuristic optimization methods. Transportation Research Record: Journal of the Transportation Research Board, No. 1999, Transportation Research Board of the National Academies, Washington, D.C., 2007, pp. 208–217.
4. Ma, T., and Abdulhai, B. Genetic Algorithm-Based Optimization Approach and Generic Tool for Calibrating Traffic Microscopic Simulation Parameters. Transportation Research Record: Journal of Transportation Research Board, No.1800, Transportation Research Board of the National Academies, Washington, D.C., 2002, pp.6-15.
5. Park, B., and Yun, I. Evaluation of stochastic optimization methods of traffic signal control settings for coordinated actuated signal systems. Presented at 85th Annual Meeting of Transportation Research Board, 2006.
6. Balakrishna, R., Antoniou, C., Ben-Akiva, M. E., Koutsopoulos, H. N., and Wen, Y. Calibration of Microscopic Traffic Simulation Models: Method and Application. Transportation Research Record: Journal of the Transportation Research Board, No. 1999, Transportation Research Board of the National Academies, Washington, D.C., 2007, pp. 198–207.
7. Paz, A., Molano, V., and Khan, A. Calibration of Micro-Simulation Traffic-Flow Models Considering All Parameters Simultaneously. Presented at 93rd Annual Meeting of Transportation Research Board,2014,pp112-134.
8. Toledo, T., Ben-Akiva, M. E., Darda, D., Jha, M., and Koutsopoulos, H. N. Calibration of Microscopic Traffic Simulation Models with Aggregate Data. Transportation Research Record: Journal of Transportation Research Board, No. 1876, Transportation Research Board of the National Academies, Washington, D.C., 2004,pp.10-19.

9. Stevanovic, A., Martin, P., and Stevanovic, J. VisSim-based genetic algorithm optimization of signal timings. Transportation Research Record: Journal of the Transportation Research Board, No.2035, Transportation Research Board of the National Academies, Washington, D.C., 2007, pp.59-68.
10. Gardes, Y., May, A. D., Dahlgren, J., and Skabardonis, A. Freeway Calibration and Application of the PARAMICS Model. Presented at 81st Annual Meeting of the Transportation Research Board, Washington, DC. 2002.
11. Lee, D. H., Yang, X., and Chandrasekar, P. Parameter Calibration for PARAMICS Using Genetic Algorithm. Presented at 80th Annual Meeting of the Transportation Research Board, Washington, DC. 2001.
12. Kim, K. O., and Rilett, L. R. Simplex-based Calibration of Traffic Micro simulation Models with Intelligent Transportation Systems Data. Transportation Research Record: Journal of Transportation Research Board, No. 1855, Transportation Research Board of the National Academies, Washington, D.C., 2003, pp.80-89.
13. Schultz, G., and Rilett, L. R. Analysis of Distribution and Calibration of Car-Following Sensitivity Parameters in Microscopic Traffic Simulation Models. Transportation Research Record: Journal of Transportation Research Board, No. 1876, Transportation Research Board of the National Academies, Washington, D.C., 2004, pp.41-51.
14. Jha, M., Gopalan, G., Garms, A., Mahanti, B. P., Toledo, T. and Ben-Akiva, M. E. Development and Calibration of a Large-Scale Microscopic Traffic Simulation Model. Transportation Research Record: Journal of Transportation Research Board, No. 1876, Transportation Research Board of the National Academies, Washington, D.C., 2004, pp.121-131.

15. Hourdakis, J., Michalopoulos, P. G., and Kottommannil, J. A Practical Procedure for Calibrating Microscopic Traffic Simulation Models. Transportation Research Record: Journal of Transportation Research Board, no. 1852, Transportation Research Board of the National Academies, Washington, D.C., 2003, pp. 130-139.
16. Dowling, R., A. Skabardonis, J. Halkias, G. McHale, and G. Zammit. Guidelines for calibration of micro simulation models: framework and application. Transportation Research Record: Journal of Transportation Research Board, No. 1876, Transportation Research Board of the National Academies, Washington, D.C., 2004, pp.1-9.
17. Paz, A., Molano, V., Martinez, E., Gaviria, C., and Arteaga, C. Calibration of traffic flow models using a memetic algorithm. Transportation Research Part C: Emerging Technologies, Vol. 55, 2015, pp. 432-443.
18. Spall, J. C. Multivariate stochastic approximation using a simultaneous perturbation gradient approximation. IEEE Transactions on Automatic Control, Vol. 37, No. 3, 1992, pp. 332:341.
19. Spall, J. C. Implementation of the simultaneous perturbation algorithm for stochastic optimization. IEEE Transactions on Aerospace and Electronic Systems, Vol. 34, No.3, 1998, pp. 817:823.
20. Goldberg, D. E. Genetic Algorithms in Search Optimization and Machine learning. Addison-Wesley. 1989.
21. Holland, J. H. Adaptation in natural and artificial systems: an introductory analysis with applications to biology, control, and artificial intelligence. University of Michigan Press, Ann Arbor, 1975
22. Metropolis, N., Rosenbluth, A., Rosenbluth, M., Teller, A., and Teller, E. Equations of state calculations by fast computing machines. Journal of Chemical Physics, Vol. 21, 1953, pp.1087-1092.

23. Kirkpatrick, S., Gelatt, C. D., and Vecchi, M. P. Optimization by simulated annealing. Science, Vol. 220, 1983, pp. 671–680.

24. Venkataraman, P. Applied Optimization with MATLAB Programming. A Wiley-Interscience Publication, John Wiley & Sons, Inc. 2001, pp.201-213.

25. Park, B., and Qi, H. Microscopic simulation model calibration and validation for freeway work zone network-a case study of VISSIM. Presented at IEEE Intelligent Transportation Systems Conference. IEEE, 2006, pp58-69.

CHAPTER 4: H-CTM FOR SIMULATING NON-LANE-BASED HETEROGENEOUS TRAFFIC‡

4.1. Introduction

Traffic simulation models are widely recognized as useful tools in transportation planning and operations (Gazis, 2002). In some cases, these models are used as a dynamic decision making aid. Considering the level detail of the models at which these represent traffic dynamics, are classified as microscopic, mesoscopic and macroscopic (Cousins et al., 2009). The choice of any one of these types of simulation models is based on needs, goals and scale of the analysis. Among those, macroscopic traffic flow models play an irreplaceable role for real-time traffic state estimation and short-term traffic prediction. Generally these models consider the traffic flow as a compressible fluid and evaluate the traffic states with the help of aggregated variables e.g. average speed, flow and density. Compared to microscopic models, these can simulate traffic state with lower number of parameters which are relatively easier to calibrate and require low computational effort for real-time application. On the contrary, the microscopic models produce output at high levels of reliability, but require correspondingly greater levels of input details and computing time. Thus, macroscopic traffic flow models are generally preferred over microscopic models for dynamic traffic state estimation.

For this study, CTM is chosen as the base model (Daganzo, 1994), which is one of the most frequently used macroscopic models for traffic simulation. It is a first order discrete and deterministic model which comply with hydrodynamic model. CTM

‡ This chapter is a modified version of a manuscript submitted in Transportation Letters (under review). Muniruzzaman, S. M., Kays, H. M. I., Hadiuzzaman, M., Shimu, T. H., Rahman, M. M. "H-CTM for Simulating Non-Lane-Based Heterogeneous Traffic".

defines three simple boundary conditions to evaluate cell to cell flow, density and speed in a very simplified way. Studies show that traffic state estimated by CTM are proven to be very close to the field data (Lin and Ahanotu, 1995). Different extensions and modifications of this model have been proposed to adapt various traffic engineering challenges, such as modeling arterial with signalized intersection (Feldman and Maher 2002), ramp metering, dynamic signal control (Lo, 2001), travel time prediction (Skabardonis and Geroliminis, 2005), queuing control (Almasri and Friedrich, 2005), dynamic route choice (Kimms and Maassen, 2011), dynamic traffic assignment (Lo, 1999) and capacity estimation after applying VSL (Hadiuzzaman and Qiu, 2013).

The parameter values used in CTM are calibrated from FD, which stands for relationship between speed-flow-density. The original work of CTM which is developed by Daganzo (1994) considered isosceles trapezoidal shaped flow-density relationship which was further modified with piecewise linear triangular shaped FD. Different shapes of FD are proposed for different traffic conditions depending upon vehicular and geometric characteristics. However, our scope of study is limited to heterogeneous non-lane-based traffic condition which shows different speed-flow-density characteristics unlike any traditional FD. Unfortunately, very few field studies are found in literature for this investigation.

The goal of this study is to develop H-CTM (Heterogeneous-Cell Transmission Model) for heterogeneous non-lane-based traffic which is expected to estimate and predict traffic state under prevailing traffic condition accurately.

The study is structured as follows: Section 4.2 reviews some previous works on macroscopic modeling and application; Section 4.3 presents the study area and data collection process; Section 4.4 investigates the structures of the FD to be used in the new model; Section 4.5 presents the mathematical formulation of basic CTM; In

Section 4.6, the proposed H-CTM is described with mathematical explanation; Section 4.7 contains the details on model calibration; validation and performance with sensitivity analysis for field applicability are discussed in Section 4.8 and finally, concluding remarks and future research scopes are presented in Section 4.9.

4.2. Literature Review

First order macroscopic flow model is used to describe the flow behavior of aggregated traffic, which result in simulating the macroscopic parameters like average speed, flow and density. This kind of modeling approach started with the noble work of Greenshilds on FD which established the interactions between the average speed-flow-density parameters (Greenshields et al., 1935). Later on, continuum concept on macroscopic flow behavior was first illustrated in LWR model (Lighthill and Whitham, 1955), which described the time and space derivatives as of order one along with speed and flow with simple linear relationship. This model also introduced shockwave speed of steady state type but couldn't explain other phenomenon like steady-state speed-density relationship and discontinuities or heterogeneity of traffic. Another limitation of LWR model is that, outflow is considered as a function of occupancy of the previous section from which it is emitted, but do not consider the preceding downstream occupancy (Mohan and Ramadurai, 2013). Sometimes it does not guarantee the convergence, like stopped traffic is predicted not to flow into an empty freeway (Daganzo, 1994). To address these issues, Daganzo (1994), formulated the Cell Transmission Model (CTM) as a discretization of first order LWR model, a special case of Godunov's scheme (Lebacque, 1996). The model divides the freeway stretch into number of cells with defined length which can capture light traffic in one tick of time and use a piecewise linear relationship between traffic flow and traffic density by triangular fundamental diagram. Though the basic CTM can capture

macroscopic traffic behavior in freeway, it cannot actually simulate heterogeneous condition.

Tuerprasert et.al. (2008) presented a new mathematical model named Multiclass M-CTM based on the basic CTM. In this model, the researchers incorporated mixed composition of vehicle types (e.g. truck, car, bus or smaller vehicles) and compared performances of basic CTM, M-CTM and microsimulator MITSIM. From the study, it is found that M-CTM is more accurate than basic CTM, particularly in uncongested networks with non-stationary vehicle composition. But the non-lane-based behavior of traffic was not included in the model. Moreover, separating different class of vehicle employs more computational effort.

Chen et.al. (2010) developed a location specific CTM (LS-CTM) of freeway traffic based on the observed variability of FD both along and across freeway segments. This model extended the original CTM by defining various shapes like triangular, inverse lambda, trapezoidal shape of FD of different lane to reproduce more complex traffic phenomena, including capacity drops, lane-by-lane interaction, nonhomogeneous wave velocities, and temporal lags. A field test on a Canadian freeway showed that the spatio-temporal evolutions of traffic flow simulated by LS-CTM can describe the traffic dynamics near bottlenecks more precisely than the original model. The model is close to the scope of H-CTM, but the lane specific FD is not very influential to heterogeneous non-lane-based traffic nature rather H-CTM can simulate this traffic state.

Ngoduy (2011) noticed that most of the existing first order continuum model cannot display the class-wise (i.e. car, bus etc.) widely scattered flow-density relationship. He found the reason behind this nature to be random variations in driving behavior. Hence he proposed stochastic FD to model this randomization. He adapted LWR continuum model for numerical simulation with global parameters and the study

revealed that the proposed model is able to capture the real traffic dynamics but is associated with large computational complicacy. Also the model performance in discrete model has not been tested with this methodology.

Liu, Wang et al. (2015) provided an analytical formulation for a mixed traffic system that includes cars and buses, which realistically replicates moving bottlenecks (MB) as well as route choice. They modified the LCTM to BUS-CTM and made it to recognize speed differentials between the free-flow speed of buses and cars by a set of defined equations (Daganzo, 1999). Also a set of speed ratios were considered between the vehicle classes, where the free-flow speed of the fastest vehicle class was not more than two times than that of the slowest vehicle class. In addition, they added capacity reduction phenomenon in CTM caused by buses hence replicating the moving bottlenecks. Using these assumptions, the model divided the original cells into sub-cells to account for the speed differentials of the vehicle classes during simulation. The numerical simulation of the model suggests that the BUS-CTM obtains more realistic results as compared with the application of the basic CTM in a mixed car–bus transportation system. Furthermore this methodology also incorporated computational complexity by considering vehicle of two different speed classes. Heterogeneous traffic comprising of 6 to 8 different speed classes of vehicles yields more complex equations while the H-CTM proposed in this paper have both simplification and versatility.

Zhang et al. (2015) proposed a model integrating a CTM with the Macroscopic FD (MFD) for urban networks and analyzed its effect by testing the proposed model and its computational efficiency in evacuation. In this study, the researchers classified the roadway into two types of networks: one is modeled with CTM, and the other one with large cell maintaining properties of the MFD. From the obtained results, it is found that the model is able to capture the shockwave and reproduce the spatio-

temporal characteristics of the evacuation traffic. Nevertheless the model is extremely biased with the evacuation only where the destination of the traffic is well defined. Moreover, in extreme situation the traffic behavior also changes compared to day-to-day habitual scenario. Though the model incorporates MFD for evacuation, this model is ineffectual in emulating heterogeneous non-lane based traffic state due to ignoring traffic class discrepancies and lane-discipline in the scope of study.

Bhavathrathan and Mallikarjuna (2012), observed that, the traffic streams in the Indian subcontinent consists of numerous vehicle classes, i.e., heterogeneous traffic with complex flow interactions. Even the recent multiclass models are inadequate to represent these complex interactions. Hence, it necessitates the development of appropriate macroscopic flow model for simulation of traffic in this nature.

Among various studies on FD, Hossain et al. (2016) developed FD for heterogeneous traffic where the authors considered vehicles comprising of mix speed classes and having non-lane-based traffic behavior. The study site for the research was in Dhaka, Bangladesh N-3 Highway where a total 3.26 km of roadway was discretized into five links and the traffic data was collected with five video cameras. For collecting on- and off-ramp data, separate video cameras were installed. For extracting high resolution traffic data from the video footages of the cameras, an object detection algorithm was developed based on the Background Subtraction (BGS) technique for image processing (Hadiuzzaman, 2016). From this study, it is found that, heterogeneous non-lane-based traffic follows non-linear speed-density relationship. Though the constants are not equal in different links, the FD follows 3-degree polynomial structure for capturing traffic dynamics.

However, no attempt was made to use CTM for heterogeneous traffic condition till date to the authors' best knowledge. This paper proposes H-CTM that can capture the stated traffic condition.

4.3. Methodology

4.3.1. Study area

For the experimental setup, a section of the Dhaka-Mymensingh Highway (N3) is chosen as the study site (Figure 4.1). It is one of the major arterial roads in Dhaka city, details of which have been discussed in section 2.6 of Chapter 2. The geometric configuration and traffic characteristics of the site make it an ideal study location for non-lane-based heterogeneous uninterrupted traffic condition.

4.3.2. Data collection

Collection of high resolution data in heterogeneous traffic condition was the first challenge for developing the model. For this seven high resolution video cameras are installed in different locations of the test site as described in Chapter 2.

The selected site is discretized into five cells. The length of each cell is chosen so that the light vehicle cannot pass the cell distance within one simulation time step. The cell sizes vary from 320 m to 920 m. The off-ramp is located at the end of cell 2 and the on-ramp is located at the beginning of cell 3 as shown in Figure 4.1. Five video cameras are installed along the main traffic stream; each one is at approximately mid-length of each link. Therefore, the collected video data can be considered representatives in capturing the traffic states prevailing in each cell. Background Subtraction (BGS) technique is used to extract high resolution data from the videos (Hadiuzzaman, 2016).

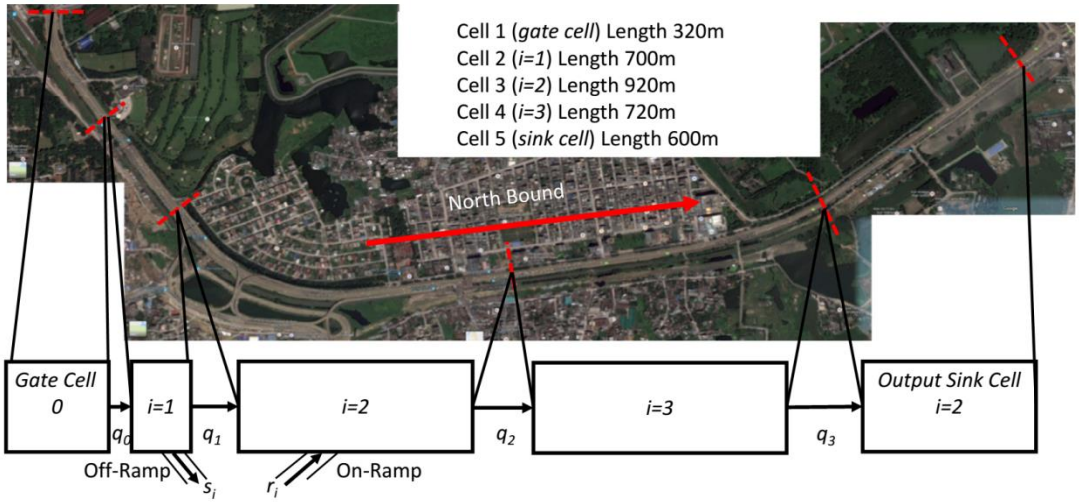

Figure 4.1: The 3.26 km stretch study site (Map courtesy: Google Map).

4.4. Fundamental Diagram

Numerous attempts are made to investigate the shape of FD for different traffic characteristics and geometric layout. For instance, Greenberg proposed logarithmic model (Greenberg, 1959), which was obtained by the integration of car-following model, Underwood developed exponential v-ρ model (Underwood, 2008) based on the results of traffic studies on the Merritt Parkway in Connecticut, Zhang (1998) proposed one-parameter polynomial model, on the other hand Papageorgiou et al. (1990) proposed the exponential model which incorporated data fitting flexibility to the Underwood model. Detailed study on FD can be found in the literature of Kühne and Gartner.

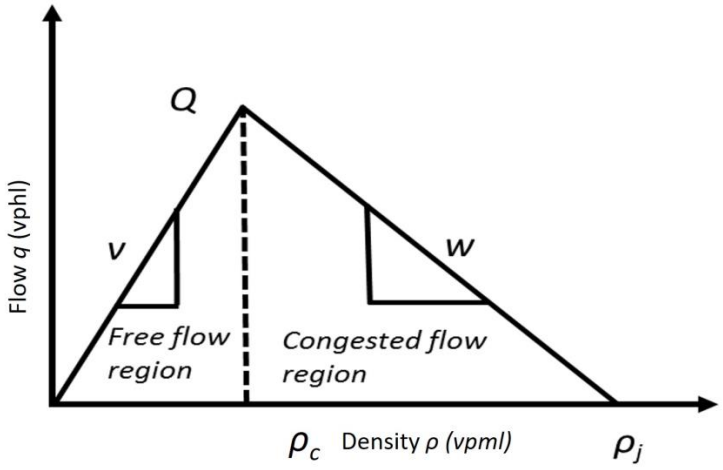

Figure 4.2: The triangular qualitative flow-density diagram, considered for the basic CTM.

The basic CTM considers the triangular flow-density relationship where the traffic state is divided into two region: the free-flow region and the congested-flow region (Figure 4.2). The model considers that, within the free-flow region, flow increases with the increment of density up to a critical point (ρc) and reaches a maximum value Q while maintaining a constant speed (v) throughout the entire stretch. After transition from free-flow to congested-flow region, the model considers the effect of backward forming shockwave (-w) which also remains constant from critical density ρc to jam density ρj. With this, the model simulates the effect of discontinuity (Equation 7).

For describing the nature of FD in heterogeneous non-lane-based traffic condition, Hossain et al. (2016) proposed a modified shape of FD, which is adopted in this paper. They collected high resolution 20 sec 2.5 hours data from traffic survey and fitted the field measured data with the well-established structure of FD model. They tested the structure of FD for linear, logarithmic, exponential and polynomial of 2nd and 3rd degree equations. The FD performances were measured based on R2 and RMSE values. From performance standards, 3rd degree polynomial equations are found to be the most optimized form of FD, though the constant term vary with the

cells (Equations 1, 2, 3). Because the speed and density characteristics are found changing with locations, vehicular interactions and also with geometric layout of roadway segments e.g. roadside friction from pedestrians, bus-bay, on- and off-ramp etc., therefore, these equations (Equations 1, 2, 3) could capture the stated field traffic condition more precisely.

For Cell 2: $$v = -2.486\times10^{-5}\rho^3 + 0.0084\rho^2 - 1.035\rho + 55.44 \quad (1)$$

For Cell 3: $$v = -1.029\times10^{-6}\rho^3 + 0.008467\rho^2 - 0.2379\rho + 27.69 \quad (2)$$

For Cell 4: $$v = -1.921\times10^{-6}\rho^3 + 0.001407\rho^2 - 0.3488\rho + 34.40 \quad (3)$$

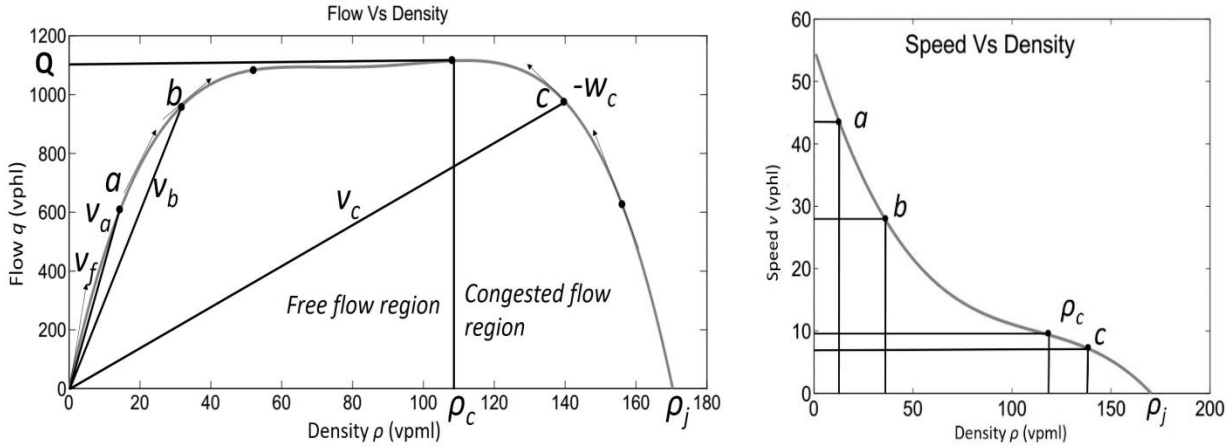

(a) Flow-Density FD (b) Speed-Density FD

Figure 4.3: FD modeled for non-lane-based heterogeneous traffic in cell 2, based on data collected on 15th April, 2015 from 1500 to 1730 hrs. (Hossain et al. 2016).

The representation of non-linear FD (Figure 4.3) for cell 2, offers an understanding of the developed non-linear FD equations (Equations 1, 2, 3). From flow-density relationship (Figure 4.3a), it is observed that the speed value is not constant both in free-flow and congested-flow region. Though the free-flow region is defined with the limit from 0 to ρc, the speed is not free-flow speed rather it is concave (Figure 4.3b) in nature while the density is increasing (0 to ρc). This means the speed is underestimated than that of lane disciplined traffic. The forward and backward

forming wave is also changing with density (Figure 4.3a), which in turn shows that the traffic flow is more unstable and discontinuous in nature. While ρ is approaching ρc, the flow values show quite stable behavior, i.e., phenomenon like stationary wave is created. This is logical in heterogeneous traffic, because when traffic of different speed class mixes together and weak lane discipline prevails, situation like stable flow may occur in case of ρ approaching ρc.

4.5. The Cell Transmission Model

Table 4.1 shows the parameters and variables used to formulate the model in this thesis. The flow conservation equation can be written as:

$$\frac{\partial \rho(x,t)}{\partial t} = -\frac{\partial q(x,t)}{\partial x} \tag{4}$$

The LWR model considers system equilibrium as per Equation (5) (Lighthill and Whitham, 1955). Incorporating this in Equation (4), the following expression (Equation 6) can be found:

$$\frac{\partial \rho(x,t)}{\partial t} = -q(\rho)\frac{\partial q(x,t)}{\partial x} \tag{5}$$

The CTM discretize the Equation (2) to obtain conservation of vehicle. CTM considers a recursion where the cell occupancy at time (t+1) equals its occupancy at time t, plus the inflow and minus the outflow (Figure 4.1):

$$n_i(t+1) = n_i(t) + \Delta t(q_i(t) + \mathrm{r}_i(t) - q_{i+1}(t) - \mathrm{s}_i(t)) \tag{6}$$

Where the flows are related to the current conditions; at time t as indicated below (Figures 4.1 and 4.2):

$$\begin{aligned} & q_i(t) = min\left\{(n_{(i-1)}(t),\ Q_i(\mathrm{t}),\ \frac{w}{v}[N_i(t) - n_i(t)]\right\} \\ & When,\ n_{(i-1)}(t) \le Q_i(\mathrm{t}),\ w = v \\ & \qquad n_{(i-1)}(t) > Q_i(\mathrm{t}),\ w \ne v \end{aligned} \tag{7}$$

Table 4.1: Model parameters and variables used in H-CTM.

Symbol	Name	Unit
N	Number of cells	dimensionless
Δt	Time step	hours
Δx_i	Cell length	miles
Q_i	Cell capacity	vehicles per hour (vph)
R_i	On-ramp capacity	vehicles per hour (vph)
S_i	Off-ramp capacity	vehicles per hour (vph)
v_i	Free flow speed	miles per hour (mph)
w_i	Back wave speed	miles per hour (mph)
ρ_j	Jam density	vehicles per mile (vpm)
ρ_c	Critical density	vehicles per mile (vpm)
β_i	Off-ramp Split ratio	[0,1], dimensionless
C_i	flow combination factor for ramp	[0,1], dimensionless
σ_i	flow distribution factor for ramp	[0,1] dimensionless
t	Period number	dimensionless
$s_i(t)$, $r_i(t)$	Off-ramp, On-ramp flow in cell i in period t	vehicles per hour (vph)
$d_i(t)$	On-ramp demand in cell i in period t	vehicles per hour (vph)
$qu_i(t)$	On-ramp queue size in cell i in period t	no of vehicles
$q_i(t)$	Flow from cell i to i + 1 in period t	vehicles per hour (vph)
$\rho_i(t)$	Density in cell i in period t	vehicles per mile (vpm)
$T(t)$	Travel time in period t	hours

4.6. The H-CTM

The basic CTM is developed based on piecewise linear triangular shape FD without any capacity lag. However, for heterogeneous traffic, the analysis of FD reveals that, the shape was considered in basic model (Hossain et al., 2016), does not remain constant over time and space for heterogeneous non-lane-based traffic. H-CTM takes the required parameter values from the most optimized FD, modeled for stated traffic condition and simulate the traffic state using modified equations. For the study, the structure of v-ρ FD is 3rd degree polynomial in nature, as a result, H-CTM replaces

the piecewise linear FD with modified non-linear v-ρ equations. Therefore, the computation of basic CTM is changed in following way:

At first H-CTM calibrate itself the initial parameter values and boundary conditions e.g. cell length, time step, initial density, on and off-ramp flows, inflow, upstream demand in the gate cell, downstream capacity etc. at 0 time step. Afterwards, it initializes on-ramp queue size as, $q_i(0) = 0$ and on-ramp flow, $r_i(0) = R_i$. In cells without an on-ramps, r_i is considered to be 0. Subsequently, the model computes on-ramp flows with following equation with constraints:

$$r_i(\mathrm{t}+1) = \min\left\{\begin{array}{l} d_i(\mathrm{t}+1) + \dfrac{qu_i(\mathrm{t})}{\Delta t}, \\ \sigma_i v_i(\rho)[\rho_j - \rho_i(\mathrm{t})], \\ R_i \end{array}\right\} \tag{8}$$

In Equation (8), the on-ramp flow is computed from the minimum value of the three term: total demand and queue generated at present time-step from on-ramp, free space available in the cell with on-ramp calculated from modified speed equations (Equation 1,2,3) with flow distribution factor and the capacity of the ramp. The σ_i factor rather replaces the w/v constant in the original equation of basic CTM (Equation 4). This factor is applicable for on-ramp and is calculated from the geometric layout of the cell.

Next the model update the queue size in the ramp from the flow conservation equation (Equation 9).

$$qu_i(\mathrm{t}+1) = \max\{qu_i(\mathrm{t}) + [d_i(\mathrm{t}+1) - r_i(\mathrm{t}+1)]\Delta t, o\} \tag{9}$$

As H-CTM initialize with calibrated parameters and the density value at 0 time step, the initial speed values are calculated from Equation (1, 2, 3). After that, the model compute cell-to-cell flows from equation 10 with the four constraints.

$$q_i(\mathrm{t+1}) = \min\begin{Bmatrix} [v_{i-1}(\rho)\rho_{i-1}(\mathrm{t}) + r_i(\mathrm{t+1})](1-\beta), \\ \mathrm{w}_i[\rho_{j(i)} - \rho_i(\mathrm{t}) - C_i\dfrac{r_i(\mathrm{t+1})}{\mathrm{v}_i(\rho)}], \\ \dfrac{1-\beta}{\beta}S_{i-1}(\mathrm{t}), \\ Q_i \end{Bmatrix} \quad (10)$$

The cell to cell flow is computed from the minimum value of the constraints. Here, the first constraint stands for the flow from i-1 cell to i cell, where the flow value is computed based on density as well as speed at that density and the on-ramp ramp flow at current time and cell, estimated from equation 8. If there presents any off-ramp in the cell, the flow will be divided according to split ratio β. The second constraint is the available free space in the cell estimated by deducting the out-going density from ρ_j. Here the backward wave is incorporated as free space is considered to propagate at backward wave speed. Considering the flow at off-ramp, if present, the third constraint will calculate the flow. If the flow is minimum toward off-ramp capacity considering β, then it will direct the flow to off-ramp. The fourth constraint is the capacity of the current cell.

After calculating cell-to-cell flow, the model will update off-ramp flows using following equations (Equation 11, 12).

$$s_i(\mathrm{t+1}) = \frac{\beta_i}{1-\beta_i}q_i(\mathrm{t+1}), \text{ when } \beta_i < 1 \quad (11)$$

$$s_i(\mathrm{t+1}) = \min\left\{w_i(\mathrm{t})[\rho_i(\mathrm{t}) + \frac{C_i r_i(\mathrm{t+1})}{v_i(\rho)}], S_i\right\}, \text{ when } \beta_i = 1 \quad (12)$$

Equation (11, 12) are logical because if β is less than 1, off-ramp flow will be a portion of mainline flow considering that off-ramp flow is less than S. If off-ramp demand exceed capacity, queue will develop in the mainline which has already been considered in Equation (10) at third constraint. If β is 1 i.e. total flow will be directed

to the off-ramp, then depending upon the available space and S, the minimum number of vehicle will enter the off-ramp.

When the model has on-ramp, off-ramp and cell-to-cell flow values, it will use density conservation equation (Equation 13) to estimate density.

$$\rho_i(\mathrm{t}+1) = \rho_i(\mathrm{t}) + \left\{ q_{i-1}(\mathrm{t}+1) + r_i(\mathrm{t}+1) - q_i(\mathrm{t}+1) - s_i(\mathrm{t}+1) \right\} \frac{\Delta t}{\Delta x_i} \tag{13}$$

The speed is then computed by following constraint of minimum value of the two.

$$V_i(k+1) = \min\left\{ v_f, abs(w) \right\} \tag{14}$$

4.7. Model Calibration

For calibration of the model, non-linear FD parameters are used (Table 4.2) (Hossain et al., 2016). The simulation setup is synchronized so as to incorporate the boundary conditions in the model. Since the model needs the description of traffic demand in its upstream gate cell and downstream sink cell for each time step for the whole simulation period, the traffic demand data collected for Cell 1 and Cell 5 are considered as known data for the model and treated as the gate cell and the sink cell respectively. So, the traffic states of the intermediate Cell 2, Cell 3 and Cell 4 are estimated by the model. Also, the on-ramp and off-ramp demand are also considered as the measured field data. The traffic flow values at the initial time step are assumed to be the measured field values for all interim cells. But after the first step, they are estimated by the model equations.

Table 4.2: Estimated FD parameters of different cells for H-CTM calibration (Hossain et al., 2016).

Cell	Free flow speed v_f (mph)	Critical density p_c (vpml)	Jam density p_j (vphl)	Capacity Q (vphl)
C2	55.44	112	170	1116
C3	27.69	325	432	1456
C4	34.40	288	376	1371

4.8. Validation of the Proposed Model

For validation of the model, the simulation results based on the mathematical structure of H-CTM, are to be compared with the real traffic data for assessing it's practical usefulness Papageorgiou (1998). Accordingly, the non-linear FD parameters Hossain et al., (2016) with boundary values are incorporated in the basic CTM to estimate traffic states over time and the results are compared with the set of measured traffic data collected on 16th of April, 2015.

The resulting speed, flow and density profiles for the intermediate links over the full simulation period are shown in Figures 4.4 (a-c). This comparison also includes the simulation data from basic CTM.

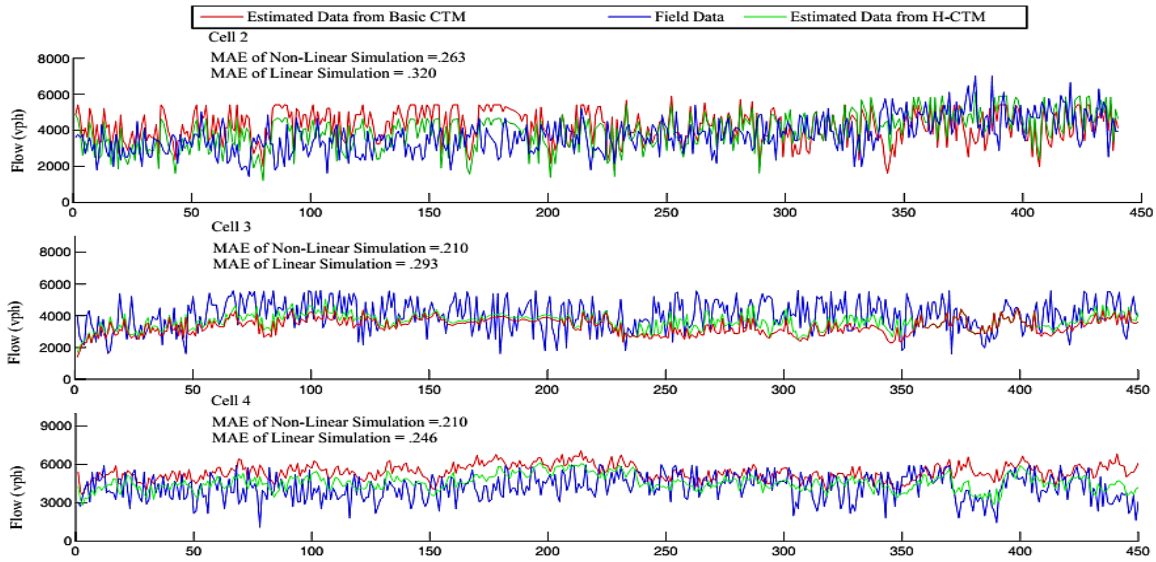

Figure 4.4: (a) Comparison of flow profiles for CTM and Hetero-CTM with field measured data at different interim cells

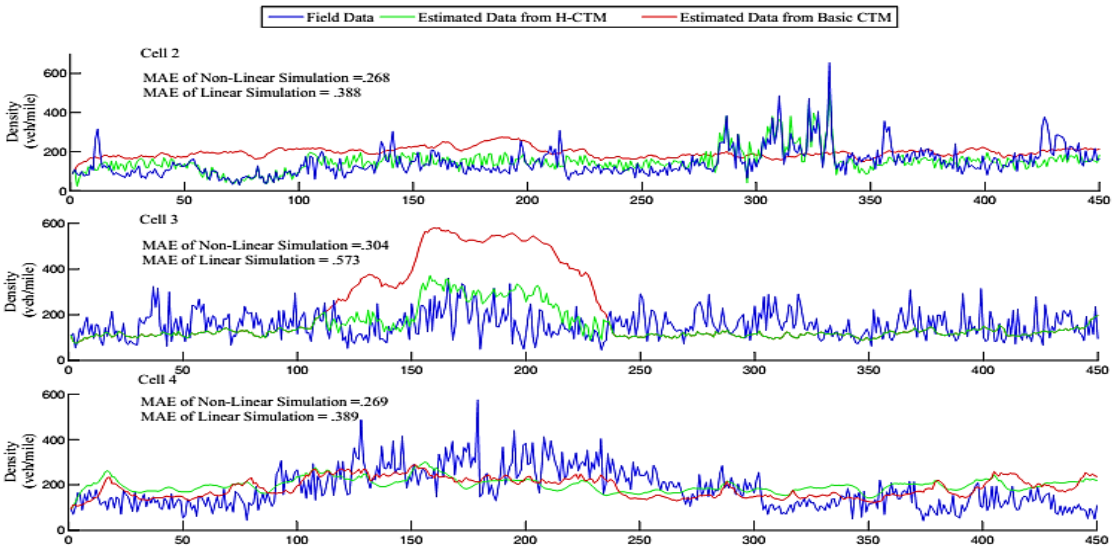

Figure 4.4: (b) Comparison of density profiles for CTM and Hetero-CTM with field measured data at different interim cells.

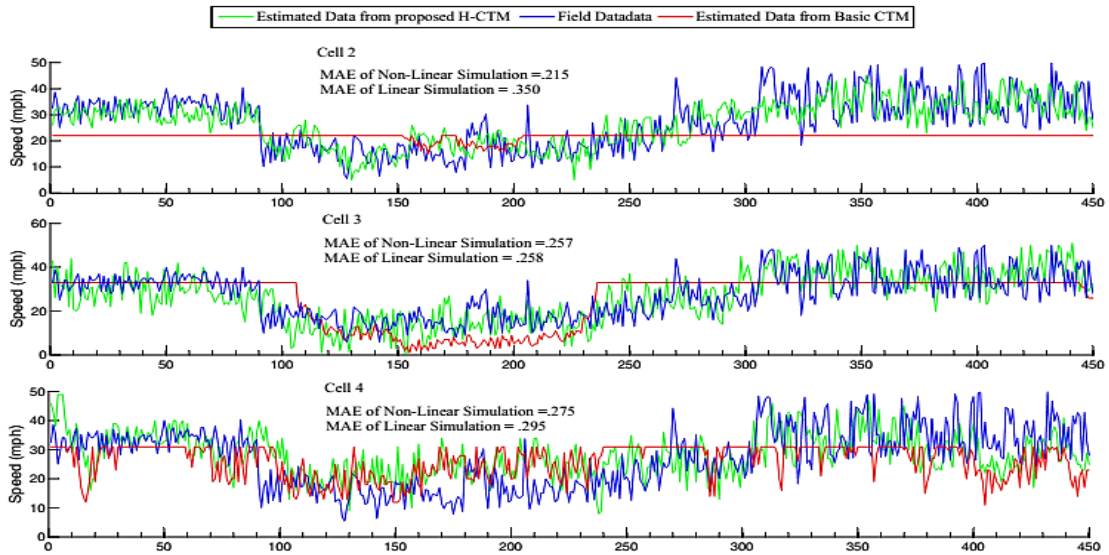

Figure 4.4: (c) Comparison of speed profiles for CTM and Hetero-CTM with field measured data at different interim cells.

For the performance measure of the model, MAE is considered as base standard which quantifies the error between estimated and measured traffic states for individual cell both for H-CTM and basic CTM. MAE is defined as:

$$MAE_i = \frac{\sum_{k=1}^{k=450} \left| (Estimated(v,\rho,q)_k - Measured(v,\rho,q)_k) \right|}{\sum_{k=1}^{k=450} Measured(v,\rho,q)_k} \quad (15)$$

From Table 4.3, it is observed that the proposed H-CTM can simulate the traffic state with an accuracy of 72.5-78.5% for speed, 77.37-79% for flow and 69.6-73.2% for density estimation while the result is compared with field data. Again it is found that proposed H-CTM is performing well compared with the basic CTM in context of MAE. The compliance of H-CTM with basic CTM is found 60 to 79% of speed, 85 to 92% of flow and 67 to 86% of density.

Table 4.3 Results of the sensitivity analysis of the Hetero-CTM with field data and basic CTM based on MAE

Change in Model Structure	**Link**	**MAE**		
		v	**q**	**ρ**
Proposed Hetero-CTM	C2	.215	.263	.268
	C3	.257	.210	.304
	C4	.275	.210	.269
Basic CTM	C2	.350	.320	.388
	C3	.258	.293	.573
	C4	.295	.246	.389
Hetero-CTM with Basic CTM	C2	.392	.143	.328
	C3	.287	.080	.271
	C4	.210	.150	.142

The accuracy of results produced by H-CTM can be considered quite satisfactory given the wide variations in operating conditions and performance characteristics of non-lane-based heterogeneous traffic. Moreover, from the validation results, it is clearly observed that it outperforms the original CTM in terms of model application. The improvement in results can be attributable to incorporation of non-linear FD. The speed equations (Equations 1, 2, 3) from the FD seems very sensitive in the model performance while the basic CTM which considers the linear FD shows poor result and cannot really capture the traffic state variations. The discontinuities and the propagation of density-change in non-lane-based heterogeneous traffic condition are quite different than other traffic systems. Moreover, the stable flow-like situation, i.e.,

stationary wave phenomenon is also very uncommon in other traffic conditions. But, the non-linear FD can capture these situation very realistically. Using these attributes, performance of basic CTM has been improved hence the newly proposed H-CTM can capture these phenomenon in its equations with constraints. Moreover, H-CTM has adopted a new parameter, flow distribution factor σ_i. These parameters influence the on-ramp flow on main-line flow. While considering the on-ramp flow, the inflow is rather subjected to the influence of its location in the cell than the influence of backward forming wave speed. With σ_i, the flow coming from on-ramp to the cell is fractionized to model the influence of its location. If the location of on-ramp is at the midpoint of the cell, then the available occupancy for ramp inflow is only accessible for half of the length of the cell. Integrating this location sensitive factor in the proposed H-CTM, the results seem to have improved because the model can take into account the location influence of the on-ramp hence the free space available for the ramp inflow is reduced by this factor. There has been some associated error in the results since the model calculates split ratio of off-ramp in 20s interval while in actual field, the change of split ratio is more dramatic.

4.9. Conclusion

A comprehensive review of literatures showed that very limited studies are found for simulating heterogeneous non-lane-based traffic condition in developing countries. This study proposes a new macroscopic flow model H-CTM which is an extension of the basic CTM incorporating the stated traffic condition. For model calibration, the basic concept on macroscopic FD in the stated traffic flow condition is incorporated. To our understanding, the main obstacle of this study was capturing high-resolution traffic data for which a practical method of high-resolution data collection technique proposed by Hossain et.al. (2016) was adopted. The principal findings of this research are listed below:

- The original CTM considering piecewise linear FD cannot really capture the traffic state accurately for non-lane-based heterogeneous traffic condition.
- The H-CTM incorporates non-linear FD modeled for heterogeneous traffic including different speed class vehicles. This model can capture this traffic state more accurately.
- From sensitivity analysis, it is found that the non-linear FD is the most important term of the H-CTM which enhances the results of basic CTM.

This study cannot be taken as a complete measure of modeling all heterogeneous non-lane-based traffic condition which is highly complex in nature especially in signalized arterials which in turn make a more complex situation to model. As future scope of research, the authors would like to recommend sensitivity investigations for checking the transferability of the model for changed application conditions.

4.10. References

1. Gazis, D.C., The origins of traffic theory. Operations Research, 2002. 50(1): p. 69-77.
2. Cousins, W., et al., Comparative study of traffic models: a concrete mass evacuation example. Department of Mathematics, University of Virginia, Charlottesville, VA, 2009. 22903.
3. Daganzo, C.F., The cell transmission model: A dynamic representation of highway traffic consistent with the hydrodynamic theory. Transportation Research Part B: Methodological, 1994. 28(4): pp. 269-287.
4. Lin, W.-H. and D. Ahanotu, Validating the basic cell transmission model on a single freeway link. PATH technical note; 1995, pp 95-103.
5. Feldman, O. and M. Maher. Optimisation of traffic signals using a cell transmission model. In 34th Annual Universities' Transport Study Group Conference, Napier University, Edinburgh. 2002.
6. Lo, H.K., A cell-based traffic control formulation: strategies and benefits of dynamic timing plans. Transportation Science, 2001. 35(2): p. 148-164.
7. Skabardonis, A. and N. Geroliminis, Real-time estimation of travel times on signalized arterials. 2005, No. Luts-Article-2009-003, pp387-406.

8. Almasri, E. and B. Friedrich, Online offset optimisation in urban networks based on cell transmission model. ITS Hanover, 2005.
9. Kimms, A. and K.-C. Maassen, Optimization and simulation of traffic flows in the case of evacuating urban areas. OR spectrum, 2011. 33(3): p. 571-593.
10. Lo, H. A dynamic traffic assignment formulation that encapsulates the cell-transmission model. in 14th International Symposium on Transportation and Traffic Theory. 1999.
11. Hadiuzzaman, M. and T.Z. Qiu, Cell transmission model based variable speed limit control for freeways. Canadian Journal of Civil Engineering, 2013. 40(1): p. 46-56.
12. Greenshields, B., W. Channing, and H. Miller. A study of traffic capacity. in Highway research board proceedings. 1935. National Research Council (USA), Highway Research Board.
13. Lighthill, M.J. and G.B. Whitham. On kinematic waves. II. A theory of traffic flow on long crowded roads. in Proceedings of the Royal Society of London A: Mathematical, Physical and Engineering Sciences. 1955, vol 229, No. 1178, pp 317-345.
14. Mohan, R. and G. Ramadurai, State-of-the art of macroscopic traffic flow modelling. International Journal of Advances in Engineering Sciences and Applied Mathematics, 2013. 5(2-3): p. 158-176.
15. Daganzo, C.F., The cell transmission model, part II: network traffic. Transportation Research Part B: Methodological, 1995. 29(2): p. 79-93.
16. Lebacque, J.-P. The Godunov scheme and what it means for first order traffic flow models. In Internaional symposium on transportation and traffic theory. 1996, pp 647-677.
17. Tuerprasert, K. and C. Aswakul. An extension of cell transmission model for heterogeneous mobility. in 15th World Congress on Intelligent Transport Systems and ITS America's 2008 Annual Meeting. 2008.
18. Chen, X., Q. Shi, and L. Li, Location specific cell transmission model for freeway traffic. Tsinghua Science & Technology, 2010. 15(4): p. 475-480.
19. Ngoduy, D., Multiclass first-order traffic model using stochastic fundamental diagrams. Transport metrica, 2011. 7(2): p. 111-125.

20. Liu, H., et al., Integrating the Bus Vehicle Class Into the Cell Transmission Model. IEEE Transactions on Intelligent Transportation Systems, 2015. 16(5): p. 2620-2630.
21. Daganzo, C.F., The lagged cell-transmission model. 1999.
22. Zhang, Z., B. Wolshon, and V.V. Dixit, Integration of a cell transmission model and macroscopic fundamental diagram: Network aggregation for dynamic traffic models. Transportation Research Part C: Emerging Technologies, 2015. 55: p. 298-309.
23. Kühne, R. and N. Gartner, Years of the Fundamental Diagram for Traffic Flow Theory: Greenshields Symposium, vol. E-C149 of Transportation Research Circular, Traffic Flow Theory and Characteristics Committee. Transportation Research Board of the National Academies. 46.
24. Hossain, S., et al. A new stochastic macroscopic model for heterogeneous traffic considering variable fundamental diagram 2. in Transportation Research Board 95th Annual Meeting. 2016.
25. Muniruzzaman, S.M., et al., Deterministic algorithm for traffic detection in free-flow and congestion using video sensor, Journal of Environment, Technology and Engineering Vol 1 (September), 2016, pp111-130.
26. Kurzhanskiy, A. and P. Varaiya, CTMSIM—An interactive macroscopic freeway traffic simulator. Department of Electrical Engineering and Computer Sciences, Berkeley, CA., USA, 2008.
27. Greenberg, H., An analysis of traffic flow. Operations research, 1959. 7(1): p. 79-85.
28. Underwoo, R., Speed, volume and density relationships: quality and theory of traffic flow, Yale Bureau of Highway Traffic,(1961), 141-188. New Haven, Connecticut, 2008.
29. Zhang, H.M., A theory of nonequilibrium traffic flow. Transportation Research Part B: Methodological, 1998. 32(7): p. 485-498.
30. Papageorgiou, M., J.-M. Blosseville, and H. Hadj-Salem, Modelling and real-time control of traffic flow on the southern part of Boulevard Peripherique in Paris: Part I: Modelling. Transportation Research Part A: General, 1990. 24(5): p. 345-359.
31. Papageorgiou, M., Some remarks on macroscopic traffic flow modelling. Transportation Research Part A: Policy and Practice, 1998. 32(5): p. 323-329.

CHAPTER 5: A NEW STOCHASTIC MACROSCOPIC MODEL FOR HETEROGENEOUS TRAFFIC§

5.1. Introduction

Macroscopic traffic flow models play an irreplaceable role in real-time traffic state estimation and short-term prediction. The models consider the traffic flow as a compressible fluid and represent the traffic states with the help of aggregated variables: flow, speed and density. As such, they include a lower number of parameters compared to the microscopic models. This results in low computational effort and relative ease of calibration for real-time application. On the contrary, the microscopic models include a large number of physical or non-physical parameters that should be appropriately specified to reproduce the traffic flow characteristics with the highest possible accuracy. The parameter estimation has intensive computational requirements and is difficult to validate because human behaviour in real traffic is difficult to observe and model. Thus, macroscopic traffic flow models are generally preferred over microscopic models for real-time traffic estimation and control.

The two most frequently used macroscopic models are the first-order cell transmission model (CTM) (Daganzo, 1994) and the second-order METANET model (Messmer and Papageorgiou, 1990). Numerous studies (Lin and Ahanotu, 1995; Muñoz et al., 2006; Papageorgiou et al., 1990) have found that traffic state estimates of these models show very close agreement with the field data. Over the years, different extensions and modifications of these models have been proposed to adapt

§ This chapter is a modified version of a published articlet in Transportation Research Record. Hossain, S., Hadiuzzaman, M., Haque, N., Muniruzzaman, S. M., Musabbir, S. R., Hasnat, M. M. "A New Stochastic Macroscopic Model for Heterogeneous Traffic Considering Variable Fundamental Diagram", in 95th Transportation Research Board (TRB) Annual Meeting, Washington, D.C., January 11-15, 2016.

for a variety of traffic engineering tasks, such as dynamic traffic assignment, estimation and prediction, control strategy design and synthesis etc. For example, the CTM has been extended in (Li, 2010), (Gomes and Horowitz, 2006) and (Hadiuzzaman and Qiu, 2013) for arterial traffic signal control, freeways with ramp metering control and Variable Speed Limit (VSL) control respectively. Likewise, many extensions of the METANET model can be found in the literature to take into account e.g., weaving effect (Yin, 2014) and lane drops (Papageorgiou et al., 1990); and have been adapted to different models of active traffic management: variable speed limits (Islam et al., 2013), ramp meter control (Papamichail et al., 2010) and combination of these two (Lu et al., 2011).

Although the conservation equation used in these models is an exact equation, the description of mean speed is essentially empirical and is derived based on a static flow-density or speed-density relationship – the Fundamental Diagram (FD). It is generally recognized that FD is dependent on flow conditions and roadway environments. Consequently, various structures of the FD have been adopted in different models to capture the intrinsic functional relationship for the whole range of traffic situations; from free flow to congested equilibrium states including non-equilibrium transitions between them. For instance, the FD corresponding to the flow-density relationship in the original CTM was assumed to be trapezoidal shaped, but it was further adapted to accommodate any continuous, piecewise differentiable FDs, such as a triangular FD. The METANET assumed an exponential speed-density relationship which was extended to explain the impact of the VSL, ramp metering etc. on traffic flow. These structures of the FD were found to reproduce the relevant traffic conditions for homogeneous traffic scenario with remarkable accuracy. However, due to different microscopic characteristics of vehicles in heterogeneous traffic compared to the homogenous condition, the aggregated macroscopic behavior is likely to be

different. This necessitates extensive investigation of FD structures for non-lane-based heterogeneous traffic. Unfortunately, very few field studies have been undertaken for this investigation. Such limited research is primarily because of the difficulty of high-resolution data collection and the complexity of reproducing the wide variation in operating and performance characteristics of vehicles in heterogeneous traffic systems.

The goal of this study is to develop a stochastic macroscopic model for an arterial roadway section of Dhaka city. The developed model is expected to accurately estimate and predict the complex nature of the prevailing heterogeneous traffic condition through appropriate modifications and extensions of the conventional traffic models. As a pre-requisite to this, the study also aims at establishing an accurate and ready-for-practice method of high resolution data collection for the stated traffic condition using image processing technique.

The chapter is structured as follows: Section 2 reviews previous works on macroscopic modeling and application; Section 3 presents the study area and details of the data collection process. Section 4 investigates the structures of the FD of different links of the study section and describes the dynamics of the proposed model. In the following section, the model's global and link-specific parameters are determined through a least squares optimization problem using measured traffic data. The main results of model performance are reported in Section 6. Finally, concluding remarks and future research scopes are given in Section 7.

5.2. Literature Review

Research on traffic flow models started from the mid-1950s, when the propagation of shock waves was modeled by (Lighhill and Whitman, 1955; Richards, 1956) based on the analogy of vehicles in traffic flow and particles in a fluid. Since then, numerous modeling approaches have been studied which describe various aspects of traffic flow

operations at different levels of detail (see the study of Hoogendoorm and Bovy, (2001) for a comprehensive review on traffic flow models). Among these, the macroscopic appr oach represents the traffic states with the help of aggregated variables and yields flow models with a limited number of equations. Most of the macroscopic models suggested so far are derived from the microscopic car-following considerations within a string of identical vehicles. However, the car-following models are only empirical and multilane traffic flow includes different types of vehicles and driving behaviors. Based on these facts, Papageorgiou (1998) convincingly argues that the deduced macroscopic model structures are unlikely to be as accurate as Newtonian physics or thermo-dynamics; rather their accuracy must be triggered via parameter calibration using real data.

The first-order macroscopic traffic flow models are mostly discretized derivatives or extensions of the LWR model. Within this category, the cell transmission model (CTM) is the most popular, owing to its analytical simplicity and ability to reproduce congestion wave propagation dynamics. Lin and Ahanotu (1995) compared the performance of the CTM under both congested and non-congested traffic conditions with data collected from a continuous segment of freeway I-880 in California. It was found that in free-flow condition, CTM provides as high as a 0.9 correlation value at a sampling interval of 6 seconds and asymptotically tends to a perfect correlation at large sampling intervals. Again, a density-based modified version (Muñoz et al., 2006) of the CTM produced density estimates which showed only 13% mean error (averaged over all the test days) with measured densities on I-210 West in Southern California during the morning rush-hour period. Further research by Daganzo (1995), Daganzo (1997) and Feldman and Maher (2002) had expanded on the CTM to model junctions, highway links with special lanes and signalized networks respectively.

However, as noted in (Zhang, 1998), (Gartner et al., 2001) and other related studies, the first-order models are unable to capture traffic instability, driver's delayed response to traffic conditions and their anticipation behavior. To overcome these shortcomings and to improve the accuracy level provided by first-order models, second-order models were developed. The most popular second-order model was suggested by Payne (1971), which has an independent speed dynamics in addition to density dynamics. He showed that the average speed in a section of a roadway is influenced by three major mechanisms: relaxation, convection and anticipation. Discretization and modifications of the Payne model have led to the origin of a family of second-order models like the models of Payne (1979), Papageorgiou (1990), Lyrintzis et al. (1994) and Liu et al. (1998). Among these, the most widely used is the METANET model, which was validated against real traffic data with remarkable accuracy at several instances. For example, Papageorgiou et al. (1990) successfully estimated the traffic states of a 6-km stretch of the southern part of Boulevard Périphérique in Paris with standard deviations of only 10.8 km/h for mean speeds and 714 veh/h for traffic volumes. But it was noted that the same parameter values of the exponential FD were used for all links in spite of the different shapes appearing from the field data at different sites. Sanwal et al. (1996) extended the METANET to model the flow under the influence of traffic-obstructing incidents. The extended model, when fitted to a 5.8 mile segment of the I-880 freeway between the Marina and Whipple exits in California, indicated quite satisfactory performance. Since the METANET contains both speed and density dynamics, it was successfully used as a candidate model for traffic control design in many studies, some of which are mentioned in the previous section. To avoid difficulty in control design and implementation, Lu et al. (2011) suggested a simplified version of the METANET, dropping the non-linear parameterization in the speed control variable. The simplified

model with a modified convection term was able to estimate the field traffic dynamics more accurately than the original model.

Comparative evaluations of first and second-order models based on real data were reported by Cremer and Papageorgiou (1981), Michalopoulos et al. (1992), Spiliopoulou et al. (2014) etc. These studies provided empirical evidence of better accuracy of second-order models compared to first-order ones. But it should be noted that the second-order models also have weaknesses. Critical review by Daganzo (1995) found logical flaws in the arguments that have been advanced to derive second order continuum models.

From these discussions it becomes evident that the macroscopic traffic flow models are mostly empirical and they have their own pros and cons. Their performances may be very different for different operating conditions; viz. lane-based homogeneous, non-lane-based heterogeneous etc. Hence, Papageorgiou (1998) suggests that the sufficiency of the traffic flow theories be decided depending on the specific utilizations. Within the vast literature on macroscopic traffic flow modeling, surprisingly few studies have addressed the heterogeneous traffic condition prevalent in many developing countries like Bangladesh, India etc. Majority of these researches (Venkatesan et al., 2008; Arasan and Koshy, 2005; Jin et al., 2010; Gunay, 2007) mainly focus on the microscopic approach of traffic flow modeling. Other works like (Chari and Badarinath, 1983) and (Gupta and Khanna, 1986) focus on developing speed, flow and density relationships for mixed traffic conditions and introduce the concept of "areal density" instead of linear density measurements.

A very limited number of first-order macroscopic models have also been developed for heterogeneous traffic. For instance, (Nair et al., 2011) views the disordered, heterogeneous traffic system as granular flow through a porous medium and extends the LWR theory using a new equilibrium speed-density relationship. This relationship

explicitly considers the pore size distribution, enabling the model to successfully capture the 'creeping' phenomena of heterogeneous queues. However, a microscopic simulation of vehicle configuration is used to determine the pore space distribution and detailed trajectory information of the disordered traffic stream is required for model calibration. Another extension (Wong and Wong, 2002) of the LWR model takes into account the dynamic behavior of heterogeneous users according to their choice of speeds in a traffic stream. The model uses an exponential form of speed-density relation and can replicate many puzzling traffic flow phenomena such as the two-capacity (or reverse-lambda) regimes occurred in the fundamental diagram, hysteresis and platoon dispersion. But being extended versions of the first-order LWR model, neither of these models have independent speed dynamics and they lack field validation. So this paper aims to introduce a second-order flow model for heterogeneous traffic which is expected to show better accuracy in estimation of measured traffic dynamics.

5.3. Methodology

5.3.1. Study area

The study site is the Tongi Diversion Road, a section of the Dhaka-Mymensingh Highway (Figure 5.1(left)), details of which have been explained in Section 2.6 of Chapter 2.

5.3.2. Data collection and processing

Collection of high-resolution traffic data required for the development of an accurate macroscopic model is a very challenging task under the existing traffic condition of the study area. This is mainly because loop detectors are unsuitable for the test site due to measurement errors caused by non-lane-based movement of vehicles activating either both or neither of two adjacent detectors. Moreover, traffic cameras for vehicle detection are absent along the corridor. Under these circumstances, video cameras are

installed at various locations of the study site to provide traffic data for the research using image processing technique, details of which have been elaborated in chapter 2. Two sets of videos were collected for the same time period on 15th and 16th April, 2015. These videos were processed and the extracted data was filtered for anomalies. Ultimately, 2.5 hours data of 15th April was used for calibration of the model parameters and the similar data set from 16th April was used for model validation. To ensure better quality of the collected data, the camera height and angle of projection were strictly maintained. As shown in Figure 5.1 (right), the mounting heights of the cameras were at least 20ft to reduce the object details detected by the algorithm and the camera angle was less than 45 degrees to avoid perception problem. However, the angle was not so small as to cause restriction in vision.

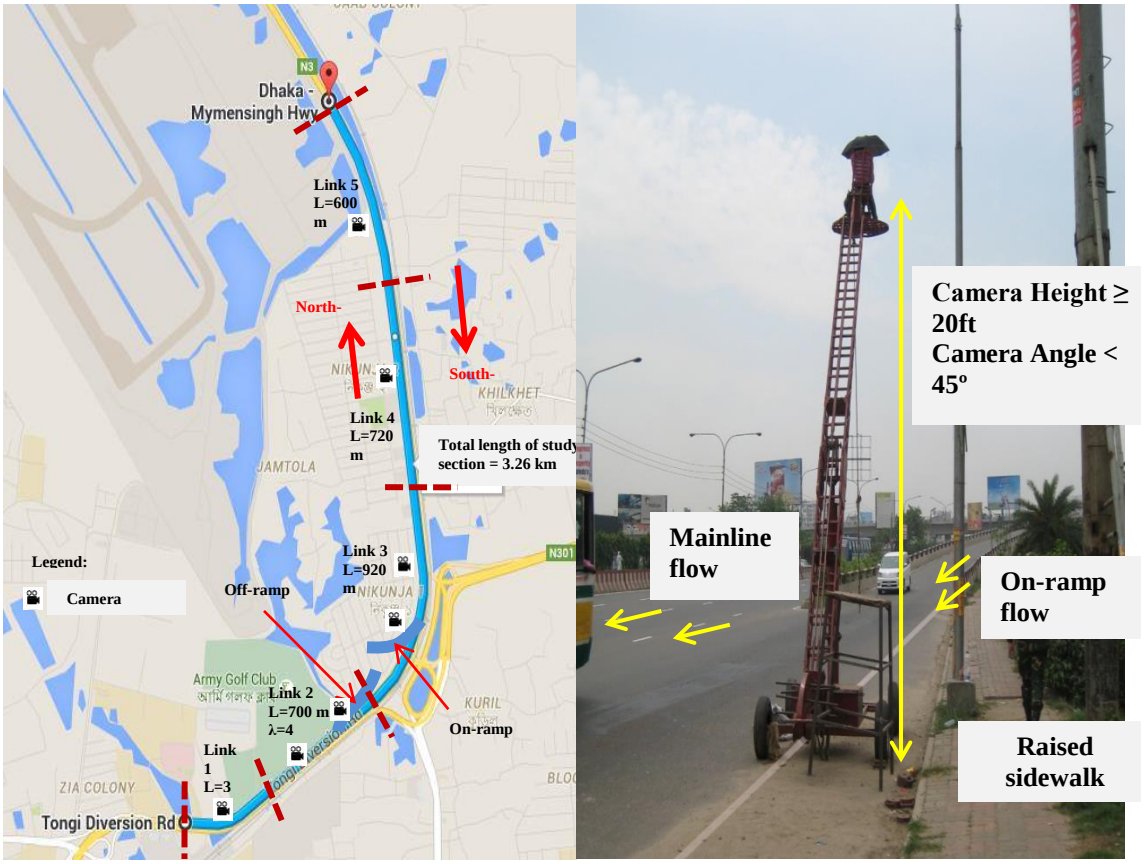

Figure 5.1: The 3.26 km study site (courtesy: Google Map) (left) and details of camera setting for data collection (right).

5.4. Model Development

5.4.1. Investigating fundamental diagram for heterogeneous traffic

The fundamental diagram (describing flow-density, speed-density or speed-flow relationship at a given location or section of the roadway) is a basic tool in understanding the behavior of traffic stream characteristics in macroscopic flow models. In the 1st order models, speed is derived directly from a steady-state speed-density ($v-\rho$) FD; whereas in the Payne model and its derivatives, the speed dynamics generates a reference speed based on the FD. Therefore, identifying the nature of this fundamental relationship is a prerequisite for any macroscopic model development. The current section aims at investigating the impact of the non-lane-based heterogeneous traffic condition on FD. More specifically, it will highlight on how the existing traffic characteristics of the test site influence the structure and parameters of the FD for the internal links L2, L3 and L4 which will be utilized for modeling purpose.

Over the years different structures of the FD have been proposed depending on the flow conditions and roadway environments. However, it is generally agreed that flow q is a concave function of density ρ defined in $[0, \rho_j]$ (ρ_j – jam density); and the corresponding v - ρ relationship is monotone decreasing. Since the FD will be used in the speed dynamics of the proposed model, only the v - ρ relationship is investigated in this section. A few functional representations of this relation from the literature are given below.

Greenshields (1934) postulated a linear relationship between speed and traffic density based on the data obtained from a rural two-lane Ohio highway. The Greenberg model (Greenberg, 1959) which is obtained by integration of the car-following model, proposed a logarithmic structure (Equation 1), observing speed-density data sets for

tunnels. The Underwood model (Underwood, 1961) proposed an exponential v-ρ relationship (Equation 2) based on the results of traffic studies on the Merritt Parkway in Connecticut.

Greenberg model:

$$v = V_m \ln\left(\frac{\rho}{\rho_j}\right) \tag{1}$$

Underwood model:

$$v = V_f e^{-\frac{\rho}{\rho_c}} \tag{2}$$

Here, ρ_c, V_f and V_m represent critical density, free-flow speed and the speed corresponding to the maximum flow or ρ_c respectively. Edie (1961) suggested using a multi-regime model to represent the traffic breakdown near critical density ρ_c. He proposed the use of the Underwood model for the free-flow regime and the Greenberg model for the congested-flow regime, thereby overcoming the flaws of both of the models. Further developments in the field of FD were directed towards generalizing the modeling approach. Examples of such developments include the one-parameter polynomial model cited in (Zhang, 1999):

$$v = v_f\left(1-\left(\frac{\rho}{\rho_j}\right)^n\right) \tag{3}$$

And the exponential model used in (Papageorgiou, 1990), which is obtained by adding parameters for data fitting flexibility to the Underwood model:

$$V(\rho) = v_f \exp\left(-\frac{1}{\alpha}\left(\frac{\rho}{\rho_c}\right)^\alpha\right) \tag{4}$$

To observe the nature of the fundamental relationship for heterogeneous traffic, the $v-\rho$ plots of the field data for different links are fitted with four general structures

evident from the literature: namely, the linear, logarithmic, exponential and polynomial forms. Table 5.1 provides a comparative study among these structures, on the basis of their goodness-of-fit. The R-Squared and Root Mean Square Error (RMSE) values reveal that the 3rd degree polynomial relationship shows the best fit with the field data for all three links. In relation to the findings of (Chari and Badarinath, 1983) which deduced a logarithmic $v-\rho$ relationship with R-Square value of 0.41 utilizing time-lapse photographic data of Hyderabad, India, it can be said that the polynomial structure shows better fit for the prevailing traffic condition.

However, the polynomial type FD structure obtained above from the direct fitting of measured $v-\rho$ data is not readily used in the speed dynamics. This is because the FD parameters are not optimized in stand-alone mode in the model dynamics. Rather, all the global and link-specific parameters are optimized simultaneously. Thus to make the FD structure more generalized and to allow for data-fitting flexibility, Zhang's one-parameter polynomial structure (Equation 3) is used in the speed dynamics of the proposed model. An additional benefit of using this structure is that two important link-specific parameters v_f and ρ_j are obtained directly during model calibration. Nevertheless, the regression analysis provides important guidelines regarding the values of v_f and ρ_j for optimization of the whole model. Figure 5.2 shows the speed vs density scatter plots of the links along with the best-fit regression lines.

An in-depth investigation of the above plots reveals that the values of the FD parameters, i.e., v_f and ρ_j vary significantly for different links. In general, the links with greater roadside friction from pedestrian activities on raised sidewalk (as observed for L3 and L4) show lower free-flow speed and greater jam density compared to the link L2 with less roadside friction. This is because the presence of roadside friction causes sluggish transition from critical to jam densities. Thus, to

capture the dynamics of heterogeneous traffic more accurately, the FD parameters are varied link-wise in the proposed model.

Table 5.1: Comparison of fitness of different structures of the fundamental diagram in heterogeneous traffic condition

Link No	**Goodness-of-fit Parameters**	**Structure of the Fundamental Diagram (v vs. ρ)**				
		$v = a_1\rho + a_2$	$v = a_1 \ln(a_2\rho)$	$v = a_1 \exp(a_2\rho)$	$v = a_1\rho^2 + a_2\rho + a_3$	$v = a_1\rho^3 + a_2\rho^2 + a_3\rho + a_4$
	R-Square	0.5800	0.6451	0.6450	0.6364	0.6460
	RMSE	6.1171	5.6233	5.6243	5.6858	5.6254
3	R-Square	0.4909	0.5951	0.6014	0.5926	0.6036
	RMSE	3.7059	3.3014	3.2791	3.3116	3.2665
4	R-Square	0.6352	0.6882	0.6969	0.6971	0.7003
	RMSE	4.3238	3.9975	3.9411	3.9442	3.9276

Note: a_1, a_2, a_3, a_4 represent the estimated coefficients of the structures.

5.4.2. Traffic dynamics

This section derives a stochastic Payne-type traffic flow model for the estimation and prediction of heterogeneous traffic states. The second-order macroscopic model is expected to depict the traffic dynamics more realistically than commonly used first-order models, owing to its independent speed dynamics in addition to the density dynamics. Similar to other discrete Payne-type models, the proposed model assumes discontinuous changes in both time and space. Thus, traffic states are described temporally and spatially at discrete steps along the roadway. The following assumptions are made in this respect: the roadway is divided into i (1, 2 ….N) links such that the length L_i of each link satisfies the step size modeling constraint i.e. $v_f T \le L_i$; each link is a homogeneous unit containing exactly one on-ramp; a link may have multiple off-ramps; each link contains at least one traffic sensor (e.g. loop detector or video camera); and each link satisfies the equilibrium traffic state

assumption individually. On the basis of these assumptions, the traffic dynamics of the proposed model are developed in the following sub-sections.

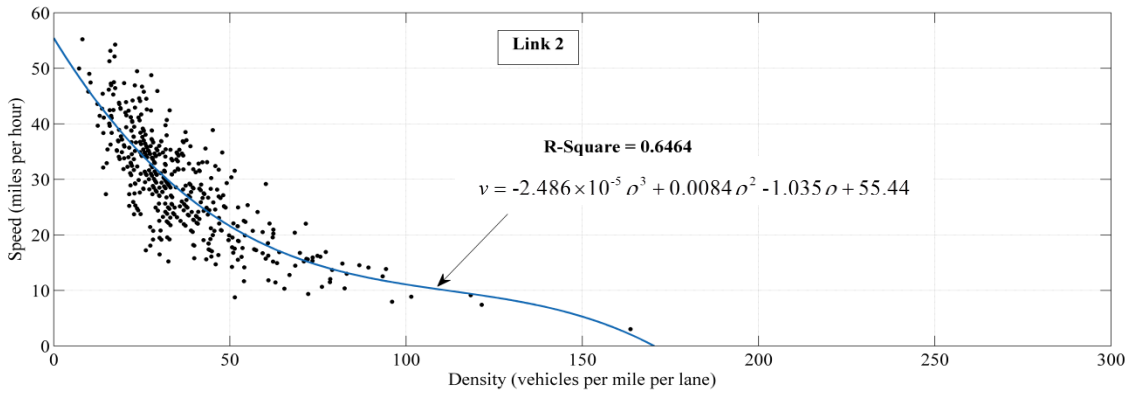

(a)

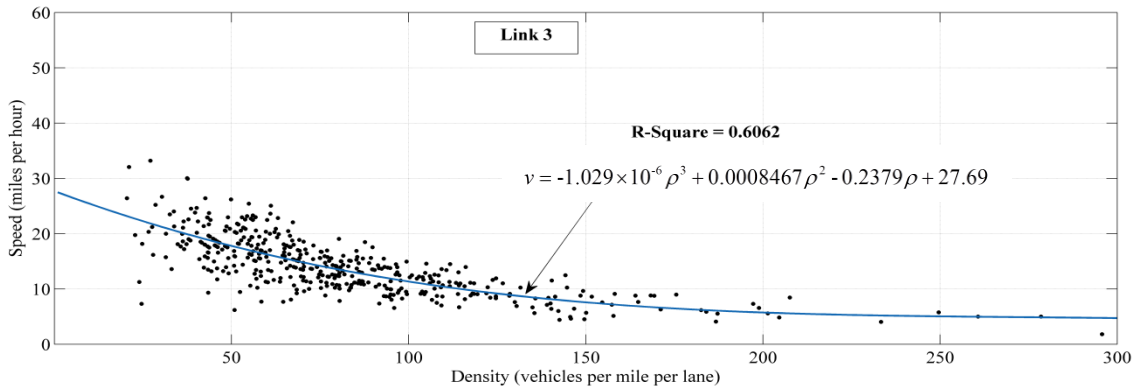

(b)

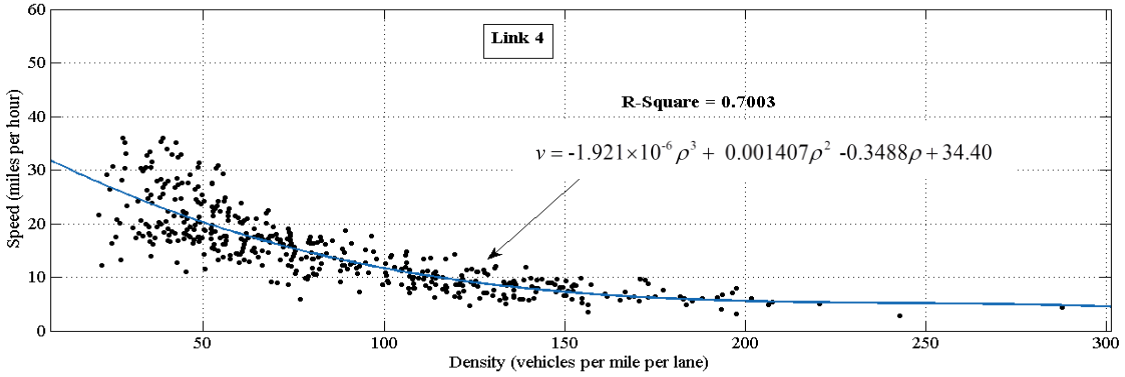

(c)

Figure 5.2: (a-c) Speed vs. density scatter plots of links 2-4 (20 seconds resolution field data used in the plots was collected from 3:00 PM to 5:30 PM on 15th April, 2015.)

5.4.2.1. Density dynamics

The density dynamics of the model is essentially the flow conservation law. Accordingly, the density evolution of the link i at time step $k+1$ equals the previous

density, plus, the inflow from the upstream link and on-ramp, minus the outflow of the link itself and off-ramp (Equation 5).

$$\rho_i(k+1) = \rho_i(k) + \frac{T}{L_i \lambda_i}\left[\lambda_{i-1} q_{i-1}(k) - \lambda_i q_i(k) + r_i(k) - s_i(k)\right] \quad (5)$$

Here, λ_i is the number of lanes of the link i. $r_i(k)$ and $s_i(k)$ are the on-ramp and off-ramp flows respectively. It is noted that Equation 5 is an exact equation and does not include any parameter to be calibrated.

5.4.2.2. Flow estimation equation

In most of the existing macroscopic models, the flow dynamics is expressed by the basic traffic flow equation, namely, flow equals density times space-mean-speed $(q = \rho * v)$. This holds true for roadways with homogeneous traffic and strict lane discipline, where the movement of vehicles is essentially one-dimensional. Thus the dynamic characteristics of a vehicle in a lane affect the motion of its followers in that lane only (Figure 5.3 (left)). But in heterogeneous non-lane-based traffic movement, as Khan and Maini (1999) mentions, traffic does not move in single file. Rather, there is a significant amount of lateral movement. Since different classes of vehicles traverse in both the longitudinal and the lateral directions, they develop a critical "influence area" around themselves as shown in Figure 5.3 (right). The nature of this influence area depends on a number of factors like, the speed of the vehicles, their sizes, acceleration and deceleration rates, maneuvering capacities and the behavior of the drivers.

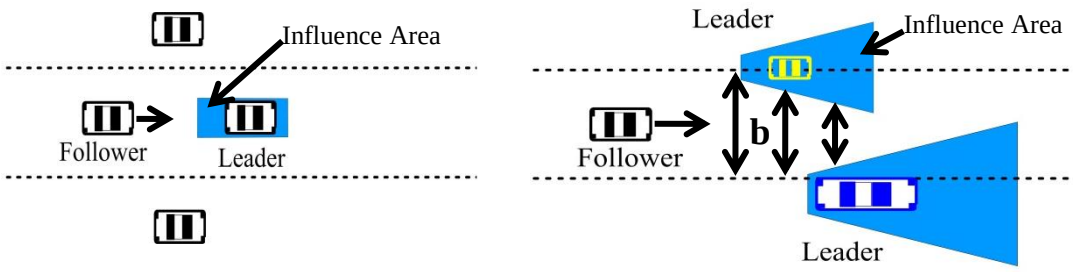

Figure 5.3: Lane-based homogeneous traffic (left) and non-lane-based heterogeneous traffic (right).

In general, traffic flow under heterogeneous condition is greater than the corresponding flow under homogeneous condition. This is because in the heterogeneous composition, the smaller vehicles occupy the gaps among the larger vehicles resulting in maximum space utilization. This space utilization is however constrained by the effect of influence area. If the available lateral clearance (denoted by b in Figure 5.3 (right)) among the influence areas of the leaders is greater than the minimum lateral clearance required for a particular class of vehicles to move, the vehicles will move forward in the traffic stream and vice-versa. In the lane-based operating condition, this available space remains constant for all classes of vehicles and is equal to the lane width of the roadway. As such, the flow computed by the basic traffic flow equation is accurate. However, in non-lane-based operating condition, the available lateral clearance varies according to the influence areas of the leaders, which again depends on a variety of static and dynamic properties of vehicles mentioned earlier. Thus, fundamental relation $q = \rho \times v$ might underestimate the actual flow. The combined effect of optimum space utilization and vehicular influence area in non-lane-based heterogeneous traffic operation could vary significantly. However, it is hard to determine such effect accurately during real-time traffic state estimation. Thus, a stochastic flow influencing term $\xi_i^q \sim N(\mu, \sigma)$ is added to the

flow equation to account for this underestimation. It is expected that the stochastic term could improve flow estimation significantly. The flow estimation equation of the proposed model is expressed as follows.

$$q_i(k) = \rho_i(k)v_i(k) + \xi_i^q(k) \tag{6}$$

5.4.2.3. Speed dynamics

The speed dynamics of the original Payne model was derived from a linear car-following model that describes the behavior and interaction of the vehicles as they follow a leading vehicle on the road. It was shown that the speed of vehicles in a link is affected by (1) the density of vehicles in that link since the speed tends to relax to the equilibrium speed on FD, (2) the speed of (slower or faster) vehicles coming from the link upstream and (3) the perception of a relatively lower or higher density in the link downstream. In the speed dynamics, these three phenomena are expressed respectively by a relaxation term, a convection term, and an anticipation term. The speed dynamics of the well-established METANET model has been derived from Payne's model. However, the anticipation term has been modified relative to Payne's model. Specifically, κ, a positive constant is added to avoid the singularity of the term when modeling low traffic density and a global anticipation parameter, υ is added to capture sensitivity of traffic speeds to the downstream traffic density. It is worthwhile to mention here that, υ is added based on the heuristic microscopic considerations of Payne's model. Thus in lane-based homogeneous traffic, where a vehicle has only one leader, υ essentially captures the sensitivity of a driver's speed to the immediate downstream density in the same lane. However, in non-lane-based heterogeneous mix, a vehicle does not have one leader, but several, perhaps on the front-left, the front-straight, and the front-right (Figure 5.3b). Hence the speed of a vehicle is influenced by the speed of a number of surrounding leaders. To account for this, a

dimensionless Car-Following (CF) parameter has been added to the anticipation term of the speed dynamics. This CF parameter, denoted by θ in Equation 7 is expected to capture the sensitivity of traffic speed to the speeds of the near-by vehicles. Similar to the flow dynamics, a stochastic speed influencing term $\xi_i^v \sim N(\mu,\sigma)$ is added to the empirical speed equation to reflect the impact of influence area on speed. Finally, the speed dynamics of the proposed model is expressed as in Equation 7 below.

$$\begin{aligned} v_i(k+1) &= v_i(k) + \frac{T}{\tau}\left[V\left[\rho_i(k)\right] - v_i(k)\right] \\ &+ \frac{T}{L_i} v_i(k)\left[v_{i-1}(k) - v_i(k)\right] - \frac{\theta}{\tau}\left[\frac{T\upsilon}{L_i}\frac{\rho_{i+1}(k)-\rho_i(k)}{\rho_i(k)+\kappa}\right] + \xi_i^v(k) \end{aligned} \tag{7}$$

Here, τ is the reaction time parameter as in the Payne's model. According to the findings of the previous section, the FD – $V\left[\rho_i(k)\right]$ in Equation 7 is represented by Equation 8:

$$V\left[\rho_i(k)\right] = v_{f,i}\left(1 - \left(\frac{\rho_i(k)}{\rho_{j,i}}\right)^{n_i}\right) \tag{8}$$

where, v_f, ρ_j and n_i are respectively the free-flow speed, jam-density and shape parameter of the fundamental diagram for link i.The set of equations (5), (6), (7) and (8) constitutes the complete stochastic second-order model for heterogeneous traffic condition proposed in this study.

5.5. Model Calibration

The model parameters which need to be estimated are the global parameters τ, υ, κ and θ; the link-specific FD parameters v_f, ρ_j and n; the mean μ_i and standard deviation σ_i of the zero-mean Gaussian flow and speed influencing terms ξ_i^q and ξ_i^v introduced in the flow and speed dynamics respectively. During the calibration

process, these parameters are chosen such that the objective function given in Equation 9 is minimized.

$$f = \sum_{i=1}^{N}\sum_{k=1}^{K}\left\{\beta\left[\hat{q}_i(k)-\tilde{q}_i(k)\right]^2+\gamma\left[\hat{v}_i(k)-\tilde{v}_i(k)\right]^2+\left[\hat{\rho}_i(k)-\tilde{\rho}_i(k)\right]^2\right\} \quad (9)$$

Here, i is over all the links and k is the time step in the calibration time period. $\hat{q}_i(k)$, $\hat{v}_i(k)$, $\hat{\rho}_i(k)$ are the flow, speed, density collected from the field on 15th April, 2015, whereas $\tilde{q}_i(k)$, $\tilde{v}_i(k)$, $\tilde{\rho}_i(k)$ are the model estimated flow, speed, density. The weight factors β and γ are chosen so that the contributions of flow, speed and density errors are comparable. From the field data, it is found that the typical speeds, flows and densities are around 30 miles/hour (mph), 1250 vehicles/hour/lane (vphpl) and 40 vehicles/mile/lane (vpmpl). Accordingly, $\beta = (40/1250)^2 = 0.001$ and $\gamma = (40/30)^2 = 1.78$ are used in the optimization. Since the model is non-linear, f can have multiple local minima for a given convergence threshold. This research uses the gradient-based optimization method "Sequential Quadratic Programming" (SQP) to minimize the objective function over a constrained parameter space. The algorithm starts with ten different initial estimates which satisfy a specified set of bounds for the acceptable values of the parameters. These points are then moved in the parameter space until the improvement in objective function reaches the predefined termination tolerance of $1x10^{-5}$. The maximum number of iterations allowed for the evaluation of the function is set to be 3000.

During the parameter optimization, the sampling time T is taken to be 20 seconds which implies that the measured traffic data be aggregated into 20 seconds interval. Then, the total number of time steps, K = (2.5 hours x 3600 second /20 second) = 450 is assigned in Equation 9. The optimized parameter set is given in Table 5.2.

Table 5.2: Optimized parameter set of the proposed model

Link-specific Parameters								Global Parameters			
Link	v_f mph	ρ_j vpmpl	n	μ_v mph	σ_v mph	μ_q vph	σ_q vph	τ h	κ	υ m^2/h	θ
L2	50.35	200	3.50	0.39	1.53	281	7.99	0.011	843021	584.55	53.0024
L3	24.50	291	3.28	0.68	2.30	992	8.85				
L4	31.80	241	3.14	1.87	12.73	448	2.64				

All the model parameters given in Table 5.2 are well optimized since none of these passes its assigned lower boundary or upper boundary values. Moreover, the trend and values of v_f and ρ_j of different links obtained from model optimization and direct regression analysis of the FD plots are in good agreement with each other. However, the values of ρ_j are slightly larger than the typical value of 200 vpmpl found in lane-based homogeneous traffic operation. This is representative of the existing heterogeneous traffic condition where space optimization by different classes of vehicles results in greater jam densities than in the lane-based homogenous condition. The value of the CF parameter θ for this study is 53. If a driver in a traffic stream adjusts his speed following the speeds of a greater number of leaders, the value of θ will increase and vice versa.

5.6. Model Validation Results

In the words of Papageorgiou (1998), empirical validation remains the final criterion measuring the degree of accuracy, and hence the usefulness, of any macroscopic traffic flow model. Accordingly, in this section, the developed model is applied with the optimized parameter values to estimate traffic states and the results are compared with the set of measured traffic data collected on the 16th of April, 2015. Since the proposed model is supposed to describe traffic dynamics for the whole density range, the flow, speed and density at the boundary links, L1 and L5 are always assumed to

be the measured field values. So, the traffic states of only the intermediate links L2, L3 and L4 are estimated by the model. Also, the ramp flows $r_i(k)$ and $s_i(k)$ of Equation 5 always take the measured values. The traffic states at the initial time step are assumed to be the measured field values for all the links. But after the first step, they are estimated by the model dynamics.

As performance measure of the model, MAE is considered which quantifies the error between estimated and measured traffic states for the individual links. MAE is defined as:

$$\mathrm{MAE}_i = \frac{\sum_{k=1}^{K=450} \left| \left(\text{Estimated } (v, \rho, \mathrm{q})_k - \text{Measured } (v, \rho, \mathrm{q})_k \right) \right|}{\sum_{k=1}^{K=450} \text{Measured } (v, \rho, \mathrm{q})_k} \tag{10}$$

From Table 5.3, it is seen that the proposed model can simulate measured traffic states with an accuracy of 83.5-89.4% for speed estimation, 75.8-89.1% for flow estimation and 84.6-86.7% for density estimation. Such accuracy can be considered quite satisfactory given the wide variations in operating and performance characteristics of heterogeneous traffic. To investigate the improvement in traffic flow simulation accuracy achieved through each of the individual factors considered in developing the final model, different changed structures of the model are validated against real traffic data. These changes include: (1) dropping the stochastic flow and speed influencing terms (and); (2) using identical FD parameters for all the links instead of variable; (3) dropping the CF parameter ; and (4) dropping the FD from the speed dynamics altogether. The function value for each case is used for overall comparison of model performance. As expected, and play a very important role in the model, which fails to converge in their absence. After that, the use of variable FD for different links contributes a higher accuracy in simulating the flow by the model. The performance

of the model degrades by 34.3%, 25.4% and 14.8% if fixed FD is considered with the parameters of links L2, L3 and L4 respectively.

Table 5.3: Sensitivity of the proposed model with respect to structural changes

Change in Model Structure	Link	MAE			f
		v	q	ρ	
Proposed Model	L2	0.106	0.109	0.133	1374 (n/a)
	L3	0.139	0.248	0.139	
	L4	0.165	0.200	0.154	
Fixed FD considering parameters of Link 2	L2	0.213	0.109	0.164	1846 (-34.3%)
	L3	0.333	0.251	0.149	
	L4	0.314	0.219	*0.129*	
Fixed FD considering parameters of Link 3	L2	0.107	*0.107*	0.150	1723 (-25.4%)
	L3	*0.099*	0.248	0.202	
	L4	0.179	0.290	0.242	
Fixed FD considering parameters of Link 4	L2	*0.101*	*0.107*	0.135	1578 (-14.8%)
	L3	*0.104*	0.248	0.146	
	L4	0.172	0.262	0.195	
Without θ	L2	0.212	*0.108*	0.164	1537 (-11.9%)
	L3	*0.109*	0.249	0.140	
	L4	*0.160*	0.239	*0.148*	
Without FD	L2	0.142	0.162	0.225	2386 (-73.6%)
	L3	*0.134*	0.300	0.284	
	L4	0.211	0.360	0.330	

(Note 1: In the table, the numbers in the first bracket denote the percentage change in overall model performance compared to the proposed model. Negative sign indicates that the overall performance of the model degrades due to the specific structural change.)

(Note 2: The italic number refers to a model structure that performs better compared to the proposed model structure in simulating the specific traffic parameter for the specific link. However, in those cases, the MAE values for proposed model and the specific case are found to be almost same.)

Dropping the CF parameter θ from the model results in an 11.9% increase in function value as compared to the full model. Interestingly, the simulation results show that the model performance degrades the most without the FD in the speed dynamics. Without FD, the error for traffic state estimation increases by 73.6% compared to the proposed model. Hence, in relation to the findings of Lu *et al.* (2011) (which concluded that model matching with FD and without FD does not make a significant difference on average for homogeneous traffic), it is seen that FD plays the most important role in the model for heterogeneous operating condition.

5.7. Sensitivity of Mainline Demand on Model Performance

In this section, the performance of the developed macroscopic model is tested for various demand profiles. This performance evaluation is necessary to check the model accuracy from free flow to congested flow conditions. However, obtaining expected demands for such analysis from field is very time consuming and costly. In this context, micro simulation model provides a platform to obtain variable demands in a controlled environment. As such, a field-data-based simulation study with different demand scenarios is conducted using VISSIM to evaluate the model performance. With a simulation warm-up period of 15 minutes, VISSIM is run for 2 hours and 45 minutes for different traffic demand levels as shown in Figure 5.4. In the figure, the blue line represents the field demand of 16th April, 2015 which has been considered as moderate for this experimentation. This demand is artificially increased by 20% and decreased by 20% to simulate high demand and low demand respectively. These demand profiles are fed into VISSIM to obtain link-wise ground truth traffic states. Moreover, the developed macro model is run for the same demand profiles and the simulated traffic states are collected to compare with the ground truth. The computed MAEs are shown in Table 5.4.

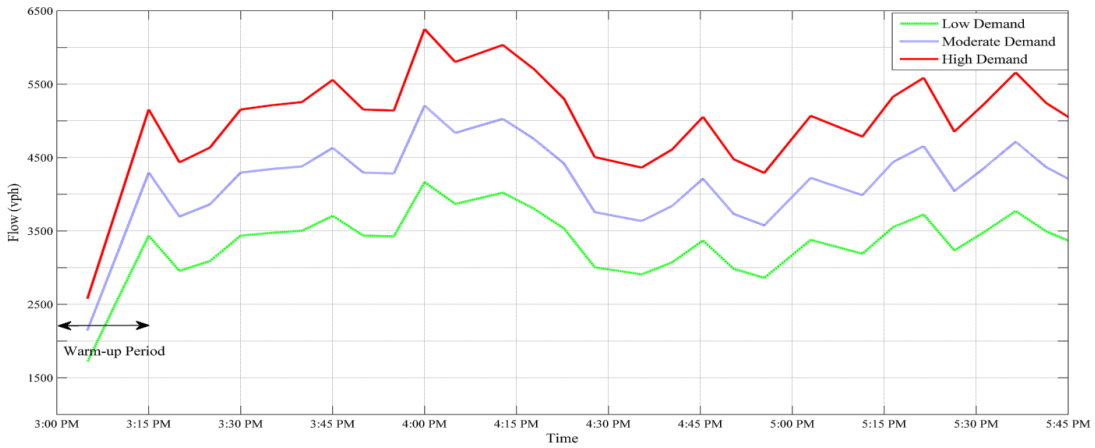

Figure 5.4: Demand profiles for mainline simulation in VISSIM

Table 5.4: Performance evaluation of the proposed model for different demand profiles

Link	Volume/Capacity	MAE		
		v	q	ρ
L2	0.76	0.050	0.066	0.080
	0.90	0.072	0.070	0.064
	1.16	0.104	0.058	0.063
L3	0.58	0.074	0.119	0.088
	0.69	0.073	0.112	0.080
	0.89	0.135	0.092	0.076
L4	0.62	0.120	0.092	0.094
	0.73	0.063	0.078	0.129
	0.95	0.118	0.087	0.140

Here, it is observed that the developed macro model estimates speed of link L2, where no spatial-temporal side friction exists with greater accuracy in relatively light demand conditions. Specifically, in comparison to moderate demand profile, the prediction accuracy of speed increases by 2.20% for light traffic demand and decreases by 3.20% for high traffic demand. With the increase in demand, the speed estimation accuracy decreases slightly, perhaps owing to the increasing complexity of heterogeneous traffic dynamics in congested traffic conditions. However, the model estimates flow and density with remarkable accuracy over the whole range of traffic demand. This could be due to the stochastic nature of the speed and density dynamics of the proposed model. By contrast, no specific trend is observed in traffic state estimation by the model for links L3 and L4. This is because of the presence of greater roadside friction in these two links.

5.8. Conclusions

A comprehensive review of the vast literature on macroscopic traffic flow modeling revealed very limited studies on the understanding of traffic flow for non-lane-based heterogeneous traffic in developing countries. Difficulty of high-resolution data collection and the complex nature of the traffic dynamics have been pointed out as the main reasons behind such limited research in this sector. As such, this study mainly

focuses on developing a practical method of high-resolution data collection and proposing a macroscopic flow model having both speed and density dynamics for the stated traffic condition. To this end, an in-depth investigation is done for understanding the macroscopic speed-flow-density relationships in the prevailing heterogeneous-flow condition. The main findings of this investigation are listed below:

i. Differences in microscopic non-lane-based heterogeneous traffic characteristics result in different macroscopic behavior of the traffic stream in comparison to the lane-based homogeneous operating condition.

ii. According to the regression analysis of the field data, the FD (speed-density) has a 3rd degree polynomial structure for all the links investigated, which differs from the findings of (Chari and Badarinath, 1983). However, comparison of the R-Square values obtained in the previous studies reveals better fitness of the polynomial structure for the current traffic condition.

iii. Although the structure of the FD remains the same over the links, the parameters (v_f and ρ_j) obtained from the regression analysis of measured $v-\rho$ plots, appear to be affected by roadside friction. In particular, increment of pedestrian activities on raised sidewalk along the study section increases the associated link jam density and reduces free-flow speed.

iv. State-of-art state estimation equations tend to underestimate the actual traffic states in non-lane-based heterogeneous condition due to the effect of vehicular influence area.

v. Moreover, the anticipation behavior of drivers in such traffic condition is dependent on the speed of multiple leaders instead of just the immediate downstream density.

Based on the above findings, this research proposes a new macroscopic traffic flow model having the following special features: (1) both the flow and speed dynamics have a normally distributed stochastic term with particular mean and standard deviation parameter; (2) the FD in the speed dynamics follows Zhang's (1999) one-parameter polynomial structure to allow for generalization and data-fitting flexibility; and (3) the parameters of the FD are variable over the links.

In the model calibration stage, simultaneous optimization of FD parameters and driver-related parameters were conducted. Interestingly, the optimized values of v_f and ρ_j obtained here follow similar trend to the values obtained when FD was calibrated in stand-alone mode (Figure 5.2). Thus, the optimized parameters capture the existing traffic conditions of the respective links quite well. Finally, to determine the individual contributions of the proposed model features, different structural variations of the final model are investigated. It was estimated that the link-specific FD parameters and the stochastic traffic state influencing terms ξ_i^q and ξ_i^v improve the model performance the most, followed by the CF parameter θ. Another interesting finding is that the proposed model performs most poorly in the absence of FD in the speed dynamics, which is in contrast to the findings of (Lu et al., 2011) for lane-based homogeneous traffic. Thus it can be concluded that FD affects the traffic states very seriously for heterogeneous composition and cannot be dropped off from the speed dynamics for simplicity in control design.

This study cannot be viewed as a complete understanding of the highly complex heterogeneous traffic operation. Several features of the proposed model could be the subject of more extensive research, including the nature of the stochastic state influencing terms which are assumed to be normally distributed in this study.

Moreover, sensitivity investigations should be done for checking the transferability of the model for changed application conditions.

5.9. References

1. Daganzo, C. F. The cell transmission model: A dynamic representation of highway traffic consistent with the hydrodynamic theory. *Transportation Research Part B: Methodological* 28, no. 4, 1994, pp. 269-287.
2. Messmer, A., and M. Papageorgiou. METANET: A macroscopic simulation program for motorway networks. *Traffic Engineering and Control* 31, no. 8-9, 1990, pp. 466-470.
3. Lin, W.-H., and D. Ahanotu, Validating the basic cell transmission model on a single freeway link. *PATH technical note; 95-3*, 1995.
4. Muñoz, L., X. Sun, R. Horowitz, and L. Alvarez. Piecewise-linearized cell transmission model and parameter calibration methodology. In *Transportation Research Record: Journal of the Transportation Research Board* 1965, 2006, pp. 183-191.
5. Papageorgiou, M., J.M. Blosseville, and H. Hadj-Salem. Modelling and real-time control of traffic flow on the southern part of Boulevard Peripherique in Paris: Part I: Modelling. *Transportation Research Part A: General* 24, no. 5, 1990, pp. 345-359.
6. Li, Z. Modeling arterial signal optimization with enhanced cell transmission formulations. *Journal of Transportation Engineering* 137, no. 7, 2010, pp. 445-454.
7. Gomes, G., and R. Horowitz. Optimal freeway ramp metering using the asymmetric cell transmission model. *Transportation Research Part C: Emerging Technologies* 14, no. 4, 2006, pp. 244-262.
8. Hadiuzzaman, M., and T. Z. Qiu. Cell transmission model based variable speed limit control for freeways. *Canadian Journal of Civil Engineering* 40, no. 1, 2013, pp. 46-56.
9. Yin, Y. Traffic Flow Modelling to Improve Traffic State Prediction. PhD dissertation, University of Alberta, 2014.
10. Islam, M., M. Hadiuzzaman, J. Fang, T. Z. Qiu, and K. El-Basyouny. Assessing mobility and safety impacts of a variable speed limit control strategy.

In *Transportation Research Record: Journal of the Transportation Research Board* 2364, 2013, pp. 1-11.

11. Papamichail, I., A. Kotsialos, I. Margonis, and M. Papageorgiou. Coordinated ramp metering for freeway networks–A model-predictive hierarchical control approach. *Transportation Research Part C: Emerging Technologies* 18, no. 3, 2010, pp. 311-331.
12. Lu, X. Y., P. Varaiya, R. Horowitz, D. Su, and S. Shladover. Novel freeway traffic control with variable speed limit and coordinated ramp metering. In *Transportation Research Record: Journal of the Transportation Research Board* 2229, 2011, pp. 55-65.
13. Lighthill, M. J., and G. B. Whitham. On kinematic waves. I. Flood movement in long rivers. II. A theory of traffic flow on long crowded roads. In *Proceedings of the Royal Society of London A: Mathematical, Physical and Engineering Sciences*, vol. 229, no. 1178, The Royal Society, 1955, pp. 281-345.
14. Richards, P. I. Shock waves on the highway. *Operations research* 4, no. 1, 1956, pp. 42-51.
15. Hoogendoorn, S. P., and P. H. Bovy. State-of-the-art of vehicular traffic flow modelling. *Proceedings of the Institution of Mechanical Engineers, Part I: Journal of Systems and Control Engineering* 215, no. 4, 2001, pp. 283-303.
16. Papageorgiou, M. Some remarks on macroscopic traffic flow modelling. *Transportation Research Part A: Policy and Practice* 32, no. 5, 1998, pp. 323-329.
17. Daganzo, C. F. The cell transmission model, part II: network traffic. *Transportation Research Part B: Methodological* 29, no. 2, 1995, pp. 79-93.
18. Daganzo, C. F., W. H. Lin, and J. M. Del Castillo. A simple physical principle for the simulation of freeways with special lanes and priority vehicles. *Transportation Research Part B: Methodological* 31, no. 2, 1997, pp. 103-125.
19. Feldman, O., and M. Maher. Optimisation of traffic signals using a cell transmission model. In *34th Annual Universities' Transport Study Group Conference, Napier University, Edinburgh*. 2002, pp 43-51.
20. Zhang, H. M. A theory of non-equilibrium traffic flow. *Transportation Research Part B: Methodological* 32, no. 7, 1998, pp. 485-498.
21. Gartner, N., C. J. Messer, and A. K. Rathi. Traffic flow theory: A state-of-the-art report. *Technical report, Transportation Research Board, USA*, 2001.

22. Payne, H. J. Models of freeway traffic and control. *Mathematical Models of Public Systems (Simulation Council Proceedings),* Vol. 1, 1971, pp.51–61.
23. Payne, H. J. FREFLO: A macroscopic simulation model of freeway traffic. *Transportation Research Record* 722, 1979, pp. 68–77.
24. Papageorgiou, M. Dynamic modeling, assignment, and route guidance in traffic networks. *Transportation Research Part B: Methodological* 24, no. 6, 1990, 471-495.
25. Lyrintzis, A. S., G. Liu, and P. G. Michalopoulos. Development and comparative evaluation of high-order traffic flow models. *Transportation Research Record: Journal of the Transportation Research Board* 1457, 1994, pp. 174–183.
26. Liu, G., A. S. Lyrintzis, and P. Michalopoulos. Improved high-order model for freeway traffic flow. *Transportation Research Record: Journal of the Transportation Research Board* 1644, 1998, pp. 37-46.
27. Sanwal, K. K., K. Petty, J. Walrand, and Y. Fawaz. An extended macroscopic model for traffic flow. *Transportation Research Part B: Methodological* 30, no. 1, 1996, pp. 1-9.
28. Lu, X. Y., T. Z. Qiu, R. Horowitz, A. Chow, and S. Shladover. METANET model improvement for traffic control. In *14th International IEEE Conference on Intelligent Transportation Systems, Washington, DC, USA*, 2011, pp. 2148-2153.
29. Cremer, M., and M. Papageorgiou. Parameter identification for a traffic flow model. *Automatica* 17, no. 6, 1981, pp. 837-843.
30. Michalopoulos, P. G., P. Yi, and A. S. Lyrintzis. Development of an improved high-order continuum traffic flow model. *Transportation Research Record* 1365, 1992, pp. 125-132.
31. Spiliopoulou, A., M. Kontorinaki, M. Papageorgiou, and P. Kopelias. Macroscopic traffic flow model validation at congested freeway off-ramp areas. *Transportation Research Part C: Emerging Technologies* 41, 2014, pp. 18-29.
32. Daganzo, C. F. Requiem for second-order fluid approximations of traffic flow. *Transportation Research Part B: Methodological* 29, no. 4, 1995, pp. 277-286.
33. Venkatesan, K., A. Gowri, and R. Sivanandan. Development of microscopic simulation model for heterogeneous traffic using object oriented approach. *Transportmetrica* 4, no. 3. 2008, pp. 227-247.

34. Arasan, V. T., and R. Z. Koshy. Methodology for modeling highly heterogeneous traffic flow. *Journal of Transportation Engineering* 131, no. 7, 2005, pp. 544-551.
35. Jin, S., D. Wang, P. Tao, and P. Li. Non-lane-based full velocity difference car following model. *Physica A: Statistical Mechanics and Its Applications* 389, no. 21, 2010, pp. 4654-4662.
36. Gunay, B. Car following theory with lateral discomfort. *Transportation Research Part B: Methodological* 41, no. 7, 2007, pp. 722-735.
37. Chari, S. R., and K. M. Badarinath. Study of mixed traffic stream parameters through time lapse photography. In *Highway Research Bulletin, Indian Roads Congress*, vol. 20, 1983, pp. 57-83.
38. Gupta, A. K., and S. K. Khanna. Mixed traffic flow analysis for developing countries WST to India. In *Research for Tomorrow's Transport Requirements. Proceedings of the Fourth World Conference on Transport Research, Vancouver, Canada*, 1986, pp. 1521–1534.
39. Nair, R., H. S. Mahmassani, and E. Miller-Hooks. A porous flow approach to modeling heterogeneous traffic in disordered systems. *Transportation Research Part B: Methodological* 45, no. 9, 2011, pp. 1331-1345.
40. Wong, G. C. K., and S. C. Wong. A multi-class traffic flow model–an extension of LWR model with heterogeneous drivers. *Transportation Research Part A: Policy and Practice* 36, no. 9, 2002, pp. 827-841.
41. Greenshields, B. D. A study of traffic capacity. *Highway Research Board, Proceedings*, Vol. 14, 1934, pp. 448-481.
42. Greenberg, H. An analysis of traffic flow. *Operations research* 7, no. 1, 1959, pp. 78-85.
43. Underwood, R. T. Speed, volume and density relationships: Quality and Theory of Traffic Flow, *Yale Bureau of Highway Traffic, New Haven, Conn.*, 1961, pp. 141-188.
44. Edie, L. C. Car-following and steady-state theory for non-congested traffic. *Operations Research* 9, no. 1, 1961, pp. 66-76.
45. Zhang, H. M. A mathematical theory of traffic hysteresis. *Transportation Research Part B: Methodological* 33, no. 1, 1999, pp. 1-23.
46. Khan, S., and P. Maini. Modeling heterogeneous traffic flow. *Transportation Research Record: Journal of the Transportation Research Board* 1678, 1999 pp. 234-241.

CHAPTER 6: CONCLUSION

6.1. Summary

This research begins with the development of a novel and robust technique, for detecting non lane based heterogeneous traffic using video sensor. Then VISCAL, an automated calibration tool for microscopic simulation parameters in VISSIM environment, based on three heuristic optimization algorithms GA, SPSA and SA was introduced. Then a first order and second order macroscopic model were developed to accurately estimate the prevailing traffic in Bangladesh. Finally the compatibility of the developed macroscopic models with microscopic model under various traffic conditions was conducted to determine the traffic demand influencing macroscopic simulation performance. Significant conclusions from this research are summarized chapter-wise below.

Chapter 2 accentuates on developing a novel traffic detection algorithm. The developed algorithm follows deterministic approach. The algorithm uses only two different parameters: (1) static background; and (2) threshold parameter. The first one initializes the background for background subtraction model and applies correction over the frames to be analyzed. The latter parameter decides whether the pixel belongs to traffic.

The algorithm achieves high accuracy of detection through small computational effort. Specifically, it achieves overall classification accuracy (>95%) with very small computational resource (500 frames per second) as compared to the most efficient algorithms identified in the recent study. Another important feature of the algorithm is that it detects traffic in three prevalent conditions such as stationary, slowly moving, and fast moving.

The innovation of the algorithm involves the use of transparency effect for frame correction to deal with challenges affecting the accuracy of traffic detection such as illumination variation, shadow, and camera displacement. The qualitative analysis shows that compared to others the proposed algorithm can detect vehicles accurately and suffers least amount of false positive and false negative, under different traffic conditions. The quantitative analysis of the algorithm shows stable Precision-Recall Relationship for both moving and stationary vehicle. The precision, recall, and percent correct classification values are 0.935, 0.906, and 0.992 respectively.

The RMSE values computed from ground truth and estimated traffic parameters show that the proposed algorithm outperforms others. While estimating the traffic parameters, a set of equations were developed which can be readily adopted with other detection algorithms. Unlike others, developed algorithm establishes correlations between traffic parameters and algorithm evaluation parameters (False Positive Rate, and False Negative Rate) to determine the applicability of any image-processing algorithm for traffic state estimation. The increment or decrement of evaluation parameters marks the characteristics of an algorithm, which dictates whether the algorithm is suitable for traffic state estimation. For background changing with time, the proposed algorithm can be adjusted for day to night transition sequence by replacing the static background parameter. Moreover, there is a certain research scope to estimate the traffic parameters at nighttime situation by extending state estimation equations developed in this study.

Chapter 3 focuses on evolving a generic calibration tool, VISCAL for microscopic simulation parameters in VISSIM environment. The optimization system of the tool is based on three heuristic algorithms: (a) GA; (b) SPSA; (c) SA. This tool offers greater flexibility to the user by providing control on every aspect of the calibration process. VISCAL includes significant features consisting of the ability to test the significance

of the appropriate decision parameter set for a particular network, to determine the most suitable objective function to reflect network characteristics, and to check the suitability of any of the three heuristic optimization algorithms for a particular network. VISCAL can be used to calibrate any type (rural, urban etc.) and extent (large, medium etc.) of network. In this study the operation of the tool is tested by a dataset obtained from a 3.26 km section of a freeway of Dhaka, Bangladesh.

Three objective functions (speed, flow, and speed-flow) from four options coded in the VISCAL system are considered for the freeway scenario. Results show that compared to GA and SA, SPSA generally obtained an acceptable set of parameters in much less time. However, it should be noted that one particular optimization algorithm would not be able to outperform the other two in all cases. For example, GA achieved best FV (MAPE) for flow based evaluation as well as multi-criteria (speed and flow) evaluation whereas; SA achieved best FV for speed evaluation of the same network.

The trade-off between time and quality is also reflected in the analysis of the freeway scenario. For instance, the SPSA converged to an optimal solution for speed-based evaluation by little iteration (only 16) compared to other two techniques (108, and 356 for GA and SA, respectively). However, the quality of FV in this case is found to be least from others. The sensitivity analysis of the objective function results showed that the combination of multi-objective criteria and GA provides the best estimates for speed and flow in the freeway scenario.

The existing features can be improved by using parallel processing to facilitate simultaneous run of all the three-optimization algorithms and four/three objective function options to reduce the computational time.

Chapter 4 concentrates on developing a new macroscopic flow model H-CTM which is an extension of the basic CTM incorporating the stated traffic condition. For model

calibration, the basic concept on macroscopic FD in the stated traffic flow condition is incorporated. The salient findings of this research are listed below:

I. The original CTM considering piecewise linear FD cannot really capture the traffic state accurately for non-lane-based heterogeneous traffic condition.

II. The H-CTM incorporates non-linear FD modeled for heterogeneous traffic including different speed class vehicles. This model can capture the traffic state more accurately.

III. From sensitivity analysis, it is found that the non-linear FD is the most important term of the model which enhance the result.

Chapter 5 mainly emphases on proposing a macroscopic flow model having both speed and density dynamics for the stated traffic condition. To this end, an in-depth investigation is done for understanding the macroscopic speed-flow-density relationships in the prevailing heterogeneous-flow condition. The main findings of this investigation are listed below:

I. Differences in microscopic non-lane-based heterogeneous traffic characteristics result in different macroscopic behavior of the traffic stream in comparison to the lane-based homogeneous operating condition.

II. According to the regression analysis of the field data, the FD (speed-density) has a 3rd degree polynomial structure for all the links investigated. However, comparison of the R-Square values obtained in the previous studies reveals better fitness of the polynomial structure for the current traffic condition.

III. Although the structure of the FD remains the same over the links, the parameters (v_f and ρ_j) obtained from the regression analysis of measured $v-\rho$ plots, appear to be affected by roadside friction. In particular, increment

of pedestrian activities on raised sidewalk along the study section increases the associated link jam density and reduces free-flow speed.

IV. State-of-art state estimation equations tend to underestimate the actual traffic states in non-lane-based heterogeneous condition due to the effect of vehicular influence area.

V. Moreover, the anticipation behavior of drivers in such traffic condition is dependent on the speed of multiple leaders instead of just the immediate downstream density.

Based on the above findings, this research proposes a new macroscopic traffic flow model having the following special features: (1) both the flow and speed dynamics have a normally distributed stochastic term with particular mean and standard deviation parameter; (2) the FD in the speed dynamics follows Zhang's one-parameter polynomial structure to allow for generalization and data-fitting flexibility; and (3) the parameters of the FD are variable over the links.

In the model calibration stage, simultaneous optimization of FD parameters and driver-related parameters were conducted. Interestingly, the optimized values of v_f and ρ_j obtained here follow similar trend to the values obtained when FD was calibrated in stand-alone mode. Thus, the optimized parameters capture the existing traffic conditions of the respective links quite well. Finally, to determine the individual contributions of the proposed model features, different structural variations of the final model are investigated. It reveals that the link-specific FD parameters and the stochastic traffic state influencing terms ξ_i^q and ξ_i^v improve the model performance the most, followed by the CF parameter θ. Another interesting finding is that the proposed model performs most poorly in the absence of FD in the speed dynamics. Thus it can be concluded that FD affects the traffic states very seriously for

heterogeneous composition and cannot be dropped off from the speed dynamics for simplicity in control design.

The predicted speed, flow and density from the developed macroscopic model were compared with those from a microscopic simulation model, VISSIM. Four levels of traffic demands viz. light, moderate, heavy and excessive demand levels were applied to evaluate the compatibility of the two models. Based on the performance of the models and comparative analysis, the following main conclusions are found:

I. The prediction of traffic states from the proposed stochastic METANET-based model is generally consistent with that from VISSIM simulation over the whole range of traffic demand levels used in this research.

II. The MAEs in traffic state estimation of various links do not show any distinct trend with the change of traffic demand levels, thus indicating that the developed macroscopic model performs quite satisfactorily for different traffic demand levels.

6.2. Recommendations for Future Research

Although traffic flow models have been studied for more than half a century in the developed world, research on this topic in developing country like Bangladesh as well as in other south-east Asian countries is extremely scarce and challenging. This is mainly due to the complexity of data collection and processing and the wide variations of driver population, vehicle components and traffic environment. Even though the current study tried to focus some effort in this sector, it cannot be viewed as a complete understanding of the highly complex heterogeneous traffic operation. In fact, it should be kept in mind that there is not a single traffic model that applies to all traffic situations. Further research to explore other forms of the traffic flow models for better representation of the heterogeneous traffic state evolution and traffic control is desirable in both theoretical analysis and field applications. In this section some

recommendations are provided for future research following the studies carried out in this study. These are listed below.

- For VISCAL two-way ANOVA can be used to determine the significant parameters for a particular microscopic model.
- The existing features of VISCAL can be improved by using parallel processing to facilitate simultaneous run of all the three-optimization algorithms and four objective function options to reduce the computational time.
- Several features of the proposed Metanet model could be the subject of more extensive research, including the nature of the stochastic state influencing terms which are assumed to be normally distributed in this study.
- Sensitivity investigations of the calibrated model parameters should be done for checking the transferability of the model for changed application conditions.
- In the compatibility analysis of microscopic and macroscopic simulation models, the effect of various time-step lengths on macroscopic model performance should be evaluated. Thus the most appropriate time-step length could be determined that will be used for on-line traffic control purpose on the studied urban freeway.
- Moreover, the impact of merging and diverging sections (at ramp locations) on macroscopic model performance should be investigated to provide experimental evidence as to whether explicit merging or diverging terms should be included in the speed dynamics of the proposed stochastic METANET-based traffic simulation model.

- Time step for the study was considered as 20 seconds. Separate study may be conducted by reducing it gradually up to five seconds to see its impact on different parameters considered.
- In future studies it is recommended that different objective functions be used for calibration of the model parameters to investigate if the result is robust. Also, other optimization algorithms can used to investigate how the optimal set of parameters depends on the choice of the algorithm.
- Finally, if field traffic states change dramatically over a very short time period, application of online calibration is recommended to adjust the model for such traffic conditions.